Fall 12-17-2021

The Role of Micrornas in the Pathophysiology of Neonatal Hypoxic-ischemic Brain Injury

Eric S. Peeples
University of Nebraska Medical Center

THE ROLE OF MICRORNAS IN THE PATHOPHYSIOLOGY OF NEONATAL HYPOXIC-ISCHEMIC BRAIN INJURY

by

Eric Peeples, M.D.

A DISSERTATION

Presented to the Faculty of
the University of Nebraska Graduate College
in Partial Fulfillment of the Requirements
for the Degree of Doctor of Philosophy

Medical Sciences Interdepartmental Area
Graduate Program
(Clinical & Translational Research Mentored Scholars Program)

Under the Supervision of Professors Zeljka Korade and Karoly Mirnics

University of Nebraska Medical Center
Omaha, Nebraska

November 2021

Supervisory Committee:
Zeljka Korade, Ph.D., D.V.M.
Ann L. Anderson-Berry, M.D., Ph.D.
Corrinne Hansen, Ph.D.
Shilpa Buch, Ph.D.
Gurudutt Pendyala, Ph.D

ACKNOWLEDGEMENTS

I would first like to thank all of my family, including my wife Lauren, my daughters Claire and Avery, and my mother Ellen, as they provided me with endless support and encouragement throughout this program. I would also like to thank my father, Bob, for instilling in me a passion for scientific investigation and inquiry, and I hope that his memory lives on in each new scientific project that I embark upon.

Additionally, I am incredibly grateful for all of the education and guidance provided by each of my mentors, including my primary supervisors/mentors Drs. Korade and Mirnics, those in my committee (Drs. Buch, Anderson Berry, Pendyala, and Hansen), as well as many others who were not in my committee but have been vital to my development as a scientist, including Drs. Joseph Vetro, Devendra Agrawal, and Donald Durden. I would also like to thank the many other scientists that have allowed me to learn from them, including Dr. Sowmya Yelamanchili and her research technologist Dalia Moore who taught me the method of extracellular vesicle extraction from brain tissue, Dr. Yunlong Huang who provided me with stem cell supernatant for extracellular vesicle extraction, and Dr. Guoku Hu who taught me a lot about microRNAs and sequencing analyses. I would also like to thank Namood-e Sahar and Bill Snyder for their support in completing some of the procedures included in these studies.

Lastly, I would like to thank all of the shared and core services for their help in these studies, including Svetlana Romanova who helped with the nanoparticle tracking analysis, as well as the DNA Sequencing Core, Bioinformatics and Systems Biology Core, and Electron Microscopy Core.

ABSTRACT

THE ROLE OF MICRORNAS IN THE PATHOPHYSIOLOGY OF NEONATAL HYPOXIC-ISCHEMIC BRAIN INJURY

Eric S. Peeples, M.D., Ph.D.

University of Nebraska, 2021

Supervisors: Zeljka Korade, Ph.D., D.V.M., Karoly Mirnics, M.D., Ph.D.

Neonatal hypoxic-ischemic brain injury (HIBI) is a devastating injury resulting from impaired blood flow and oxygen delivery to the brain at or around the time of birth. The subsequent metabolic failure and cellular injury in the brain can be partially attenuated by rapid initiation of therapeutic hypothermia, but even with prompt induction of hypothermia, more than one in four survivors suffer from major developmental disabilities – an indication of the critical need for more effective therapies. MicroRNAs (miRNA) may be able to act as therapeutic targets in neonatal HIBI; however, very little is known about the endogenous expression of miRNAs after neonatal HIBI nor the role that extracellular vesicle (EV)-delivered miRNAs may play in the neuroprotective effects of EV administration. Using temporal and regional sampling of brain tissue in a mouse model of neonatal HIBI followed by next-generation miRNA sequencing (miRNA-Seq), miRNA profiles of the different brain regions at 30 minutes and the whole brain at 24 and 72 hours after injury were obtained. EVs were then modified to optimize neuroprotection by hypoxia preconditioning, administered intranasally to the mouse model, and the EV miRNA content was analyzed by miRNA-Seq. The studies identified several

promising miRNAs for future investigations into miRNA-based therapeutic interventions. Given the multifactorial nature of neonatal HIBI, it is likely that a combination of miRNAs would need to be targeted to achieve maximal benefit. Because of this, the list of promising miRNAs was grouped by targeted pathways, and future investigations should consider assessing the effects of altering one or more miRNA from each of the miRNA clusters. Additional mechanistic studies will be necessary to demonstrate whether the differentially expressed miRNAs may be beneficial or pathologic and whether the miRNAs detected in the EVs play a significant role in the neuroprotection seen after hypoxia preconditioned EV administration. Ultimately, given their broad effect profile, ease of administration, and small size allowing for effective blood-brain barrier crossing, miRNAs represent promising targets for improving brain injury and reducing developmental impairments in neonates suffering from HIBI.

TABLE OF CONTENTS

LIST OF FIGURES

LIST OF TABLES

LIST OF ABBREVIATIONS

Ago	Argonaut
ANOVA	Analysis of variance
BCA	Bicinchoninic acid
cGMP-PKG	cGMP-dependent protein kinase G
CPM	Count per million
Ct	Cycle threshold
DAPI	4’,6-diamidino-2-phenylindole
DGCR8	DiGeorge Syndrome critical region 8
EM	Electron microscopy
ERK	Extracellular signal-regulated kinase
ESCRT	Endosomal sorting complex required for transport
EV	Extracellular vesicle
FoxO	Forkhead box O
HIBI	Hypoxic-ischemic brain injury
HIE	Hypoxic-ischemic encephalopathy
HIF	Hypoxia inducible factor
HMGCR	3-hydroxy-3-methylglutaryl-CoA reductase
IEG	Immediate early gene
IGFBP3	Insulin-like growth factor binding protein 3
IL	Interleukin

ILV	Intraluminal vesicles
IN	Intranasal
ING5	Inhibitor of growth family member 5
iNOS	Inducible nitric oxide synthase
JNK	c-Jun N-terminal kinase
KEGG	Kyoto Encyclopedia of Genes and Genomes
L1CAM	L1 cell adhesion molecule
MAPK	mitogen-activated protein kinase
miRNA	MicroRNA
miRNA-Seq	MicroRNA sequencing
MRE	MicroRNA response element
mRNA	Messenger RNA
MSC	Mesenchymal stem cell
MVB	Multivesicular bodies
NF	Nuclear factor
NLRP3	NOD-, LRR-, and pyrin domain-containing protein 3
NSC	Neural stem cell
NTA	Nanoparticle tracking analysis
OCT	Optimal cutting temperature
OGD	Oxygen and glucose deprivation
PAI-1	Plasminogen activator inhibitor 1

PBS	Phosphate buffered saline
PGK1	Phosphoglycerate kinase 1
PI3K	Phosphoinositide 3-kinase
Pri-miRNA	Primary microRNA
PTEN	Phosphotase and tensin homolog
qPCR	Quantitative polymerase chain reaction
RISC	RNA-induced silencing complex
Rora	Retinoic acid receptor-related orphan receptor A
ST18	Suppression of tumorigenicity 18
TdT	Terminal deoxynucleotidyl transferase
TGF	Transforming growth factor
TIMP-1	Tissue inhibitor matrix metalloproteinase 1
TNF	Tumor necrosis factor
TRBP	Transactivation response element RNA-binding protein
TTC	2,3,5-triphenyltetrazolium chloride
TUNEL	Terminal deoxynucleotidyl transferase dUTP nick end labeling
UCH-L1	Ubiquitin C-terminal hydrolase-L1

INTRODUCTION

Pathophysiology of Neonatal Hypoxic-Ischemic Brain Injury

Neonatal hypoxic-ischemic encephalopathy – the clinical phenotype resulting from perinatal hypoxic-ischemic brain injury (HIBI) – is estimated to affect on average 8 out of every 1,000 live births worldwide, with some regions demonstrating rates as high as 15 per 1,000 live births (1). Therapeutic hypothermia has been shown to improve outcomes in infants with HIE, but despite widespread utilization of therapeutic hypothermia in many countries, more than half of infants with moderate to severe injury die or develop severe neurodevelopmental disability (2). Because of this, there is an urgent need for the development of targeted therapies to supplement therapeutic hypothermia in these high-risk infants.

Several similar but clearly distinct terminologies are used when discussing neonatal hypoxia-ischemia. The first is asphyxia, which is the end-organ (i.e. brain, heart, kidney, etc.) effects of hypoxia-ischemia on the newborn. HIE is the brain-specific effect of asphyxia, and specifically refers to the clinical phenotype of abnormal brain activity secondary to the hypoxic-ischemic injury. The clinical diagnosis of HIE relies on the presence of signs of acidosis and hypoxia – such as low pH, elevated base deficit, or severe fetal distress or hypoxia – as well as a number of clinical examination findings suggesting abnormal brain activity and response. Since there is no clear definition of how to determine encephalopathy in the animal models, pre-clinical studies rely on terminology more specific to the abnormal brain pathology rather than brain activity or response. As such, for animal models, terms such as HIBI are preferred. Lastly, cell culture models of hypoxia-ischemia have been developed using the combination of oxygen and glucose deprivation (OGD).

Neonatal HIBI is a triphasic injury (3). The first phase starts with the initial hypoxic-ischemic insult, and the primary energy failure and hypoperfusion result in necrotic cell death in the minutes to hours after injury. This phase generally terminates shortly after the restoration of normoxia and adequate perfusion. The secondary phase starts between 6 and 12 hours after injury and continues until about 72 hours after injury. It is characterized by deteriorating mitochondrial function and an acute inflammatory response, with apoptosis being the hallmark cell death process during this phase. After the secondary phase is the tertiary phase which includes partial recovery from the injury but is also characterized by continued inflammation and gliosis (4). Importantly, between the primary and secondary phases of injury is a latent phase during which time the primary energy depletion has resolved, and the secondary metabolic failure has not yet occurred – this is the target period for hypothermia, which currently the only proven therapeutic intervention for neonatal HIE.

Therapeutic hypothermia has been shown to decrease mortality and neurodevelopmental impairment in survivors of neonatal HIE. Cooling the entire body by about 3 degrees Celsius for the first three days after injury decreases mortality and neurodevelopmental impairment in survivors but has not been shown to be beneficial in low- or middle-income countries (2, 5). Even in high resource settings, however, the neuroprotection of hypothermia is incomplete. Based on the several moderate-size clinical trials that have been performed to investigate hypothermia for neonatal HIE (6-13), 46% of infants undergoing hypothermia still died or developed major disabilities, including 22% of survivors developing cerebral palsy (2). Given the significant continued morbidity and mortality after neonatal HIE, novel therapies are urgently needed. One promising area for developing targeted therapeutic interventions in HIE is microRNAs (miRNA).

MicroRNA Synthesis and MicroRNA-Regulated Gene Expression

MiRNAs are small non-coding RNAs that modulate gene expression primarily through post-transcription silencing of messenger RNAs (mRNA, Figure 1). MiRNAs average 22 nucleotides in length and are derived from the precursor primary miRNAs (pri-miRNA) that are transcribed from DNA. The pri-miRNAs can be transcribed from introns of intragenic regions (or less commonly intragenic exons) or intergenic DNA regions (14). MiRNA genesis may occur through the canonical pathway (Figure 1) or one of several non-canonical pathways that can be Drosha-independent or Dicer-independent (15).

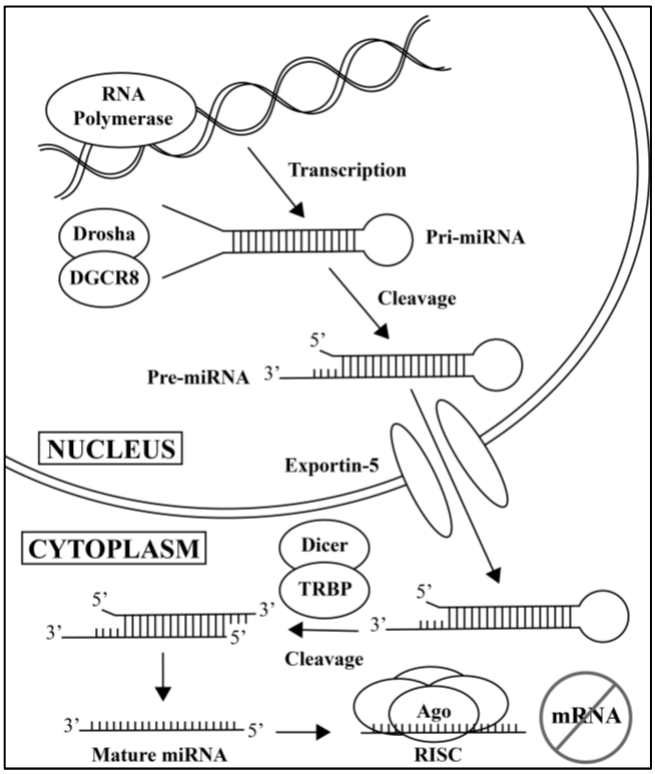

Figure 1. Canonical pathway of mature microRNA (miRNA) generation and RNA silencing*. After transcription, pri-miRNA are cleaved into pre-miRNA by Drosha and DiGeorge Syndrome Critical Region 8 (DGCR8) before being transferred to the cytoplasm where Dicer and transactivation response element RNA-binding protein (TRBP) further cleave the pre-miRNA into a mature miRNA duplex. The mature miRNA is then integrated with argonaute (Ago) proteins in the RNA-Induced Silencing Complex (RISC) to inhibit messenger RNAs (mRNA).*

The canonical miRNA genesis pathway starts with pri-miRNA processing into pre-miRNAs by the microprocessor complex which consists of the RNA binding protein DiGeorge Syndrome Critical Region 8 (DGCR8) which identifies the pri-miRNA binding motifs and the ribonuclease enzyme Drosha which cleaves the base of the hairpin pri-miRNA structure resulting in a two nucleotide 3' overhang on the resulting pre-miRNA (16). The pre-miRNA is then exported from the nucleus to the cytoplasm by the exportin-5 complex

for further cleavage by the endonuclease Dicer and its cofactor transactivation response element RNA-binding protein (TRBP) (17). This final cleavage step removes the terminal loop and results in a mature miRNA duplex with a 5p strand derived from the 5' end of the pre-miRNA and a 3p strand from the 3' end. Either strand can then be bound to argonaut (Ago) proteins in an ATP-dependent manner (18); the selection of the strand for integration with Ago depends on the thermodynamic stability at the 5' end of the miRNA duplex or a 5' U at the first nucleotide position (19).

The resulting miRNA-Ago complex is termed the RNA-induced silencing complex (RISC). The RISC targets complementary sequences on mRNAs that are specifically targeted by the miRNA guide strand in the RISC. These complementary sequences are commonly on the 5' untranslated region of the mRNA and are referred to as miRNA response elements (MRE). The degree of complementarity between the MRE and the miRNA in the RISC determines which of four silencing pathways the mRNA will undergo: target cleavage, transient binding, stable binding, or Ago unloading (20).

Effects of Hypoxia-Ischemia on Human Cord Blood MicroRNAs

To date, there have been two studies that have attempted to profile the serum miRNA changes in human newborns with HIE using high-throughput analyses (21, 22). Both of these studies assessed only cord blood changes and both used the same cohort of infants, but the studies used two different approaches to miRNA detection (next generation sequencing versus microarray). Between the two studies, the investigators identified at least 107 microRNAs that were significantly up- or downregulated in newborns diagnosed with HIE. Due to differences in reporting the miRNA species (one of the manuscripts did not regularly state which miRNA strand had altered regulation), it is difficult to exactly

compare the two study results, though there were up to seven miRNAs that were found to have altered regulation in the same direction in both studies (Table 1).

Of these, expression of miR-30b has also been confirmed to be decreased in the peripheral blood of neonates after HIE compared to controls and was strongly associated with the platelet activation marker CD62P and the plasma fibrinolytic marker plasminogen activator inhibitor 1 (PAI-1) (23). This study demonstrated persistent decreased expression of miR-30b after the immediate time of birth; however, the kinetics of miR-30b

Table 1. Umbilical cord blood microRNAs (miRNA) found to have altered expression in both previous studies of human neonates with hypoxic-ischemic encephalopathy (HIE). *For the direction of regulation, Up signifies upregulation of that miRNA in HIE versus control; Down the inverse. The Looney study did not specify the strand in their results, so definite comparisons cannot be made between the two.*

miRNAs	Looney, et al. 2015	Casey, et al. 2020
Possible Agreement Between Studies		
miR-148a	Down	
miR-148a-5p		Down
miR-16-2	Up	
miR-16-2-3p		Up
miR-181a	Down	
miR-181a-3p		Down
miR-21	Down	
miR-21-3p		Down
miR-26b	Down	
miR-26b-3p		Down
miR-30b	Down	
miR-30b-5p		Down
miR-30c	Down	
miR-30c-5p		Down
Possible Disagreement Between Studies		
miR-106b	Down	
miR-106b-5p		Up
miR-128	Down	
miR-128-3p		Up
miR-192	Down	
miR-192-5p		Up
miR-19a	Down	
miR-19a-3p		Up
miR-19b	Down	
miR-19b-3p		Up
miR-26b	Down	
miR-26b-5p		Up
miR-27b	Down	
miR-27b-3p		Up
miR-301a	Down	
miR-301a-3p		Up

expression are still not clear, as the precise timing of blood draw was not stated in this study. Additionally, miR-148a has been found to also be down-regulated after adult ischemic stroke (24), which is one of the closest relevant adult diseases to neonatal HIE. Downregulation of miR-148a is associated with increased microglial activation and release of inflammatory mediators such as tumor necrosis factor (TNF)-α, interleukin (IL)-1β, and IL-10, likely through activation of mitogen-activated protein kinase (MAPK), extracellular signal-regulated kinase (ERK), and c-Jun N-terminal kinase (JNK) (25).

Although not shown to be consistently altered in both of the high-throughput studies described above, several additional miRNAs have subsequently been confirmed by additional human studies. In a validation cohort, the same research team as the studies above re-demonstrated decreased expression of miR-199a and -374a in infants diagnosed with HIE versus controls (26). Downregulation of miR-374a in umbilical cord blood was also confirmed by a separate research team (27). Additionally, the activin-A receptor type IIb gene, which is a predicted target of miR-374a, has been shown to be elevated in infants with severe HIE (though not moderate or mild) compared to controls (28). Activin-A levels were not significantly different between groups.

An additional study by Looney, et al. evaluated umbilical cord blood levels of miR-181b and its predicted target ubiquitin C-terminal hydrolase-L1 (UCH-L1) despite demonstrating downregulation of miR-181b in only one of their three previous analyses (21, 22, 26). In this most recent study, miR-181b was significantly downregulated in infants with moderate to severe HIE compared to controls, and UCH-L1 mRNA was upregulated in infants with HIE (29).

MiR-410 downregulation after neonatal HIE has also been subsequently confirmed in circulating blood shortly after birth. Although only the Looney, et al study showed decreased expression of miR-410 in their HIE cohort, Meng, et al recently demonstrated

decreased expression of miR-410 in the circulating blood at around 6 hours after injury (30). After subsequently testing overexpression of miR-410 in a cell culture OGD model, they proposed that miR-410 and the beneficial effects of its upregulation are related to interactions with phosphatase and tensin homolog (PTEN).

Probably the most well studied hypoxia-related miRNA is miR-210. Although neither of the high-throughput studies of umbilical cord blood described above demonstrated changes in miR-210, one study that measured only miR-374a and miR-210 in cord blood did demonstrate significant decreases in both miR-210 and miR-374a expression in infants with HIE versus healthy controls (27). For miR-210, however, the inverse pattern was demonstrated in a recent study which showed increased miR-210 expression in cord blood in infants with perinatal asphyxia (31), though this study did not separate those with HIE and those with asphyxia without encephalopathy so the results may not be directly comparable between the two studies.

With the only high-throughput studies performed to date being of cord blood, this has allowed for relatively clean comparisons to be made between the study results, but has limited the understanding of any changes occurring outside the immediate moments after delivery (a time during which the insult continues to evolve and potentially progress). Additionally, both of these studies were performed with the important aim of seeking out novel microRNA biomarkers that could allow for early diagnosis and therefore potentially more effective treatment for these high-risk infants, although there are several limitations that must be considered when interpreting the umbilical cord blood miRNA expression levels. The first is that cord blood is derived from shared circulation between both mother and baby, especially when assessing very small molecules such as miRNAs that can easily cross the placenta. There is a growing body of literature demonstrating that the

development of the placenta and placental disorders significantly alter the circulating miRNA profile of the mother in both humans and animals (32, 33).

Additionally, the human studies are understandably limited to only circulating blood values (versus tissue values), so they are not specific to the brain. The findings from cord blood studies could therefore vary considerably based on the amount of systemic organ (heart, liver, kidney, etc.) injury that results from the hypoxic-ischemic injury. Even the traditional laboratory markers of hepatic injury (aspartate transaminase, alanine transaminase, prothrombin time, and activated partial thromboplastin time) as well as of kidney injury (creatinine) can vary greatly between moderate and severe neonatal HIE (34). An adequate biomarker would need to detect both moderate and severe HIE, as both are thought to require treatment with therapeutic hypothermia. Due to the noise caused by miRNAs produced by other organs, circulating miRNAs likely do not reflect brain injury with the necessary specificity for an adequate biomarker.

Lastly, consistent with the triphasic nature of neonatal HIBI, miRNA expression also varies over time after ischemic injury. Thought to be related to the multiphasic nature of the expression of hypoxia inducible factor 1 subunit α (HIF1α) and other hypoxia-regulating genes after ischemia, several miRNAs have been shown to have multiple phases of expression throughout the first 72 hours after injury. For instance, miR-335 was shown to be downregulated in the first hours after middle cerebral artery occlusion, followed by significant upregulation around 24 hours, and then downregulation again after 24 hours (35). As a consequence of this multi-phasic expression pattern, miR-335 mimic has been shown to be neuroprotective when administered immediately after injury but miR-335 antagonist was neuroprotective when administered at 24 hours after injury, corresponding to inverse endogenous expression at each of those time points (35).

MicroRNA Expression Profiles After Injury

No high-throughput miRNA analyses in neonatal HIBI have been performed outside of the cord blood studies above; however, several studies have assessed individual miRNA expression in the first hours or days after injury. One study in humans at 24-48 hours after HIE demonstrated elevations in miR-21 that were associated with elevated HIF1 levels (36). Another study assessed dried blood spot miRNA values at 18-19 hours after neonatal HIE, demonstrating good correlation between dried blood spot levels and whole blood samples, but showed no difference in any of the five miRNAs that they assessed: let-7b, miR-21, miR-29b, miR-124, and miR-155 (37).

The expression of miR-210 outside of the immediate injury period has been evaluated in a few studies, including one human study. In a study using a piglet model of HIBI, plasma miR-210 increased from pre-injury to immediately post-injury by 3.5-fold, but was then back to baseline levels by 30 minutes and remained near baseline at 9.5 hours after injury (38). This study did not assess brain levels of miRNAs, which may explain the difference between their findings and those of investigators evaluating brain miR-210 levels in the rat model of HIBI. In the rat model, studies have demonstrated significantly higher brain miR-210 expression at 3, 6, 12, and 24 hours after HIBI compared to sham operated normoxic control animals (39, 40). Specifically, miR-210 was significantly upregulated in the microglia at 24 hours after injury (40). Another rat study demonstrated decreased expression of miR-210 in the brain at 72 hours after neonatal HIBI compared to controls (41). In the one human study specifically assessing miR-210 levels after the immediate injury period, investigators demonstrated significant elevations (1.8-fold) of peripheral blood miR-210 expression at 72 hours of life in infants who had suffered perinatal asphyxia versus healthy controls (42), which was again inverse to the brain-specific levels seen in the rodent study.

Taken together, it is possible that the elevated miR-210 levels in the peripheral blood at 72 hours in the human study but not at 9.5 hours in the piglet study may demonstrate a delay in the detection of circulating miRNAs given the superior sensitivity of the brain analyses. This would not account for the difference between the downregulation seen in the brain in the rat study at 72 hours versus the upregulation in the circulating blood of the humans at 72 hours, which may speak more to the lack of specificity of the circulating blood microRNAs for detecting changes in brain-related miRNAs. Differences in technique and species expression, however, must also be strongly considered.

In the cord blood study performed by Looney, et al, miR-374a was the most highly downregulated miRNA in infants with HIE compared to healthy controls, which they subsequently confirmed in a validation study (21, 43). The decreased miR-374a expression in cord blood was further demonstrated by another group, showing ~4-fold decreased expression compared to healthy control newborns (27). Despite the consistent downregulation in human umbilical cord blood, miR-374a levels were found to be upregulated in the plasma of the piglet model after HIBI (38). Levels were elevated immediately after injury, but then decreased rapidly so that, although still elevated at 30 minutes, were back to baseline by 3.5 hours after injury.

MiR-181a was also evaluated in the piglet model, with upregulation compared to controls only at 1 hour after injury, but not before or after that time point (22). Of note, this finding was inverse to what has been shown in the human cord blood studies. Upregulation of miR-181a shortly after ischemic brain injury is supported by studies in adult ischemic stroke demonstrating upregulation 30 minutes after injury in a rat model (44), and reduced infarct size and improved neurological deficits when mice were administered miR-181a antagonist at 60 minutes after injury (45). This protection may be related to inhibitory effects of miR-181a on glucose-regulated protein 78, which is a heat

shock protein found primarily in the endoplasmic reticulum (46). One potential issue with using circulating miR-181a as a biomarker of ischemic brain injury, however, is that it is not specific to the brain and has also been found to be upregulated after myocardial ischemia (47), which may also occur after neonatal asphyxia. Additionally, in one study of adult stroke, miR-181a was found to only be upregulated in the brains of male mice, with no difference after injury in female mice (48).

Much like the miR-181a studies described above, several other investigators have begun to investigate the therapeutic potential of altering miRNA expression before, during, and after brain injury.

MicroRNAs as Therapeutic Targets for Hypoxic-Ischemic Brain Injury

MiRNAs are thought to play a significant role in modulating the neuroinflammation after HIBI and therefore may act as effective targets for therapeutic intervention (49). Much of the literature to date regarding miRNAs in neonatal HIBI has focused on a class of miRNAs known as hypoxamiRs. HypoxamiRs, including the commonly studied miR-21 and -210 but also miR-335, -137, and -376c, are miRNAs that are regulated by hypoxia but also in turn regulate cell response to decreased oxygen (50). These hypoxamiRs have been shown to play a significant role in several pathological states, from cardiac injury to cancer (51, 52), and altering miRNA levels in the brain may provide neuroprotection after HIBI (35, 53, 54). Due to their small size (21-25 nucleotides in length), miRNAs are more likely to cross the blood-brain-barrier than other larger molecules currently being tested as therapeutics (55). As such, miRNA-based interventions may be able to provide targeted therapy to supplement hypothermia in neonates suffering after HIBI, but the question of which miRNA(s) to target remains a significant hurdle in the path toward developing successful miRNA-based therapies.

A few groups have attempted to modulate miR-210 expression to attenuate brain injury after hypoxia-ischemia. In the one study of brain miR-210 levels described above, miR-210 was persistently upregulated between 3 and 24 hours after injury (39). As such, most of the interventional studies have attempted to decrease miR-210 through administration of antagonists. In an adult stroke model, inhibition of miR-210 reduced stroke-induced cerebral infarction and edema, decreased behavioral deficits after stroke, and suppressed post-stroke inflammatory reaction when administered either prior to or 4 hours after injury (56). Similarly, exosome-mediated delivery of miR-210 24 hours after stroke improved survival and increased angiogenic factors (57).

In models of neonatal HIBI, miR-210 inhibition improves expression of glucocorticoid receptors (39), suppresses microglia-mediate inflammation, in part through sirtuin 1 and ten-eleven translocation 2 and subsequent increase of nuclear factor (NF)-kB (40, 58), ameliorates mitochondrial dysfunction caused by miR-210-associated downregulation of the iron-sulfur cluster assembly protein (59), and results in decreased cerebral edema and IgG leakage into brain parenchyma, suggesting improvement in blood-brain barrier integrity (60). Only one potentially contradictory study has been published in neonatal HIBI, demonstrating decreased apoptosis after intracerebroventricular injection of miR-210 mimic (61). The authors did not specifically state the timing of when the injections were performed relative to the injury, however, making it difficult to truly compare their results to the other studies that have all demonstrated consistent neuroprotective effects of miR-210 antagonism.

Other miRNAs that have been successfully altered in neonatal HIBI include miR-374a, -204, -124, and -454. Overexpression of miR-374a through intracerebroventricular injection of miR-374a mimic attenuated brain injury and inhibited release of pro-inflammatory cytokines in neonatal rat model, potentially through NOD-, LRR-, and pyrin

domain-containing protein 3 (NLRP3) inflammasome alteration (62). These effects could also be related to alterations in the PTEN and phosphoinositide 3-kinase (PI3K) pathways which have also been shown to be affected by miR-374a (50). Although there have been some inconsistencies in post-injury levels of miR-374a between humans and animal models, as described above, the beneficial effects of miR-374a overexpression would be consistent with decreased levels seen in human umbilical cord blood. Similar neuroprotective benefits have been demonstrated with the administration of miR-204 mimic, resulting in increased neuronal proliferation and decreased neuronal apoptosis (63). Overexpression of miR-124 promoted cell survival and attenuated neuronal apoptosis, resulting in improved testing of memory and neurological function at one and two months after injury (64). Administration of miR-454 mimic improved cell viability in OGD injured neurons, likely related to effects on suppression of tumorigenicity 18 (ST18) expression (65), and lastly, knockdown of miR-326 upregulated the expression of the δ-opioid receptor, improved cell survival, and decreased caspase-3- and Bax-related apoptosis (66).

When searching for therapeutic targets, it is important to note that the studies performed on humans and piglets assessing the circulating miRNA levels were seeking to discover biomarkers for diagnosis and prognosis – not therapeutic targets. As such, a better understanding of the changes in brain miRNA levels after HIBI will be vital to the future investigation of miRNA-based interventions. Supporting the disconnect between the circulating levels and therapeutic promise, of the miRNAs that were described above as having been tested in neonatal HIBI animal models and shown to have some benefit, only miR-454 and -374a were shown to be altered in the human umbilical cord blood studies, and neither miRNA was differentially expressed in both of the studies (21, 22).

Free circulating miRNAs have a half-life that may be as short as 90 minutes (67). However, miRNAs can be administered intranasally (39, 68), providing easy and efficient brain delivery by bypassing the blood-brain barrier and minimizing possible off-target systemic effects compared to intravenous administration (69). Several groups have demonstrated that small RNAs can be successfully administered intranasally in rodent models of brain injury, with adequate brain tissue penetration within 30 minutes after administration of 0.5-1 nmol of miRNA (53, 68, 70). Another method to extend the miRNA half-life and improve brain tissue targeting is by binding the miRNAs to nanoparticles to decrease their uptake by the reticuloendothelial system or to insert the miRNAs into protective vessels such as extracellular vesicles (EV).

Extracellular Vesicles and Other Therapeutic Vessels for MicroRNAs

EVs are a heterogeneous group of membrane-bound vesicles that are released by various types of cells (71) and carry a variety of cargo including miRNAs, proteins and lipids (72). EVs exist in the central nervous system, mediating interactions between neurons and glia to support neuronal survival (73, 74). Due to their ability to cross the blood brain barrier (75), they have become a strong candidate for both serum biomarkers of brain injury as well as for therapeutic intervention. EVs derived from mesenchymal stem cells (MSC) have been shown to decrease microgliosis and reactive astrogliosis in a rat model of preterm inflammatory white matter injury after intraperitoneal injection (76). When administered intravenously to a mouse model of adult stroke, MSC-derived EVs provided improvement in neuronal survival and angioneurogenesis, with results similar to a comparison group receiving MSCs (77).

EVs, as classified by the International Society of Extracellular Vesicles, range in diameter from 20-1000 nm, and consist of several subclasses, including exosomes, ectosomes, microvesicles, shedding vesicles, microparticles, exosome-like vesicles,

nanoparticles, and apoptotic bodies (78). The importance of EVs lies in their ability to mediate cell-to-cell communication; as such, they play significant roles in both normal physiological processes as well as various pathological conditions.

The biogenesis of EVs occurs either dependent or independent of the Endosomal sorting complex required for transport (ESCRT) pathway (79-81). In the ESCRT dependent pathway, intraluminal vesicles (ILVs) are formed within large multivesicular bodies (MVBs) by invagination of late endosomal membranes that then accumulate proteins and cytosolic components or are trafficked to lysosomes for degradation (81). The ESCRT-independent pathway has been shown to be mediated via raft-based microdomains that are highly enriched in sphingomyelinases (82). Two lipid metabolism enzymes (neutral sphingomyelinase and phospholipase D2) have been shown to generate lipids in the limiting membrane of MVBs, which induce inward budding and, thus, formation of ILVs in an ESCRT-independent manner (79, 80).

The composition of the EV is primarily governed by the physiological state of its environment as well as the type of producer cell. While the membranes of all EVs are enriched with cholesterol (83, 84), glycosphingolipids (83), and phosphatidylserine (84, 85), the exact lipid profile of specific EVs tends to be similar to, yet distinguishable from that of its cell of origin (86). The nucleic acid content of EVs is also variable, including various types and quantities of DNA, ribosomal RNA, mRNA, and non-coding RNAs such as miRNAs.

It is now widely believed that much of the therapeutic benefits of stem cell transplantation lies in the cell-to-cell signaling factors transported by EVs. The miRNA cargo contained within the EVs are specifically and strongly associated with the positive effects of stem cell transplantation. Although the EVs carry a range of potentially therapeutic molecules including RNAs and proteins, a recent study demonstrated that

administering mesenchymal stem cell-derived EVs to OGD-injured neurons decreased apoptosis and improved cell survival; however, this protection was lost when the EVs were pretreated with RNase but not when pretreated with proteinase (87). The ability of EVs to carry wide therapeutic payloads makes them ideal candidates for this type of intervention. EVs modified to overexpress certain miRNA have showed improved neurogenesis and functional recovery in models of adult stroke (88, 89); however, no studies have been performed in neonatal models.

Ischemic and/or hypoxic preconditioning has long been known to alter the cellular environment in a manner that is protective against future hypoxic-ischemic injury. Given the significant role that EVs play in intercellular communication, it is feasible that they may also contribute to the protective effects of preconditioning. Supporting this theory, investigators have demonstrated that infusion of preconditioned EVs resulted in significant attenuation of infarct size in a mouse model of ischemic stroke compared to EVs that were not preconditioned (90). The EV preconditioning not only affects several of the EV protein markers, but also results in significantly altered miRNA profiles compared to naïve EVs (91). This is consistent with studies of the brain tissue which have also demonstrated a significant role of miRNA expression in the effects of preconditioning (92). Previous studies have demonstrated that altering EV miRNA expression results in improved therapeutic efficacy (93), but to date, no study has assessed the neuroprotective effect of hypoxia preconditioned EVs after neonatal HIBI.

Gaps in the Current Literature

As described above, although some studies have begun to assess plasma levels at or around the time of injury, very little is known about the brain miRNA changes after neonatal HIBI. The studies that have been performed in the brain to date have focused only on one or a few miRNAs, limiting the ability for identifying novel therapeutic targets. Given that

the high-throughput studies of plasma samples have all been performed in the first minutes or hours after injury, minimal known about any miRNA signaling outside the first hours after injury. Additionally, HIBI does not affect all regions of the brain equally and, although global brain expression patterns need to be investigated since miRNA-based interventions are unlikely to affect only the injured tissue, investigations of brain region-specific miRNA patterns may provide more sensitive insight into the roles miRNAs play in neonatal HIBI.

Lastly, EVs are promising therapeutic vessels for several types of small molecules, including miRNAs; however, no study to date has attempted to use intranasally administered EVs for neuroprotection after neonatal HIBI. Although naïve stem cell-derived EVs may provide some neuroprotection, there are emerging data to suggest that preconditioning EVs with hypoxia may provide superior neuroprotection. Given the link between EV miRNA contents and the beneficial effects of stem cell transplantation, it is likely (but yet unknown) that the additional benefit of hypoxia preconditioned EVs may lie in the miRNA content.

Dissertation Aims

In order to attempt to fill some of the gaps in the literature described above, the studies included in this dissertation sought to address three specific aims.

The first aim was to evaluate the whole brain miRNA expression patterns at 24 hours and 72 hours after HIBI in a neonatal mouse model. To attempt to differentiate the effects of hypoxia alone versus combined hypoxia-ischemia, two control groups were used: one true sham normoxia control and one sham control that was exposed to hypoxia but not ischemia. Additionally, the contralateral HIBI expression pattern was analyzed given the predilection of many studies to use the contralateral brain tissue as a sort of internal control

in this animal model, but the lack of any description in the literature about the validity of this practice for miRNA analyses.

The second aim sought to assess the brain region-specific miRNA expression patterns at 30 minutes after neonatal HIBI and attempt to link alterations in miRNA expression with mRNA changes. The 30-minute time point was chosen to attempt to maximize both the comparability of the results to the human studies of umbilical cord blood (i.e. 0 minutes) and the chances of demonstrating meaningful changes in expression given that previous studies of piglets in the first hours after HIBI showed that the peak expression changes for many miRNAs were around one hour after injury.

The third and final aim was to compare the neuroprotective effects of intranasal EV administration after neonatal HIBI. For this aim, naïve neural stem cell-derived EVs were compared with EVs derived from hypoxia-preconditioned brain tissue. EVs were administered at 30 minutes and 24 hours after injury, and the effects of EV administration on brain tissue viability and apoptosis were measured. To begin evaluating the mechanism of EV-mediated neuroprotection, miRNA sequencing was performed on the hypoxia-preconditioned EVs.

Taken together, these aims seek to provide a comprehensive analysis of endogenous miRNA signaling in the brain after neonatal HIBI in order to aid in identifying novel therapeutic targets. Additionally, the final aim will begin evaluating the interplay EV-induced neuroprotection and the EV miRNA contents, thus confirming and/or expanding on the number of potential therapeutic miRNAs.

METHODS

Development of Mouse Models of Hypoxia and Hypoxic-Ischemic Brain Injury

All studies described were approved by the University of Nebraska Medical Center Institutional Animal Care and Use Committee.

Timed pregnant CD1 mouse dams were obtained from Charles River Laboratory (Wilmington, MA). After delivery, pups were maintained in a 12-hour light and 12-hour dark environment with the dam and littermates. At postnatal day 9, pups of both sexes were randomized to the relevant injury/treatment groups for each study (Table 2). The HIBI groups were induced with 5% isoflurane and then were anesthetized with 2.5% isoflurane through a nose cone (VetFlo Anesthesia System, Kent Scientific Corp., Torrington, CT). While under anesthesia, pups were labelled sequentially by tail tattoo. They were then rotated to a supine position and the ventral neck sterilized with isopropyl alcohol and 2% chlorhexidine. Analgesia was provided by injection of 2 mg/kg sterile bupivacaine at the incision site. A small vertical incision was made in the midline of the ventral neck. The neck was dissected in order to identify and isolate the right common carotid artery from the vagus nerve (94). After isolation, the common carotid artery was cauterized, and once

Table 2. Injury/treatment groups used throughout all studies described here. *HIBI, hypoxic-ischemic brain injury induced by unilateral carotid artery ligation and 30 minutes of 8% oxygen; EV, extracellular vesicle; PBS, phosphate-buffered saline; NSC, neural stem cell*

	Group	N
Chapter 1 (3 groups)	Sham	8 (4 at each time point)
	HIBI	8 (4 at each time point)
	Hypoxia only	8 (4 at each time point)
Chapter 2 (2 groups)	Sham	4
	HIBI	4
Chapter 3 (5 groups)	Hypoxia only	3 (for brain EV extraction)
	Sham + PBS	10 (6 TTC/protein; 4 TUNEL)
	HIBI + PBS	10 (6 TTC/protein; 4 TUNEL)
	HIBI + NSC EVs	10 (6 TTC/protein; 4 TUNEL)
	HIBI + Brain EVs	10 (6 TTC/protein; 4 TUNEL)

hemostasis was confirmed, the neck was closed with sterile surgical glue. Surgeries took no longer than five minutes. The sham control group underwent the same anesthesia, tattooing, analgesia, and neck dissection, but once the carotid artery was identified and isolated, the neck was closed without vessel ligation. Hypoxia only groups also received the sham surgery. After surgery, pups were transferred to a recovery cage.

During the surgery and the immediate recovery period, the pups were maintained at normothermia on far infrared heating pads. The pups underwent serial examination every ten minutes during and after the surgery until breathing, activity, and righting reflex normalized. Once the pups were fully recovered, they were returned to the dam and littermates for a two-hour recovery period. After recovery, groups were again separated, and the HIBI and hypoxia only groups underwent 30 minutes at 8% oxygen in a hypoxia chamber (BioSpherix, Parish, NY) at normothermia maintained by infrared heating pads. The sham control group spent the same 30 minutes separated from the dam but in a warm normoxic environment.

Tissue Collection and Storage

For the studies described in Chapter 1, half of the pups in each group were sacrificed at 24 hours and the other half at 72 hours after injury. The whole brain was extracted as quickly as possible, and the hemispheres separated. Each hemisphere was cut into 1 mm coronal sections and then submerged in RNAlater Stabilizing Reagent (Invitrogen, Carlsbad, CA) until RNA extraction. For hypoxia only and sham control groups, the right hemisphere was used for analyses. For HIBI pups, ipsilateral (right) and contralateral (left) hemispheres were processed separately. For the studies in Chapter 2, all pups were sacrificed at 30 minutes after completion of hypoxia or normoxia. After dissecting out the brains and separating the hemispheres, each hemisphere was further dissected into regions. First, the brainstem was removed, and the cerebellum separated. The

striatum/thalamus was then separated from the remaining tissue, exposing the hippocampus, which was subsequently isolated from the cortex. Each region was immediately frozen on dry ice and stored at -80°C until analysis.

For the studies in Chapter 3, 30 minutes after the second EV administration, the pups underwent deep anesthesia isoflurane through a nose cone. The pups were then placed supine and a bilateral thoracotomy performed to expose the heart. A 14-gauge needle was inserted into the left ventricle followed by incision of the right atrium for drainage and subsequent perfusion with 5-10 mL of ice-cold phosphate buffered saline (PBS). For 2,3,5-triphenyltetrazolium chloride (TTC) staining and western blot, brains were immediately dissected after PBS perfusion. For immunofluorescent histology, once the fluid from the right atrium turned clear and the liver appeared pale, animals subsequently underwent perfusion with 5 mL of 10% formalin. Following formalin perfusion and fixation, the brain was removed intact and placed in a vial containing 10% formalin overnight. After formalin fixation, the tissue was dabbed gently to remove excess formalin, washed twice with PBS, and then placed in 15% sucrose for 12-24 hours and then placed in 30% sucrose.

Extracellular Vesicle Extraction from Brain Tissue

For the studies in Chapter 3, two groups of EVs were prepared: hypoxia preconditioned brain tissue-derived (brain-EV) and neural stem cell (NSC)-derived EVs (NSC-EV). NSC-EVs were extracted from an existing mouse induced neural progenitor cell line (supernatant graciously provided by Dr. Yunlong Huang). The cell extraction and tissue culture protocol has been described previously (95). Briefly, after NSC passage, the NSC supernatant was collected for EV extraction, diluted in PBS, and transferred to an ultracentrifuge tube. To prepare the brain-derived EVs, P9 CD1 mouse pups were exposed to 8% oxygen for 30 minutes as described above. Immediately after hypoxia exposure, the animals were sacrificed, and the brain tissue extracted and frozen at -80°C

for EV extraction. The frozen brain tissue was finely minced in a tissue digestion solution of papain and exosome-free Hibernate A (200-300 mg tissue with 3 mg papain and 3.5 mL Hibernate A) and incubated for 15 minutes at 37°C. Enzyme digestion was stopped using ice cold exosome-free Hibernate A. The homogenate was then centrifuged at 300 g for 10 min at 4°C and the supernatant transferred to an ultracentrifuge tube.

The brain-EV and NSC-EV suspensions both underwent ultracentrifugation at 100,000 g for 70 min at 4°C. The pellet was washed with PBS and then underwent another round of ultracentrifugation at 100,000 g. The supernatant was removed after the wash and the pellet was resuspended in PBS and stored at -80°C until use.

Evaluation of Extracellular Vesicle Characteristics

Standard EV characteristics have been proposed by the International Society for Extracellular Vesicles (96). To ensure the necessary EV characteristics were present, first the EV size, shape, and concentration were estimated by nanoparticle tracking analysis (NTA) and electron microscopy (EM). NTA was performed on the NanoSight NS300 (Malvern Panalytical, Malvern, United Kingdom) as described previously (97). Samples for EM imaging were spotted onto formvar/silicon monoxide coated 200 mesh copper grids (Ted Pella Inc., Redding, CA). Grids were glow discharged for 60 seconds at 20μA with a GloQube glow discharge unit (Quorum Technologies, Lewes, United Kingdom) prior to use. Samples were negatively stained with NanoVan (Nanoprobes Inc., Yaphank, NY) and examined on a Tecnai G2 Spirit TWIN (FEI Co., Hillsboro, OR) operating at an accelerating voltage of 80kV. Images were acquired digitally with an AMT digital imaging system. EV characteristics were also confirmed using protein electrophoresis and western blot, as described below.

Intranasal Administration of Extracellular Vesicles to Mouse Model of HIBI

At P9, pups were randomly assigned to one of four groups (Table 2): 1) unilateral right-

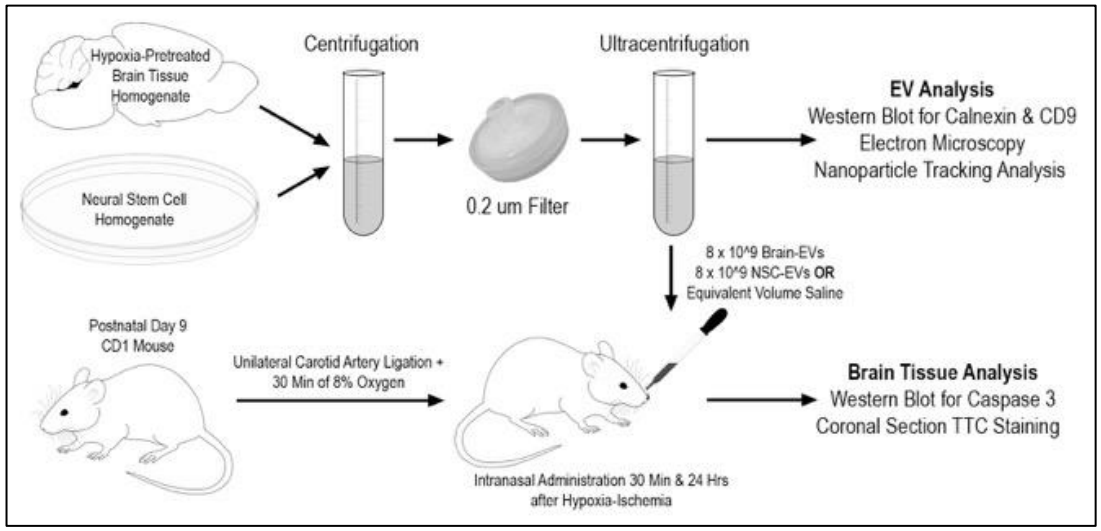

Figure 2. Procedure for intranasal administration of extracellular vesicles (EVs) in the postnatal day 9 mouse model of hypoxic-ischemic brain injury. *NSC, neural stem cell; TTC, 2,3,5-triphenyltetrazolium chloride*

sided carotid artery ligation followed by hypoxia and intranasal (IN) saline treatment; 2) unilateral carotid artery ligation followed by hypoxia and IN administration of neural stem cell-derived EVs; 3) unilateral carotid artery ligation followed by hypoxia and IN administration of endogenous mouse brain EVs exposed to hypoxia; and 4) sham surgery of carotid dissection without ligation followed by normoxia (21% oxygen) and IN saline administration. Thirty minutes prior to EV administration, the nasal passages of the mice were prepared by IN injection of 2 μL of 2% hyaluronidase. Then 10 μL of EV solution (8 x 10^9 EVs/ 10 μL) or PBS was administered to the mice intranasally, corresponding to assigned treatment group. These intranasal administrations were performed 30 minutes following hypoxia and repeated at 24 hours after hypoxia (Figure 2).

Brain Tissue and Extracellular Vesicle RNA Extraction

For Chapters 1 and 2, between 15 and 20 mg of brain tissue at a time was thawed on ice and transferred into a dounce homogenizer with Qiazol Lysis Reagent (Qiagen, Hilden, Germany). The tissue was fully homogenized, and the RNA extracted using the RNeasy Lipid Tissue Mini kit (Qiagen). Briefly, 200 µL of chloroform was added to each sample and the tube shaken vigorously for 15 seconds followed by incubation at room temperature for 3 minutes. The sample was then centrifuged at 12,000 x g for 15 minutes at 4°C in order to separate the aqueous phase containing the RNA from the organic and lipid phases. The upper phase was transferred to a new tube and combined with one volume of 70% ethanol and vortexed. The RNA was then extracted using the spin columns supplied in the kit with serial buffer washes, on-column DNase digestion, and finally elution of the RNA by addition of RNAse-free sterile water.

RNA concentration and integrity was determined through spectrophotometry (DeNovix DS-11, Wilmington, DE). Only samples with ratios of 260/280 nm absorbance >1.9 were used for analyses.

For Chapter 3, aliquots with 6.5×10^{15} EVs were mixed with Qiazol Lysis Reagent, and the RNA extracted using the RNeasy Mini kit (Qiagen) as described above.

Next Generation miRNA Sequencing

For the miRNA sequencing performed in all three chapters, RNA samples extracted from brain tissue (chapters 1 and 2) or from brain-EVs (chapter 3) underwent quality confirmation through parallel capillary electrophoresis on a Fragment Analyzer (Agilent, Santa Clara, CA) and then were processed for miRNA-Seq. MiRNA-Seq libraries were prepared from 200 ng RNA per sample with the NEXTFLEX Small RNA Kit (PerkinElmer,

Waltham, MA) per the manufacturer's instructions. The libraries were then sequenced on the Illumina NextSeq 550 platform (San Diego, CA).

mRNA Panel

For the mRNA analyses in Chapter 2, RNA samples underwent quality confirmation through parallel capillary electrophoresis on a Fragment Analyzer (Agilent) followed by the CodeSet Hybridization protocol with the nCounter Mouse Neuroinflammation probes (Nanostring, Seattle, WA). Samples are hybridized by combining 8 µL master mix (Reporter CodeSet and hybridization buffer), 5 µL of sample, and 2 µL of the capture ProbeSet, and incubated overnight at 65°C in a thermal cycler. The next morning, the samples are transferred to the nCounter MAX/FLEX (Nanostring) device, where the digital analyzer counts the fluorescent target molecules. Finally, data are downloaded from the digital analyzer and loaded in nSolver for normalization and analysis.

Quantitative Polymerase Chain Reaction (qPCR)

For Chapters 1 and 2, miRNA-Seq and mRNA panel findings were validated by qPCR for the miRNAs and mRNAs that were highly differentially expressed and/or were previously reported to have biological relevance in neonatal HIBI (Table 3). For miRNA qPCR, the miRCURY LNA Reverse Transcription Kit (Qiagen) was used to generate cDNA from 200 ng of RNA. Template RNA was adjusted to a concentration of 5 ng/µL and 2 µL was added to the reverse transcription mix of 2 µL reaction buffer, 4.5 µL RNase-free water, and 1 µL enzyme mix, mixed, and incubated at 42°C for 60 minutes. The mix was then heated to 95°C for 5 minutes to inactivate the enzyme, cooled back to 4°C, and stored at -20°C until use.

Table 3. Sequences for each microRNA (miRNA) messenger RNA (mRNA) quantitative polymerase chain reaction primer

miRNA	**Sequence (5' to 3')**
miR-1195	UGAGUUCGAGGCCAGCCUGCUCA
miR-137-3p	UUAUUGCUUAAGAAUACGCGUAG
miR-155-5p	UUAAUGCUAAUUGUGAUAGGGGU
miR-2137	GCCGGCGGGAGCCCCAGGGAG
miR-335-5p	UCAAGAGCAAUAACGAAAAAUGU
miR-376c-3p	AACAUAGAGGAAAUUUCACGU
miR-6240	CCAAAGCAUCGCGAAGGCCCACGGCG
miR-665-3p	ACCAGGAGGCUGAGGUCCCU
mRNA	
ATF3 Forward	CCAGGTCTCTGCCTCAGAAG
Reverse	CAAAGGGTGTCAGGTTAGCAA
BDNF Forward	ATTAGCGAGTGGGTCACAGC
Reverse	TCAGTTGGCCTTTGGATACC
EGR1 Forward	GAGCACCTGACCACAGAGTC
Reverse	CGAGTCGTTTGGCTGGGATA
FOS Forward	GGTGAAGACCGTGTCAGGAG
Reverse	CCTTCGGATTCTCCGTTTCT
NFKB2 Forward	GGCCGGAAGACCTATCCTAC
Reverse	AGGTGGGTCACTGTGTGTCA
SOCS3 Forward	GGTCACCCACAGCAAGTTTC
Reverse	GGTACTCGCTTTTGGAGCTG
SRXN1 Forward	ATGTACCTGGGAGCATCCAC
Reverse	GCTGCATGTGTCTTCTGAGC

The miRNA qPCR was performed using the miRCURY LNA SYBR Green qPCR kit (Qiagen) with manufacturer generated primers for each of the target mature miRNAs (Table 3). The cDNA solution was first diluted 1:60 in RNase-free water to a final volume of 600 µL and then added to a pre-mixed reaction mix of SYBR Green Master Mix, PCR primer mix, and RNase-free

water. The solution was mixed thoroughly, dispensed into PCR tubes, centrifuged briefly, and then placed into the thermal cycler. Cycles were set for 2 minutes at 95°C for heat activation, and then 40 cycles of alternating 10 second denaturation at 95°C and 60 seconds annealing at 56°C. Cycle threshold (Ct) values were downloaded from the device, normalized to the U6 small nuclear RNA as an endogenous control, and analyzed. All qPCR samples were run in triplicate.

For mRNA qPCR, a similar process was followed, but the RevertAid First Strand cDNA Synthesis Kit (Thermo Scientific, Rockford, IL) was used for the cDNA synthesis and the PowerUp SYBR Green Master Mix (Applied Biosystems, Waltham, MA) was used for the standard qPCR. For mRNA analyses, values were normalized to the housekeeping gene phosphoglycerate kinase 1 (PGK1). For both miRNA and mRNA analyses, Ct values and expression levels were calculated by the ΔΔCt method (98). Expression fold-change in the HIBI group compared to controls was reported after $\log_2$ transformation.

Infarct Area Measurement

For the EV studies in Chapter 3, the PBS-perfused brains were immediately sectioned into 2 mm coronal sections using an acrylic brain matrix (Kent Scientific). The section at the optic chiasm (starting at 1 mm from the rostral aspect of the brain) was incubated in 2% TTC for 20 minutes at room temperature and then placed in 10% formalin for fixation. Following this staining and fixation process, the TTC stained brain sections were scanned and digitized. The area of viable non-infarcted tissue (seen as pink with the TTC stain) on the ipsilateral hemisphere and the contralateral hemisphere were measured separately using Image J software (NIH, Bethesda, MD). The percent of viable ipsilateral tissue was estimated by dividing the ipsilateral area by the contralateral area.

Protein Electrophoresis and Western Blot

For Chapter 3, protein electrophoresis and western blot were used both to characterize EVs as well as for an outcome marker using homogenized brain tissue. For the brain tissue analyses, the remaining ipsilateral brain tissue from the PBS-perfused brain was homogenized in RIPA buffer with a dounce homogenizer. The total protein concentration of the homogenate was analyzed by bicinchoninic acid (BCA) protein assay (Thermo Scientific) and 20 ug of sample protein was prepared and loaded onto a pre-cast 4-12% NuPAGE Bis-Tris gel (Invitrogen). For EV characterization, ~2.5 x 10^{14} EVs were loaded into each well.

After electrophoresis, the protein was transferred to a PVDF membrane which was then incubated with primary antibodies for caspase-3 (R&D Systems, Minneapolis, MN) and beta-actin antibody (Invitrogen) for use as the loading control. EV characterization membranes were incubated with calnexin (Invitrogen) or CD9 (Invitrogen) and beta-actin primary antibodies. Following incubation, the membrane was washed and then anti-rabbit IgG HRP-linked antibody (1:3000, Cell Signaling Technology, Danvers, MA) was added and incubated at room temperature shaking for 60 minutes. The membrane was washed again and developed in Radiance HRP substrate for chemiluminescence imaging on the Azure 600 Western Blot Imaging System (Azure Biosystems, Dublin, CA). Band densities were analyzed using Image J software as previously described (99) and normalized using the band quantification of the beta-actin loading control.

Brain Tissue Sectioning

For Chapter 3, after formalin and sucrose fixation, the fixed brains were processed for sectioning. First, the brains were placed in Optimal Cutting Temperature (OCT) solution and re-frozen at -80°C. The tissue was then mounted to a specimen disk and 10

μm sections obtained on a cryostat microtome (Leica Biosystems, Buffalo Grove, IL). Sections were collected in PBS and stored at 4°C until staining.

TUNEL Staining and Brain Section Imaging

For terminal deoxynucleotidyl transferase dUTP nick end labeling (TUNEL) staining, brain sections were post-fixed in a 2:1 mix of ethanol and acetic acid for 5 minutes and then washed twice in PBS. The tissue was gently blotted with a laboratory wipe to remove excess liquid and then immediately submersed in equilibration buffer for at least 10 seconds before removing buffer to apply terminal deoxynucleotidyl transferase (TdT) enzyme and incubating at 37°C for one hour in a humidified chamber. After incubation, the section was submersed in stop/wash buffer and incubated for 10 minutes at room temperature. After washing, the section was placed in anti-digoxigenin conjugate solution and then incubated for another 30 minutes at room temperature. Finally, the section is washed in PBS at least four times and then stained with 4',6-diamidino-2-phenylindole (DAPI) as a nuclear counterstain. The sections were then covered in aqueous mounting medium and a coverslip applied.

Fluorescent imaging was performed on the ImageXpress Pico Automated Cell Imaging System (Molecular Devices, San Jose, CA). After obtaining images of each section, the ImageXpress automated cell counting system was used to count TUNEL+ cells and DAPI+ cells in sections through the striatum (~3.5 mm from the rostral edge of the brain) using a mouse brain atlas to determine landmarks for consistency between brains.

Bioinformatics and Statistical Analyses

For all miRNA sequencing, results were aligned to mature mouse miRNA from miRBase using bowtie2 alignment, and differential expression analysis performed using EdgeR. In Chapter 1, two samples with alignment <25% were excluded and replaced with

new samples with alignment above 25%. A false discovery rate <0.05 or p-value <0.05 for these exploratory studies were considered significant. Conservation between mammalian species for each of the miRNAs was assessed using microRNAviewer (100). MiRNAs that demonstrated >90% sequence homology between species were considered to be “highly conserved.”

In Chapter 1, expression pattern relationships between controls, ipsilateral HIBI, and contralateral HIBI, were assessed using a stepwise approach combining significance and magnitude of change approach. First, miRNA species with an average raw count of <10 were filtered out, as these low expressors tend to give rise to more unreliable data. Then counts per million (CPM) were calculated for each sample and the CPM was $\log_2$ transformed to establish differential expression for ipsilateral-control, ipsilateral-contralateral, and contralateral-control comparisons. For this analysis, differentially expressed miRNA species were defined by an uncorrected p-value of 0.05 and a magnitude change of 30% in at least one of the three comparisons. These data underwent unsupervised two-way (gene vs. sample) hierarchical clustering based on Euclidian distance using the Morpheus program (Broad Institute, Cambridge, MA). This procedure was separately performed for samples obtained at 24 or 72 hours.

Correlation between high-throughput results (i.e. miRNA-Seq and Nanostring) and qPCR results in Chapters 1 and 2 were performed using linear regression with Prism version 9.2.0 (GraphPad, La Jolla, CA). Goodness of fit was determined using the R^2 value.

The miRNA KEGG pathway analyses in Chapter 2 were performed using Diana Tools (101) using Tarbase annotations, a p-value threshold of 0.05, and enrichment analysis by Fisher’s exact test with hypergeometric distribution. The mRNA Kyoto Encyclopedia of

Genes and Genomes (KEGG) pathway analyses were performed using Ingenuity Pathway Analysis (Qiagen). For both analyses, pathway data were stratified by -log(p-value).

Network visualization of mRNA-mRNA and miRNA-mRNA networks in Chapter 2 were obtained using Cytoscape (Institute for Systems Biology, Seattle, WA). The mRNAs demonstrating significant differential expression in each region were mapped to the BioGRID Mus musculus interactions archive (version 4.4.200). The nodes from the significant mRNAs were selected, and networks were generated two degrees of connection (undirected) between those mRNA and the other mRNA included in the Nanostring Neuroinflammation panel. Those mRNAs with less than two connections were excluded from the network. Node fill color relates to the log fold change of mRNA in hypoxic-ischemic brain injury compared to controls. The same process was used for the miRNA-mRNA networks, with the following exceptions. Starting with the miRNAs that demonstrated significant differential expression, the miR2Gene pathway analysis (102) was used to predict miRNA-mRNA interactions.

In Chapter 3, comparative analyses between the four injury/treatment groups were performed using one-way analysis of variance (ANOVA) and the Mann Whitney U test for individual group comparisons. P-values of <0.05 for ANOVA and <0.025 for Mann Whitney test (Bonferroni correction for two comparisons – HIBI+PBS vs. each of the two EV treatment groups) were considered significant.

CHAPTER 1: TEMPORAL CHANGES IN MIRNA EXPRESSION AFTER NEONATAL HYPOXIC-ISCHEMIC BRAIN INJURY

Material from: Peeples ES, et al, Temporal brain microRNA expression changes in a mouse model of neonatal hypoxic-ischemic injury, published 2021, publisher – Springer Nature.

Rationale

As most of the previous studies assessing endogenous miRNA expression after HIBI were seeking to use miRNA expression as an early biomarker of injury, rather than assessing for therapeutic targets, they have primarily used peripheral blood for miRNA measurements (21, 22, 38, 103). As mentioned above, however, the circulating miRNA levels are unlikely to adequately reflect the brain microenvironment given that the peripheral blood contains miRNAs from every organ, not just the brain, and those results should therefore be used with caution when attempting to identify therapeutic targets for neuroprotection. Additionally, although it has been shown that gene expression may remain altered as late as school age in children who suffered neonatal HIBI (104), previous miRNA studies in neonatal HIBI have primarily focused on changes in the seconds (cord blood) or first few hours after injury (21, 22, 38, 103).

The expression pattern of miRNAs changes rapidly in the first minutes to hours after neonatal HIBI (22, 38) and clinically neonatal encephalopathy is often not diagnosed within the first hour after injury (average age at entry to the large hypothermia trials ranged from 1.9 to 4.7 hours after injury (2)). As such, miRNA expression will likely have shifted significantly from birth by the time that therapy is initiated. The miRNA expression patterns in cord blood or immediately after injury in animal models, therefore, has limited utility in the development of miRNA-targeted interventions that would most likely be administered

over the course of hypothermia (approximately 2-72 hours after injury). Although some studies have profiled the expression of a few selected brain miRNAs outside of the first few hours after neonatal HIBI, the global profile of miRNA expression changes 24 to 72 hours after neonatal HIBI has not yet been established.

Designing interventions to effectively target miRNAs after neonatal HIBI will require a greater knowledge of the subacute miRNA expression changes that occur after injury. To that aim, the goal of this study was to assess changes in brain-specific miRNA expression at 24 and 72 hours after injury in a mouse model of term neonatal HIBI. In order to provide a comprehensive miRNA profile, next-generation miRNA-Seq was used and subsequently validated by qPCR. The results of this study will provide important differential expression information necessary to design future studies targeting miRNA expression in the first 72 hours after neonatal HIE.

HIBI Versus Hypoxia at 24 and 72 Hours After Injury

Analyses were performed between four different groups (Figure 3): normoxia controls, hypoxia only, ipsilateral HIBI, and contralateral HIBI. Figure 4 demonstrates miRNAs with significant differential expression in the first comparison: hypoxia only compared to normoxia controls. This analysis demonstrated 51 miRNAs with significant differential expression at 24 hours (Figure 4A), 129 at 72 hours (Figure 4B), and 38 at both time points (Figure 4C). Thirty-three of the 38 that were altered at both time points were found to be highly conserved between mammalian species. Notably, all miRNAs that were differentially expressed at both time points after hypoxia only were expressed in the same direction (positive or negative) at both time points.

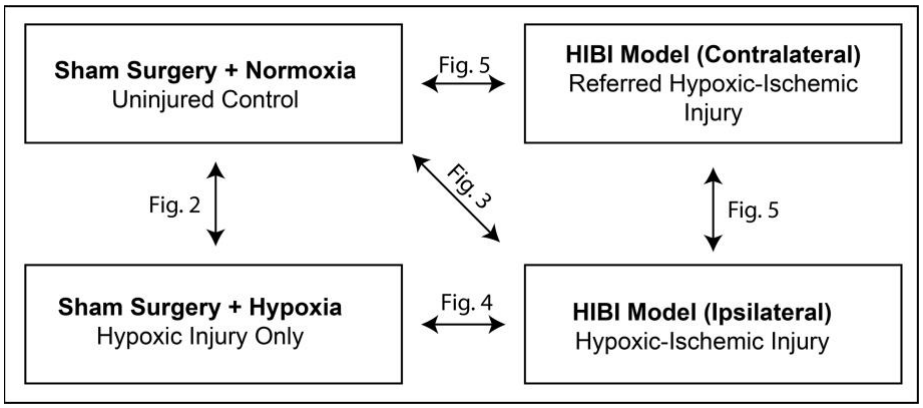

Figure 3. Group comparisons made throughout temporal microRNA study, *with references to the relevant figures that contain each of the comparisons. Hypoxic-ischemic brain injury (HIBI) model consists of unilateral carotid artery ligation with 30 minutes of hypoxia at 8% oxygen. Sham surgery includes dissection and visualization of carotid artery but no ligation. The hypoxia only group received sham surgery followed by 8% oxygen for 30 minutes.*

HIBI Versus Normoxic Controls at 24 and 72 Hours After Injury

A similar analysis was performed between the ipsilateral (lesioned) HIBI samples and the normoxia controls (Figure 5). Figure 5A shows volcano plots for the miRNAs at 24 and 72 hours, providing a visual display of the number of miRNAs with a significant p value and the associated $\log_2$ fold-change. Overall, 16 miRNAs were found to have significant differential expression at 24 hours after HIBI (Figure 5B), and 26 at 72 hours after HIBI (Figure 5C). Five of these miRNAs had significant altered expression at both 24 hours and 72 hours: miR-137-3p, -2137, -335-5p, -376c-3p, and -5126 (Figure 5D). The conservation of miR-5126 has not been well described; however, the other four miRNAs are highly conserved between mammalian species. Of note, miR-2137 and miR-5126 maintained similar relative expression directionality at both 24 and 72 hours after injury (both were upregulated at both time points after HIBI). MiR-335-5p, -137-3p, and 376c-3p demonstrated multi-phasic expression, with all three being upregulated after ipsilateral HIBI at 24 hours after injury but downregulated at 72 hours.

To attempt to differentiate effects of hypoxia versus hypoxia-ischemia, Figure 6 demonstrates the miRNAs with significant differential expression at 24 and 72 hours after HIBI compared to the differential expression in hypoxia only versus controls at each of the time points. The five miRNAs that were differentially expressed after HIBI at both time points are listed at the top of the figure (within the dashed box) for ease of comparison. With only a few exceptions, the direction of expression after hypoxia only and HIBI were similar between the two comparisons at 24 hours (Figure 6A) but were more often inverse to each other at 72 hours (Figure 6B). Figure 6C is a Venn diagram demonstrating the overlap of miRNAs with significant differential expression for the hypoxia only and HIBI groups at each time point.

qPCR was subsequently performed on each of the miRNA-Seq samples to validate the high-throughput findings. Figure 7 demonstrates strong correlation (R^2=0.634) between qPCR $\log_2$(fold-change) and miRNA-Seq $\log_2$(fold-change) for each of those samples. miR-665 was an outlier for the correlated values, and subsequent post-hoc exclusion of miR-665 values improved the R^2 to 0.743. In addition to running qPCR on the miRNA-Seq samples, three additional brains per group were used for qPCR, for a total of 6 samples per group. Figure 8 summarizes the total $\log_2(\Delta\Delta Ct)$ fold-change qPCR results for all six biological replicates in each of the analyzed miRNAs, compared to the miRNA-Seq $\log_2$(fold-change) values.

mRNA Pathways Associated with Dysregulated miRNAs

To aid in understanding the pathways affected by the upregulated miRNAs in this study, a literature search was performed to identify the most commonly identified mRNAs involved in neonatal HIBI; 63 such mRNAs were identified (listed in Table 4 (105-110)). A list of miRNAs known to be associated with each of the mRNAs was obtained from

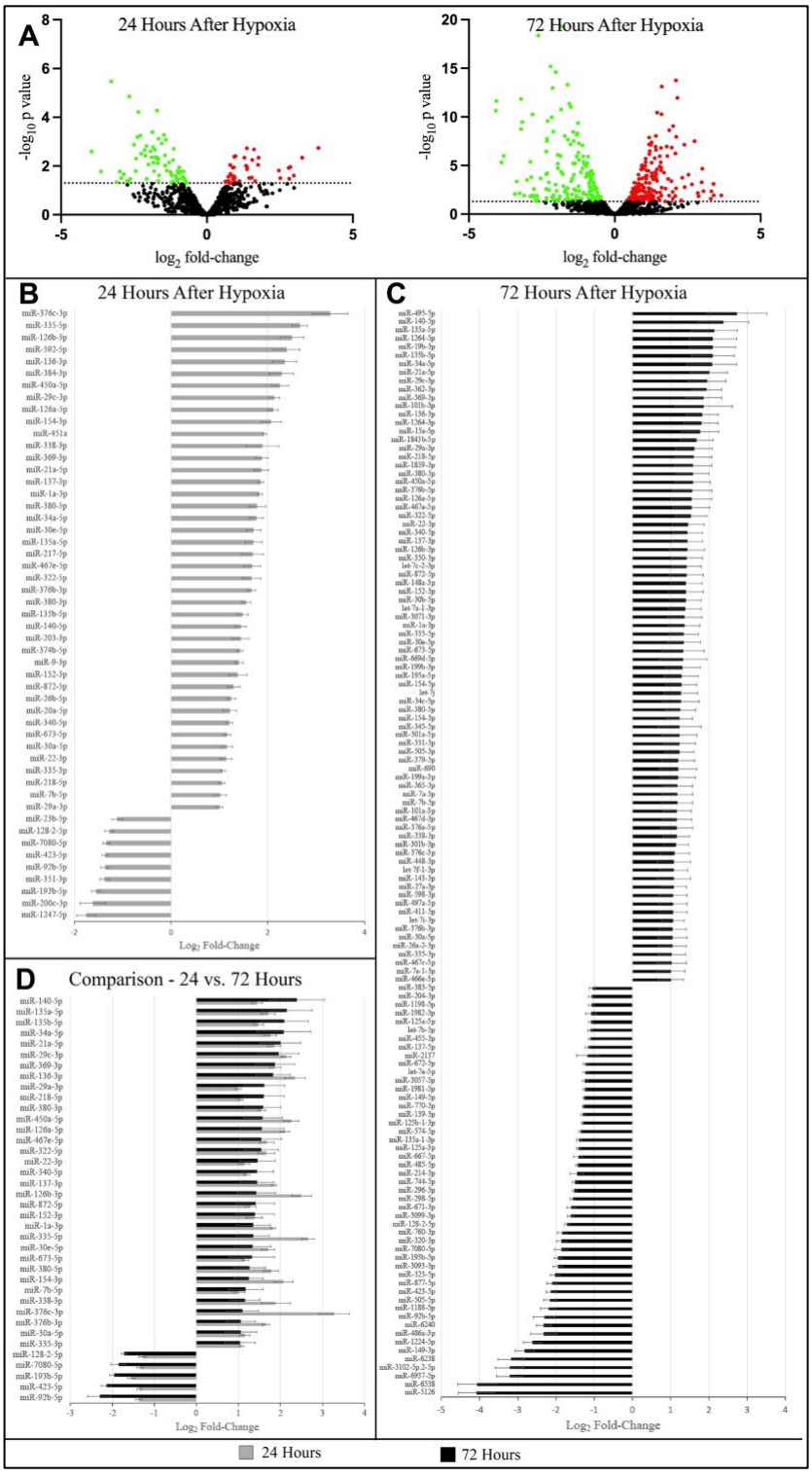

Figure 4. MicroRNAs with significant differential expression in hypoxia only injury compared to uninjured controls. *Volcano plots demonstrate total number of microRNAs with significant p values (above dashed line) and corresponding log_2 fold-change. The microRNAs with significant differential expression (defined by log_2 fold-change > 1, p value and/or false discovery rate < 0.05, and average count per million reads > 10) are shown below, stratified by their altered expression at B) 24 hours, C) 72 hours, and D) both.*

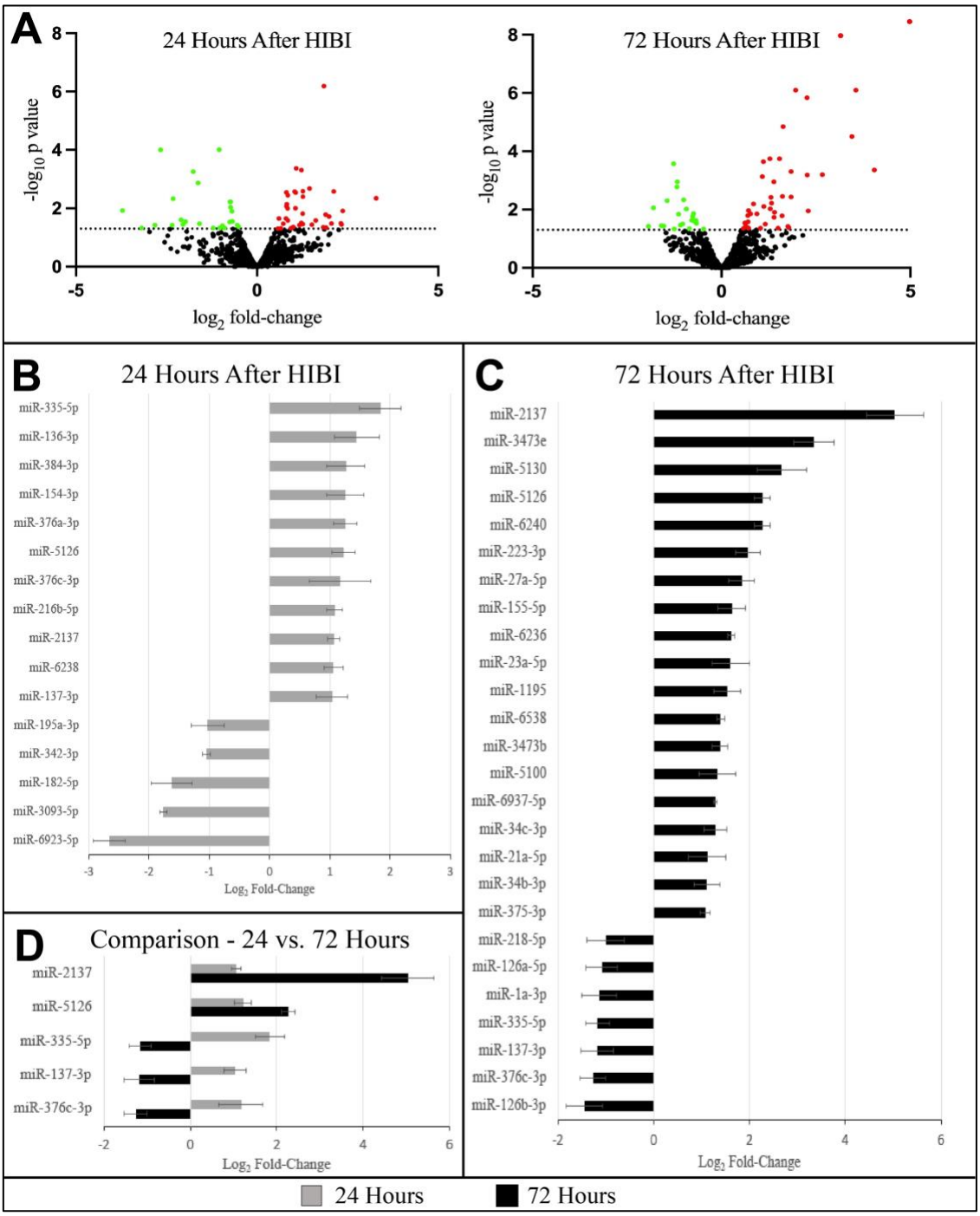

Figure 5. MicroRNAs with significant differential expression in ipsilateral hypoxic-ischemic brain injury (HIBI) compared to uninjured controls. *Volcano plots demonstrate total number of microRNAs with significant p values (above dashed line) and corresponding log_2 fold-change. The microRNAs with significant differential expression (defined by log_2 fold-change > 1, p value and/or false discovery rate < 0.05, and average count per million reads > 10) are shown below, stratified by their altered expression at B) 24 hours, C) 72 hours, and D) both.*

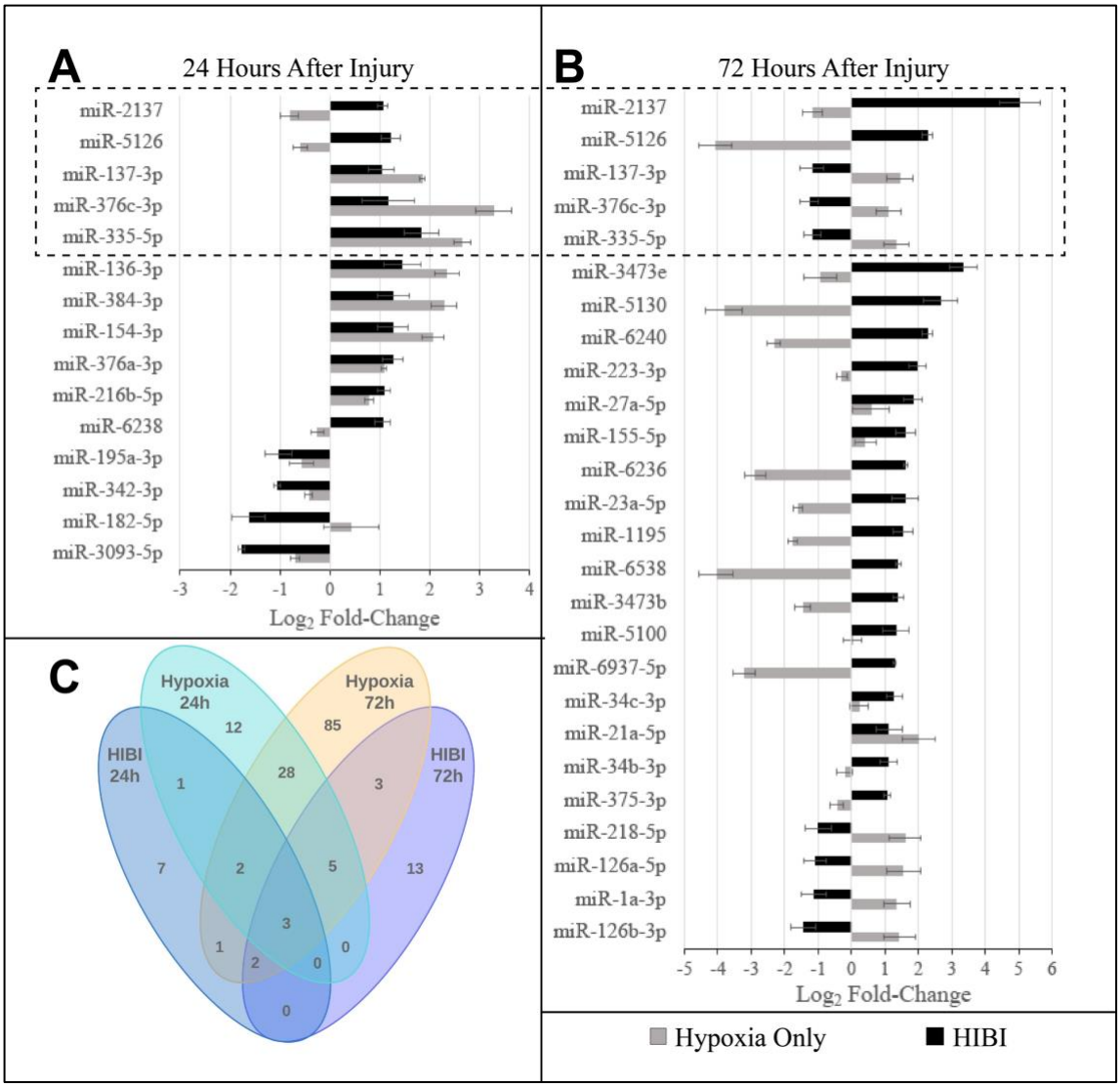

Figure 6. MicroRNAs with significant differential expression in ipsilateral hypoxic-ischemic brain injury (HIBI) compared to controls (black bars), *with associated differential expression of the same miRNAs in hypoxia only compared to controls (grey bars) at A) 24 hours or B) 72 hours. The five microRNAs that were significantly differentially expressed at both time points are enclosed in the dashed box. Significance defined by HIBI versus control comparison with log_2 fold-change > 1, p value and/or false discovery rate < 0.05, and average count per million reads > 10. A Venn diagram in C shows the number of significantly differentially expressed microRNAs under each condition and time point.*

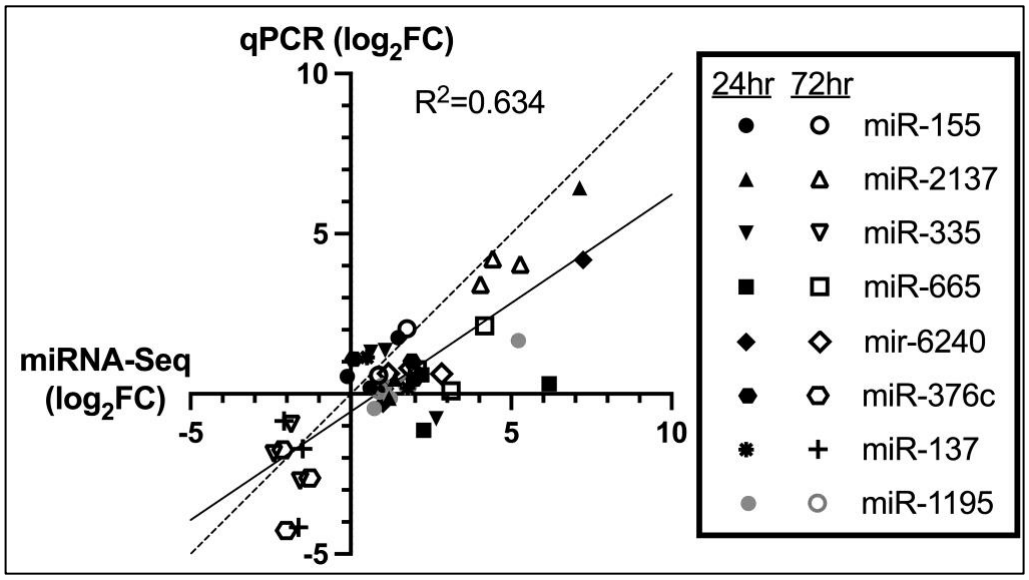

Figure 7. Correlation between next-generation microRNA sequencing (miRNA-Seq) and quantitative polymerase chain reaction (qPCR) validation *of eight highly expressed and/or physiologically relevant microRNAs. The x-axis values are miRNA-Seq log_2 fold-change (log_2FC, ipsilateral hypoxic-ischemic brain injury versus control) values and y-axis are qPCR ΔΔCt log_2FC values. Filled shapes are from the samples obtained at 24 hours and the open shapes are from the samples obtained at 72 hours. The solid line represents the best-fit regression of the data points with strong correlation (R^2=0.634) and the dashed line represents the ideal correlation line (x=y). The top right and lower left quadrants contain the majority of samples, which all demonstrated concordant log_2FC directionality between miRNA-Seq and qPCR, while the top left and lower right quadrants show the few samples with discordant directionality.*

miRTarBase and then compared to the list of miRNAs with significant differential expression from our study. Table 5 lists those differentially expressed miRNAs from our study that were associated with one or more of the identified mRNAs, as well as the experimental group and time point at which that miRNA demonstrated significant altered expression.

Validity of Using Contralateral Brain as Control for HIBI miRNA Studies

Lastly, as contralateral brain tissue has often been proposed as a valid internal control for unilateral HIBI models, the pattern of differential miRNA expression was evaluated between the normoxia controls, ipsilateral HIBI, and contralateral HIBI groups using two-way, unsupervised hierarchical clustering. Figure 9 demonstrates the clustering results.

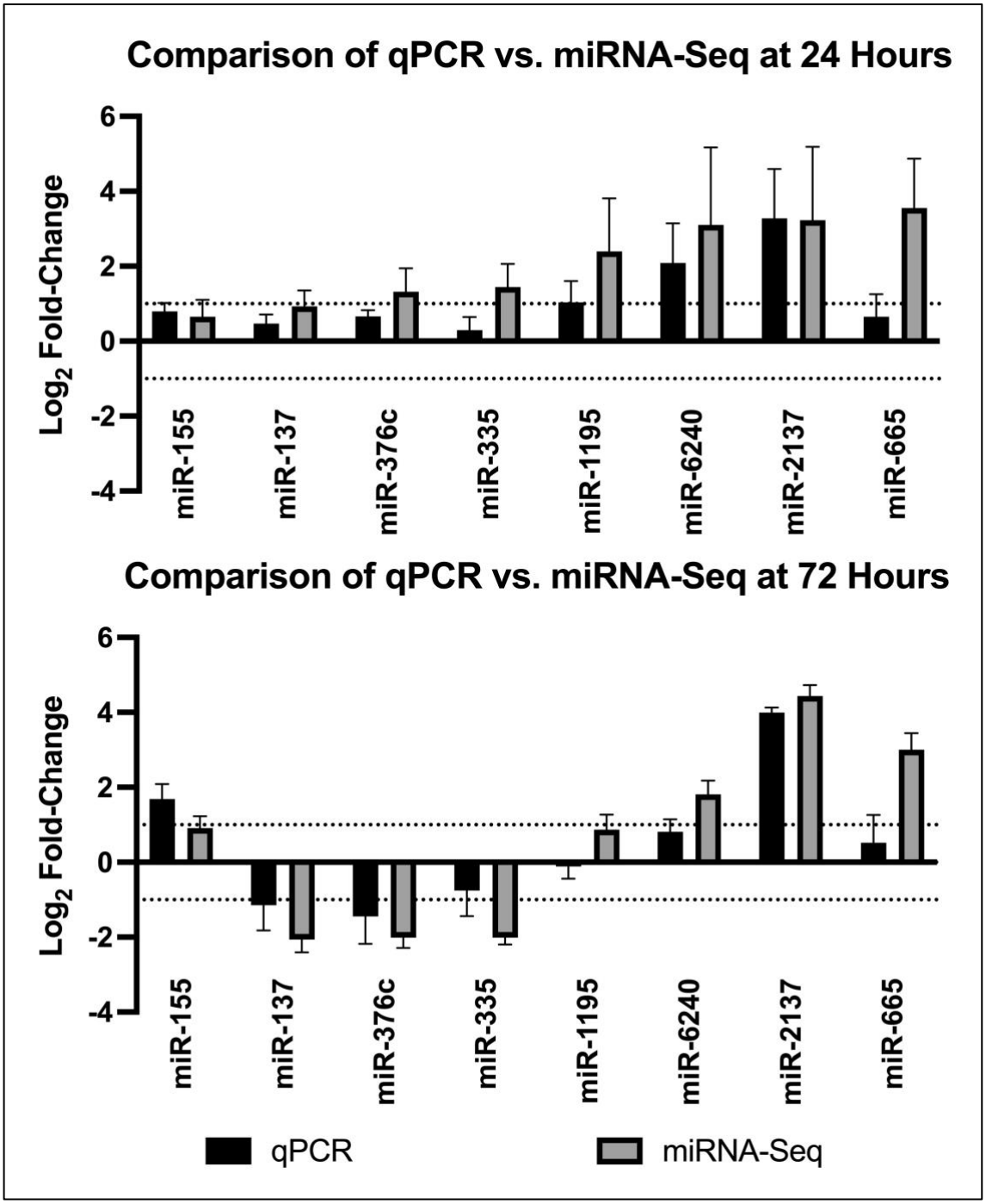

Figure 8. Log_2 differential expression values (ipsilateral hypoxic-ischemic brain injury versus control) for next-generation microRNA sequencing (miRNA-Seq) and quantitative polymerase chain reaction (qPCR) validation *of eight highly expressed and/or physiologically relevant microRNAs. Dashed lines demonstrate log_2>1 or <-1 significance thresholds.*

***Table 4. Messenger RNAs (mRNA) associated with neonatal hypoxic-ischemic brain injury**, as identified by literature search (21-26). The mRNAs were matched with associated microRNAs (miRNA) that demonstrated significant differential expression in the current study.*

mRNA	Gene Name	Associated miRNA
Adam9	ADAM Metalloproteinase Domain 9	30e-5p, 362-3p, 140-5p
Adrb2	Adrenoceptor Beta 2	30e-5p
Alox5	Arachidonate 5-Lipoxygenase	None
Angpt14	Angiopoietin 14	None
Angpt2	Angiopoietin 2	None
Anxa2	Annexin A2	155-5p, 218-5p
Anxa4	Annexin A4	34a-5p
Atg10	Autophagy Related 10	192-5p, 362-3p
Bag3	BAG Cochaperone 3	34a-5p
Bdnf	Brain Derived Neurotrophic Factor	376b-5p, 15a-5p
Casp6	Caspase 6	34a-5p
Casp7	Caspase 7	192-5p, 106a-5p, 34a-5p, 23a-5p
Casp8	Caspase 8	29c-3p, 29b-3p, 29a-3p, 5119, 665, 34a-5p, 376b-3p
Chrm5	Cholinergic Receptor Muscarinic 5	None
Chrna5	Cholinergic Receptor Nicotinic Alpha 5 Subunit	None
Clcf1	Cardiotrophin Like Cytokine Factor 1	218-5p
Csf1	Colony stimulating factor 1	335-5p, 30e-5p
Csrnp1	Cysteine and Serine Rich Nuclear Protein 1	None
Ctsc	Cathepsin C	375
Ctsl	Cathepsin L	362-3p
Ctss	Cathepsin S	None
Cyba	Cytochrome B-245 Alpha Chain	None
Cybb	Cytochrome B-245 Beta Chain	34a-5p
Cyp1b1	Cytochrome P450 Family 1 Subfamily B Member 1	340-5p, 148b-5p
Dap	Death Associated Protein	30e-5p, 335-5p
Ddx58	DExD/H-Box Helicase 58	218-5p, 3058-5p, 298-5p
Dusp1	Dual Specificity Phosphatase 1	101a-3p, 200c-3p
Dusp5	Dual Specificity Phosphatase 5	335-5p, 92a-3p
Eno2	Enolase 2	30e-5p, 93-3p, 1195, 665-3p, 218-5p, 669d-5p, 339-5p
F3	Coagulation Factor 3	223-3p, 375, 106a-5p, 335-5p
Fzd4	Frizzled Class Receptor 4	375, 192-5p, 29c-3p, 665
Gfap	Glial Fibrillary Acidic Protein	335-5p
Gria	Glutamate Ionotropic Receptor AMPA	None

Grik4	Glutamate Ionotropic Receptor Kainate Type Subunit 4	335-3p, 339-5p
Grin2a	Glutamate Ionotropic Receptor NMDA Type Subunit 2A	136-5p, 362-3p
Hspa12a	Heat Shock Protein Family A Member 12A	15a-5p, 339-5p
Hspb8	Heat Shock Protein Family B Member 8	193b-5p
Il11	Interleukin 11	None
Il13ra1	Interleukin 13 Receptor Subunit Alpha 1	155-5p
Il1r1	Interleukin 1 Receptor Type 1	135b-5p, 192-5p
Il1rn	Interleukin 1 Receptor Antagonist	None
Il23a	Interleukin 23 Subunit Alpha	None
Il2rg	Interleukin 2 Receptor Subunit Gamma	None
Junb	JunB Proto-Oncogene	155-5p, 3960
Lcn2	Lipocalin 2	None
Lrrc25	Leucine Rich Repeating Containing 25	None
Mapt	Microtubule Associated Protein Tau	136-5p
Nes	Nestin	155-5p
Nfat5	Nuclear Factor of Activated T Cells 5	30e-5p, 335-5p, 877-5p, 1a-3p, 106a-5p, 155-5p, 149-3p, 1249-5p, 1195, 362-3p, 744-5p
Npy2r	Neuropeptide Y Receptor Y2	19b-3p
Nrp1	Neuropilin 1	335-5p, 338-3p, 218-5p
Ogfrl1	Opioid Growth Factor Receptor Like 1	192-5p, 665
Pdcd2	Programmed Cell Death 2	None
Procr	Protein C Receptor	375
S100a4	S100 Calcium Binding Protein A4	None
S100b	S100 Calcium Binding Protein B	29a-3p, 29b-3p
Scg2	Secretoneurin	362-3p
Spp1	Osteopontin	335-5p, 340-5p
Tlr1	Toll Like Receptor 1	335-5p
Tlr7	Toll Like Receptor 7	186-3p
Tmbim1	Transmembrane BAX Inhibitor Motif Containing 1	362-3p
Tnf	Tumor Necrosis Factor	298-5p, 155, 223, 296-3p, 34a-5p
Uchl1	Ubiquitin C-Terminal Hydrolase L1	877-5p, 92a-3p, 218-5p

Table 5. Differentially expressed microRNAs (miRNA) associated with one or more hypoxic-ischemic brain injury (HIBI)-associated messenger RNAs (mRNA) *identified by literature search. The direction of differential expression for each group, relative to controls, at each time point (24 or 72 hours after injury) are designated by up (upregulation in HIBI versus controls) or down (downregulation in HIBI versus controls) arrows.*

	Differential Expression				
	Hypoxia		HIBI		
miRNA	24h	72h	24h	72h	Predicted mRNA Targets
miR-1a-3p	↑	↑		↓	Nfat5
miR-101a-3p		↑			Dusp1
miR-1195				↑	Eno2, Nfat5
miR-135b-5p	↑	↑			Il1r1
miR-140-5p	↑	↑			Adam9
miR-149-3p		↓			Nfat5
miR-15a-5p		↑			Hspa12a
miR-155-5p				↑	Anxa2, Il13ra1, Junb, Nes, Nfat5, Tnf
miR-19b-3p		↑			Npy2r
miR-193b-5p	↓	↓			Hspb8
miR-200c-3p	↓				Dusp1
miR-218-5p	↑	↑		↓	Anxa2, Clcf1, Ddx58, Eno2, Nrp1, Uchl1
miR-223-3p				↑	F3, Tnf
miR-23a-5p		↓		↑	Casp7
miR-29a-3p	↑	↑			Casp8, S100b
miR-29c-3p	↑	↑			Casp8, Fzd4
miR-296-3p		↓			Tnf
miR-298-5p		↓			Ddx58, Tnf
miR-30e-5p	↑	↑			Adam9, Adrb2, Csf1, Dap, Eno2, Nfat5
miR-335-5p	↑	↑	↑	↓	Csf1, Dap, Dusp5, F3, Gfap, Grik4, Nfat5, Nrp1, Spp1, Tlr1
miR-338-3p	↑	↑			Nrp1
miR-34a-5p	↑	↑			Anxa4, Bag3, Casp6, Casp7, Casp8, Cybb, Tnf
miR-340-5p	↑	↑		↓	Cyp1b1, Spp1
miR-362-3p		↑			Adam9, Atg10, Ctsl, Grin2a, Nfat5, Scg2, Tmbim1
miR-375-3p				↑	Ctsc, F3, Fzd4, Procr
miR-376b-5p	↑	↑			Casp8
miR-669d-5p		↑			Eno2
miR-744-5p		↓			Nfat5
miR-877-5p		↓			Nfat5, Uchl1
miR-93-3p	↑				Eno2

These analyses revealed that the pattern of 107 miRNAs differentially expressed at 24 hours strongly separated the three experimental groups (vertical dendrogram in Figure 9A), with the normoxia control group showing the most distinct separation. It is notable that the miRNA expression in the contralateral hemisphere was closer to the patterns seen in ipsilateral HIBI than to the normoxia controls at 24 hours. In contrast, at 72 hours (Figure 9B), the contralateral HIBI samples appeared to demonstrate recovery, showing an expression pattern with greater similarity to the miRNA profile in the normoxia controls. At 72 hours, a strong miRNA lesion signature started to emerge in the ipsilateral tissue, providing greater separation from the other two groups. Comparisons between the miRNA expression in the contralateral HIBI samples versus controls at 24 hours after injury are also shown in Figure 10. Between the contralateral HIBI and control groups, there were no miRNAs with significant differential expression at 72 hours after injury.

Summary

The results from this study provide a comprehensive assessment of the subacute brain miRNA expression changes at 24 and 72 hours after hypoxia or HIBI, resulting in several novel conclusions: 1) hypoxia alone results in significantly altered expression at both 24 and 72 hours of several miRNAs, many of which are hypoxamiRs; 2) HIBI resulted in considerable phase-specific expression, with few miRNAs demonstrating significant differential expression at both time points, and most of those demonstrating inverse differential expression at 24 hours compared to 72; and 3) at 24 hours, most miRNAs with significant differential expression had differential expression in HIBI similar in direction (positive or negative) to hypoxia, but at 72 hours HIBI miRNAs tended to have inverse

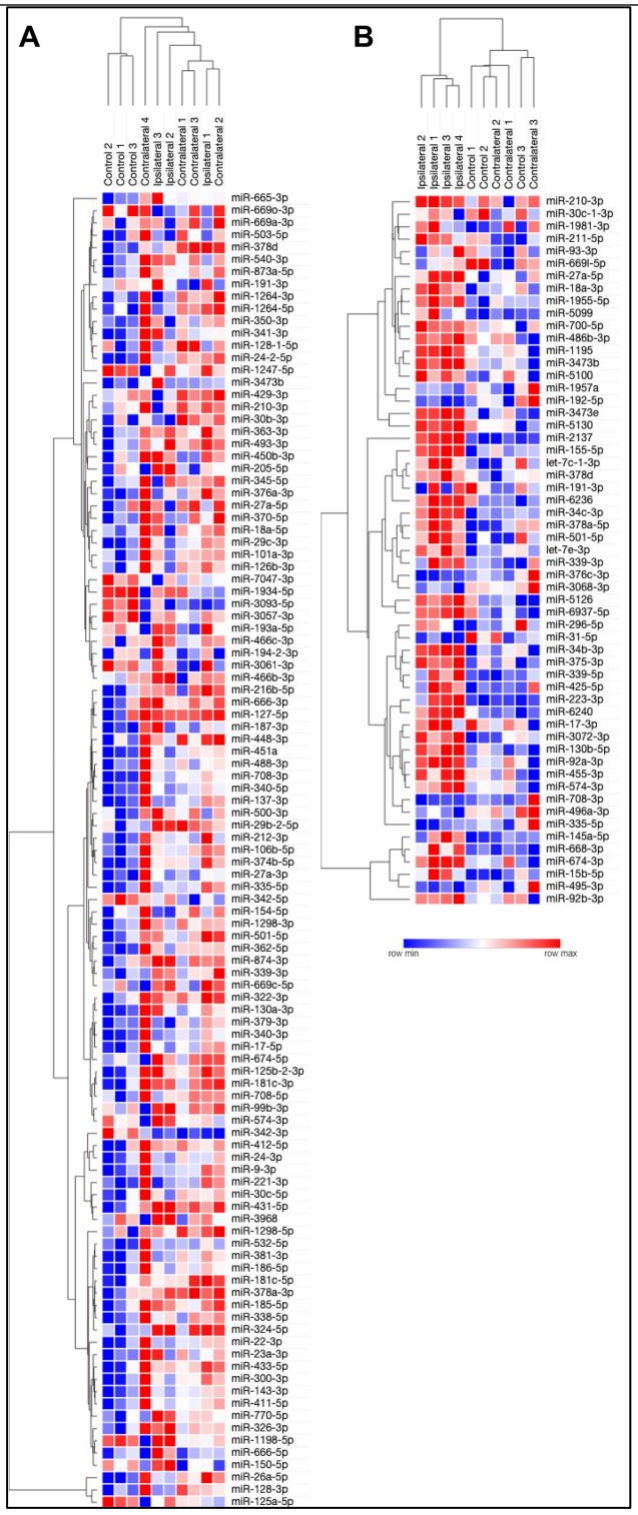

Figure 9. Two-way unsupervised clustering of differentially expressed microRNAs at 24 hours and 72 hours. *Rows represent microRNA species and columns represent samples. Each square represents an expression of a single microRNA species in a single sample, color-coded for magnitude of change relative to other samples in the comparison. The unsupervised clustering A) fully separated the control samples from the ipsilateral and contralateral hypoxic-ischemic brain injury (HIBI) samples at 24 hours and B) clearly separated out the ipsilateral HIBI samples from the control and contralateral HIBI samples at 72 hours after injury.*

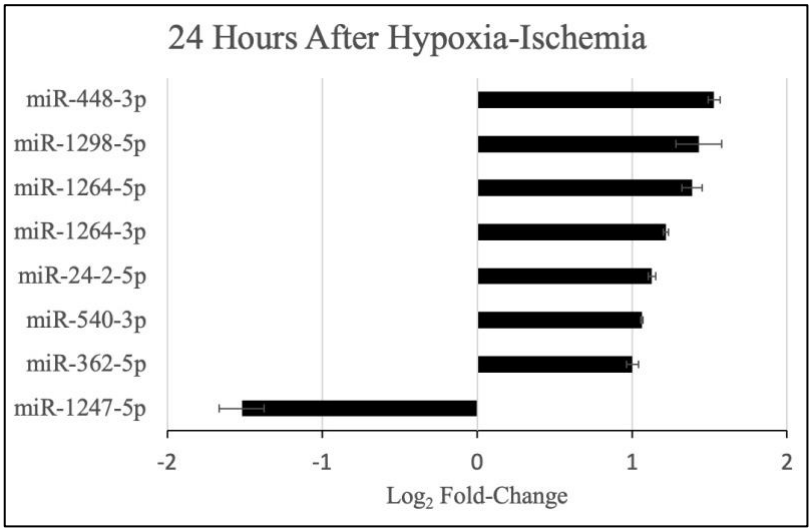

Figure 10. MicroRNAs with significant differential expression in contralateral hypoxic-ischemic brain injury (HIBI) compared to uninjured controls. *The microRNAs with significant differential expression (defined by log_2 fold-change > 1, p value and/or false discovery rate < 0.05, and average count per million reads > 10) at 24 hours after injury. No miRNAs demonstrated significant differential expression between these two groups at 72 hours.*

directionality to hypoxia. Lastly, based on the relationships between the miRNA expression in ipsilateral HIBI vs. contralateral HIBI vs. normoxia controls and found that the ipsilateral injured brain was more similar to controls than was the contralateral brain at 24 hours, though the contralateral brain became more similar to controls than ipsilateral brain by 72 hours.

This study's limitations included a modest sample size. Due to the exploratory and descriptive nature of the study, the minimal number of samples that would provide for valid statistical analyses were used for miRNA-Seq. In order to help overcome the lower sample size for miRNA-Seq, however, qPCR was performed as a validation for several of the key miRNAs. Due to the modest sample size, this study was unable to assess for differences in expression between sexes, which may affect miRNA expression (111). Additionally, given the descriptive methods, it was not possible to assess whether the alterations in miRNA expression that were demonstrated were harmful and part of the pathophysiology of the HIBI or were part of the endogenous cellular repair mechanisms. Lastly, this study

used whole brain samples so cannot delineate possible region-specific miRNA expression changes within the brain.

In conclusion, this study provides a global assessment of the subacute changes in brain miRNA expression after hypoxia or HIBI in mouse models of injury. This is the first study to include brain-specific miRNA sequencing as late as 72 hours after injury. As investigators continue to advance research into targeted miRNA-based interventions for neonatal HIBI, it will be very important to account for the multi-phasic expression patterns that were observed in this study to identify optimal timing for the individual interventions. One of the remaining gaps in knowledge relates to region-specific miRNA changes, which will be addressed in the next study.

CHAPTER 2: REGIONAL CHANGES IN MIRNA AND MRNA EXPRESSION AFTER NEONATAL HYPOXIC-ISCHEMIC BRAIN INJURY

Rationale

Although the study described in Chapter 1 provided for a description of the temporal changes in brain miRNA expression after neonatal HIBI and demonstrated several miRNAs with altered regulation in the brain as a whole, no studies to date have assessed brain region-specific miRNA changes after injury. The brain has been shown to have a unique baseline miRNA profile compared to other tissues, and each brain region also has a specific expression signature (112). These baseline differences may result in significantly different regional miRNA responses in disease processes, such as neonatal HIBI, that tend to preferentially affect certain regions of the brain more than others.

Although all regions of the brain are exposed to the systemic hypoxia that is introduced in the unilateral carotid artery ligation HIBI model, the reduction in blood flow resulting in the ischemic injury does not affect all brain regions equally. In one of the initial descriptions of this model by Dr. Vannucci, he described the most significant reductions in regional blood flow as occurring in the striatum and thalamus (2-3 times the reduction seen in areas such as the subcortical white matter), which correlated closely with the distribution and extent of ischemic neuronal necrosis that was primarily seen in the striatum, thalamus, and posterior cortical regions (113). At the same time, Dr. Vannucci's group noted no change or increased blood flow to the cerebellum and brainstem after HIBI in this model, consistent with an injury produced by occluding only the anterior cerebral circulation (carotid artery).

Based on this knowledge of this variable blood flow distribution and injury, the goal of this study was to evaluate the brain region-specific miRNA changes after neonatal HIBI in the mouse model. The primary regions of interest were chosen from the literature described above, and were the cortex, striatum/thalamus, and cerebellum. As described in the introduction, most clinical and pre-clinical studies of miRNA profiling after neonatal HIBI have assessed levels within the first hour after injury (21, 22). All of the human studies were obtained immediately after delivery (i.e. cord blood) but the previous piglet models demonstrated peak dysregulation of many miRNAs at one hour after injury. As such, to allow for comparison with the previous clinical studies (of cord blood at 0 minutes after injury) but also ensure time for miRNA dysregulation to occur (peak at 60 minutes after injury), the region-specific miRNA levels assessed in this study were all obtained at 30 minutes after injury.

Regional Brain miRNA Changes 30 Minutes After Injury

Figure 11 demonstrates the miRNAs with significant differential expression after neonatal HIBI compared to controls in each region. There were 39 miRNAs that were differentially expressed in the cerebellum (16 upregulated; 23 downregulated), 12 in the striatum/thalamus (11 upregulated; 1 downregulated), and 21 in the cortex (18 upregulated; 3 downregulated).

In all, 61 unique miRNAs demonstrated significant differential expression in one or more region studied (Figure 12A); nine of which had significant differential expression in more than one region. Of those miRNAs affected in multiple regions, miR-410-5p, -1264-3p, 1298-5p, -5126, and -34b-3p all had inverse differential expression in the cortex and striatum/thalamus compared to the cerebellum, potentially suggesting specificity for ischemia given that the cerebellum undergoes hypoxia but not ischemia in this model.

MiR-6240, -3963, 3473a, and -3473b all had differential expression in the same direction for the three regions, suggesting that they may be primarily affected by the hypoxic insult

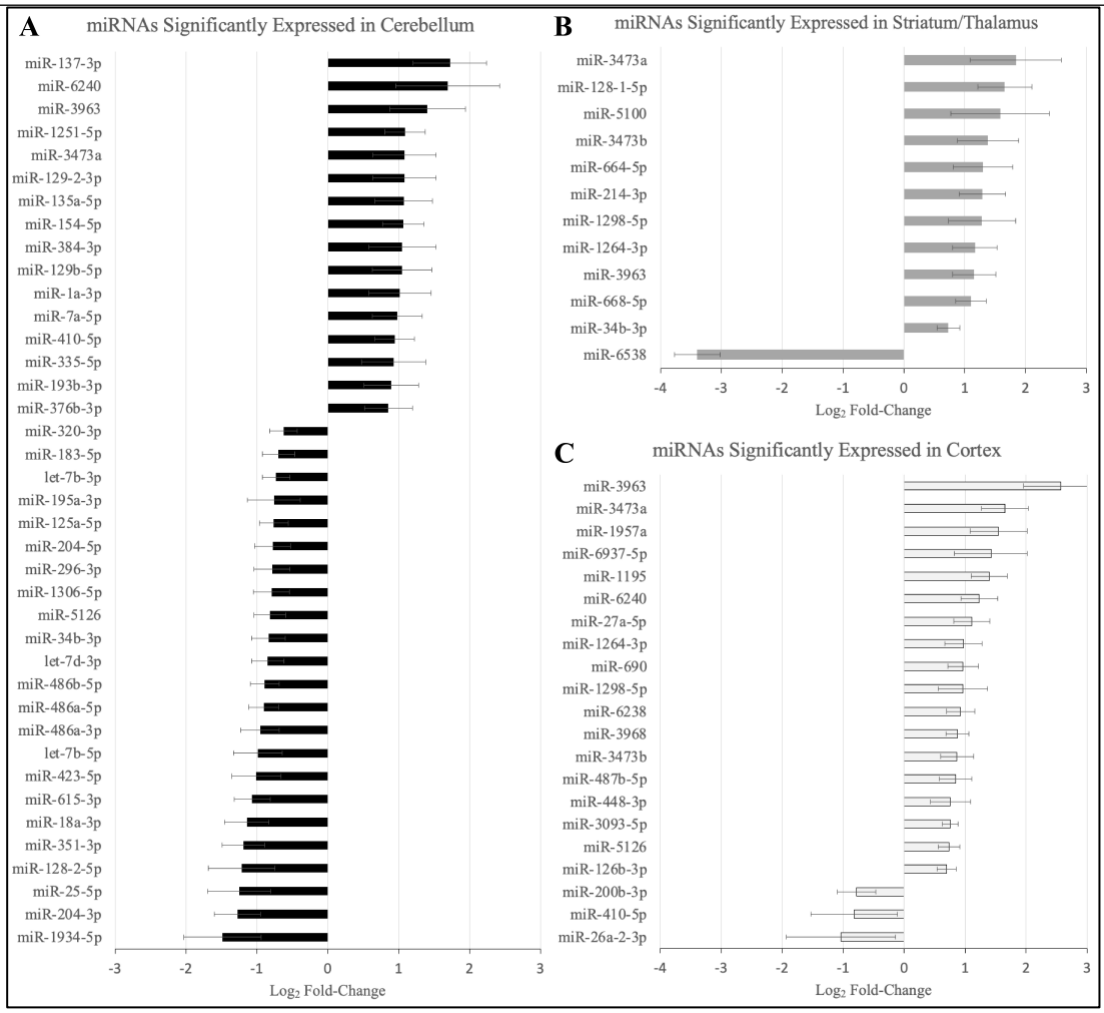

Figure 11. MicroRNAs with significant differential expression at 30 minutes after hypoxic-ischemic brain injury *in the A) cerebellum, B) striatum/thalamus, and C) cortex. Significance defined by fold-change > 1.5, p value and/or false discovery rate < 0.05, and average count per million reads > 10.*

(Figure 12B). The differentiation between cerebellar miRNA signaling and that of the cortex, striatum, and thalamus was confirmed by two-way unsupervised clustering (Figure 12C) demonstrating a clear separation of three of the four cerebellum samples from those of the other two regions.

Lastly, assessment of the canonical pathways that are predicted to be affected by the miRNAs that were upregulated at 30 minutes after HIBI was performed by KEGG pathway

analysis (Figure 12D). The KEGG analysis demonstrated that the miRNAs with altered regulation in this study primarily alter metabolic pathways, including that of fatty acid metabolism and biosynthesis, lysine metabolism, steroid biosynthesis, AMPK signaling, and sphingolipid metabolism. Many of the traditional hypoxia and cell death pathways, including mammalian target of rapamycin (mTOR), MAPK, and HIF1 were also included in the KEGG analysis, but were lower in significance.

Regional Brain mRNA Changes 30 Minutes After Injury

In order to further evaluate the effects of miRNA alterations on mRNA levels in the early period after HIBI, mRNA levels were also assessed at 30 minutes after injury using the Nanostring Neuroinflammation Panel. Figure 13 shows the 44 mRNAs that were differentially expressed in at least one region; 16 demonstrating significant differential expression in two or more regions (Figure 13A). Of note, all mRNAs that had significant differential expression demonstrated increased expression after HIBI relative to controls (Figure 13B). Only a few mRNAs in the figure showed downregulation in any of the three regions (for instance, Eomes in the cerebellum and cortex); however, in each case this downregulation did not reach statistical significance.

KEGG mRNA pathway analysis demonstrated that the mRNAs that are upregulated at 30 minutes after HIBI are largely involved in inflammatory and cell death pathways, including interleukin (IL-3, -8, -10, -17A), TNF receptor, HIF1α, and PI3K signaling (Figure 13C). For the mRNA KEGG analysis, 335 pathways were identified as significant; the top 50 were included in the figure.

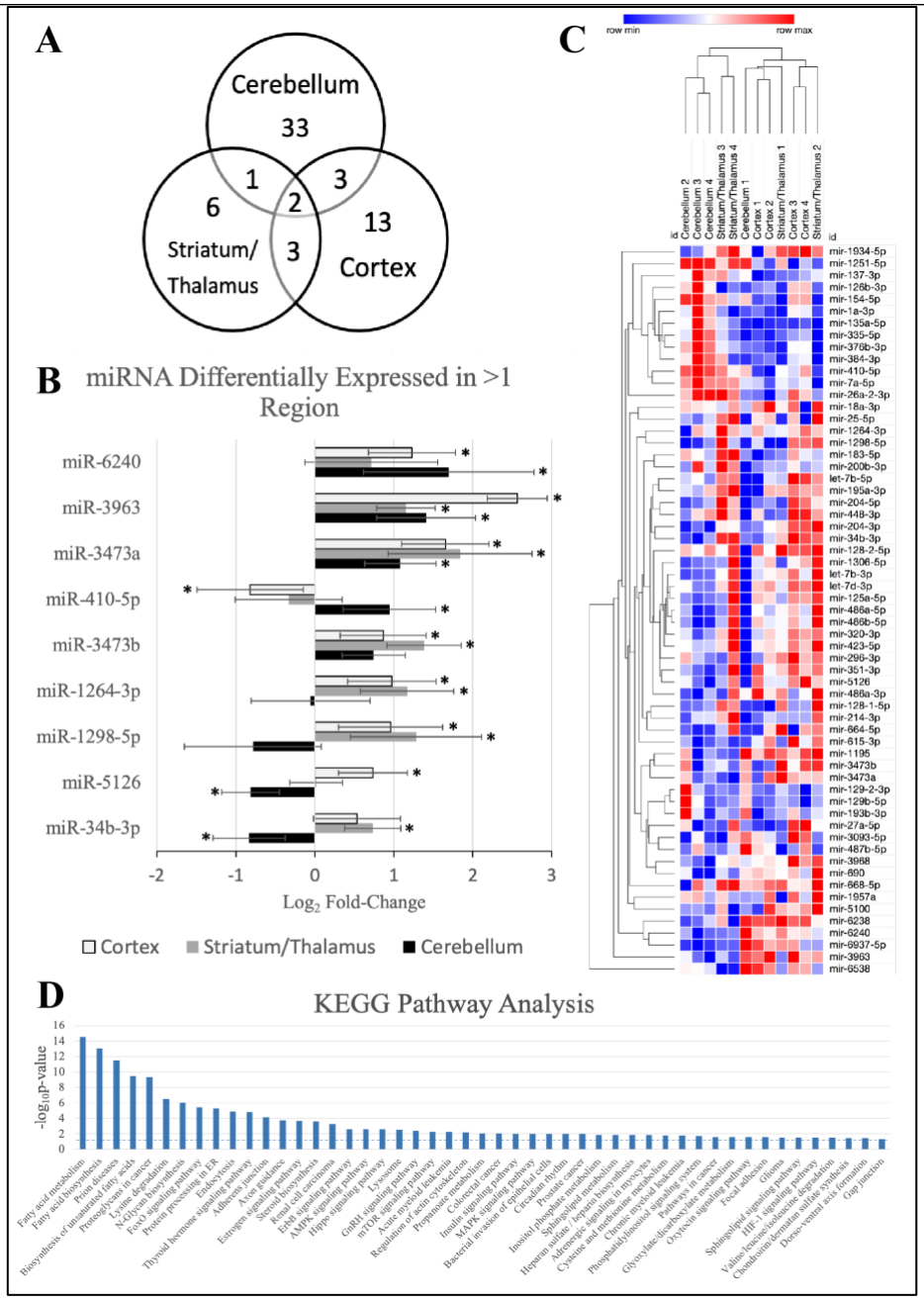

Figure 12. MicroRNAs (miRNA) with significant differential expression in more than one region. *A) Venn diagram demonstrating the number of miRNAs with significant differential expression and the overlap between each region; B) differential expression of the nine miRNAs with significant differential expression in more than one region (*regional expression significant, as defined by fold-change > 1.5, p value < 0.05, and average count per million reads > 10); C) two-way unsupervised clustering of differentially expressed microRNAs demonstrating separation of the majority of the cerebellum samples from the cortex and striatum/thalamus samples. Rows represent microRNA species and columns represent samples. Each square represents expression in a single sample, color-coded for magnitude of change relative to controls; and D) KEGG pathway analysis of the miRNAs with significant differential expression.*

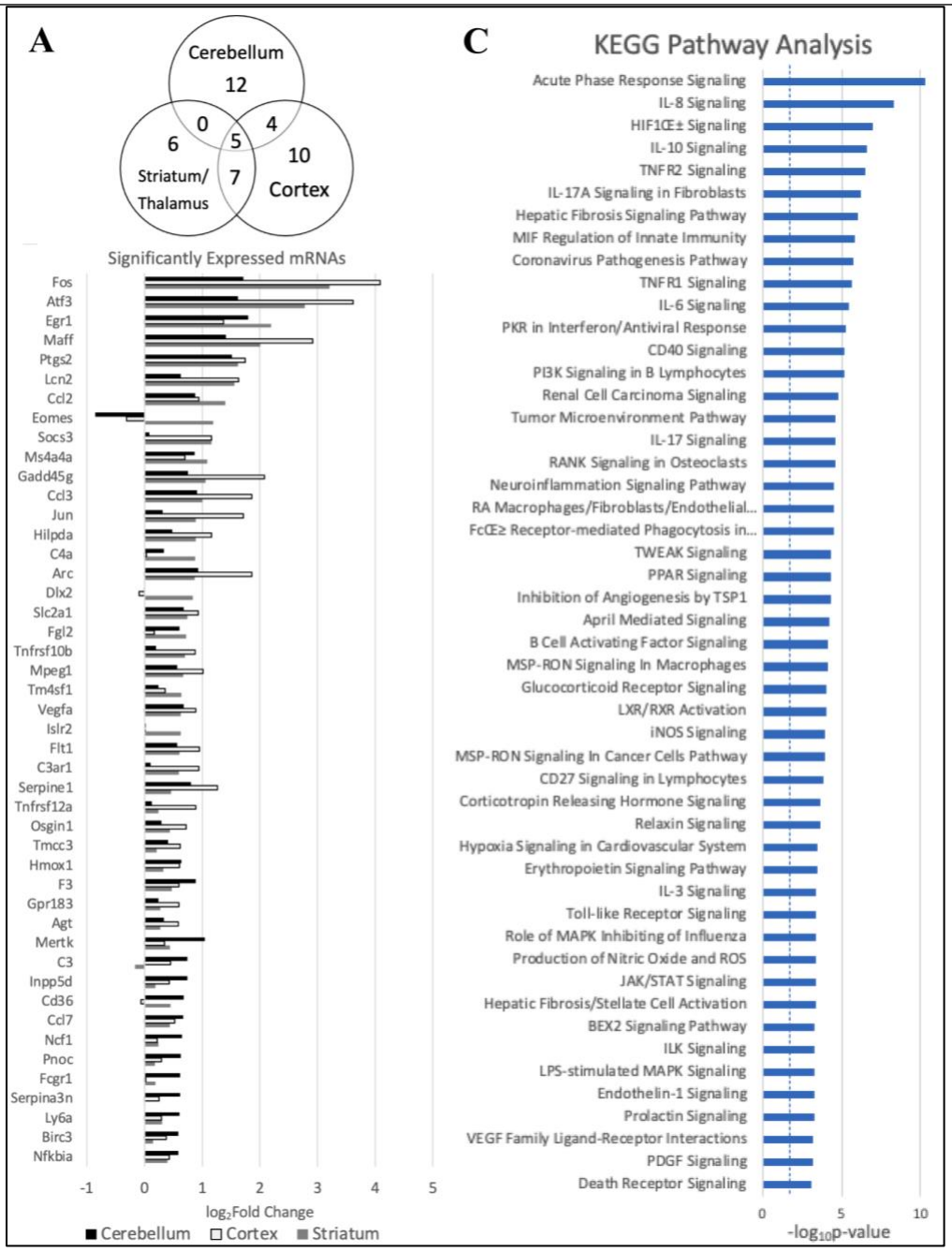

Figure 13. Messenger RNAs (mRNA) with significant differential expression in more than one region. *A) Venn diagram demonstrating the number of mRNAs with significant differential expression and the overlap between each region; B) differential expression of the mRNAs with significant differential expression in at least one region (significance defined by fold-change > 1.5 and p value and/or false discovery rate < 0.05); and C) KEGG analysis demonstrating the canonical pathways affected by all of the mRNAs demonstrating significant differential expression.*

mRNA-mRNA Networks

Figure 14 demonstrates the mRNA-mRNA network connections between those mRNAs with significant differential expression 30 minutes after HIBI and up to two degrees of connection with the other mRNAs analyzed in this study. The differentially regulated genes that were consistently demonstrated to be highly integrated into all three regional networks included Atf3, Fos, Arc, Jun, and Tlr.

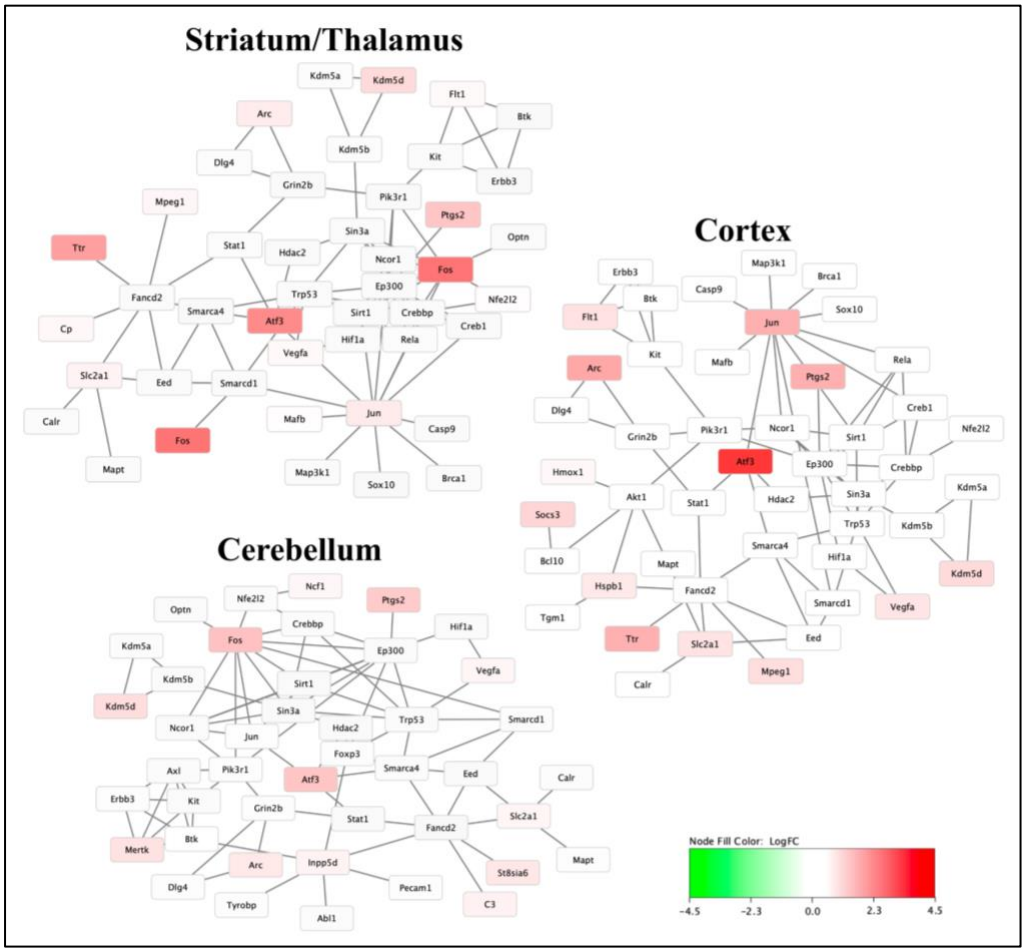

Figure 14. Messenger RNA (mRNA) networks in each region *representing the mRNA with significant differential expression after hypoxic-ischemic brain injury versus controls and two degrees of connection between those mRNA and the other mRNA analyzed in this study. Not shown are any mRNAs with no, or only one, connection. Node fill color relates to the log fold change of mRNA in hypoxic-ischemic brain injury compared to controls.*

Networks of miRNA-mRNA Interactions

Two miRNA species that were significantly differentially expressed in the cortex were closely associated with mRNAs that were also found to have significant differential expression: miR-1195 and -690 (Figure 15). MiR-1195 was associated with Tnfsf10b and miR-690 with Egr1. There were no significant miRNA-mRNA networks in either the striatum/thalamus or the cerebellum.

qPCR Validation of Nanostring Analyses

For validation of high-throughput mRNA data, qPCR was performed on each of the samples for seven of the mRNAs with significant differential expression. Figure 16 shows very strong correlation (R^2=0.894) between the Nanostring values and the qPCR values for all three regions and all seven mRNA species.

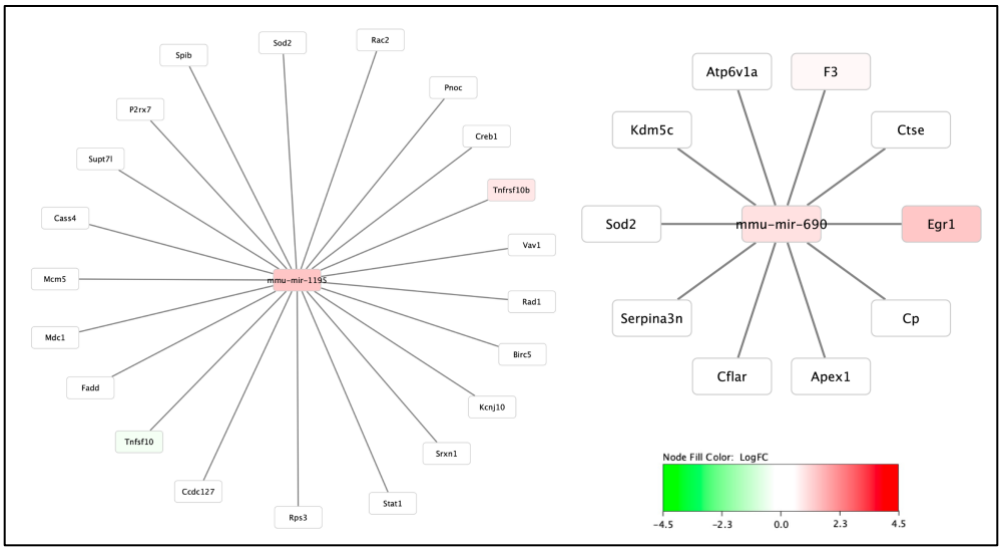

Figure 15. MicroRNA to messenger RNA (miRNA-mRNA) networks in the cortex. *The only two miRNAs that demonstrated significant differential expression at 30 minutes and were closely linked to mRNAs also significantly altered at 30 minutes after injury were miR-1195 and -690. Neither the striatum/thalamus nor cerebellum expression data resulted in significant miRNA-mRNA networks*

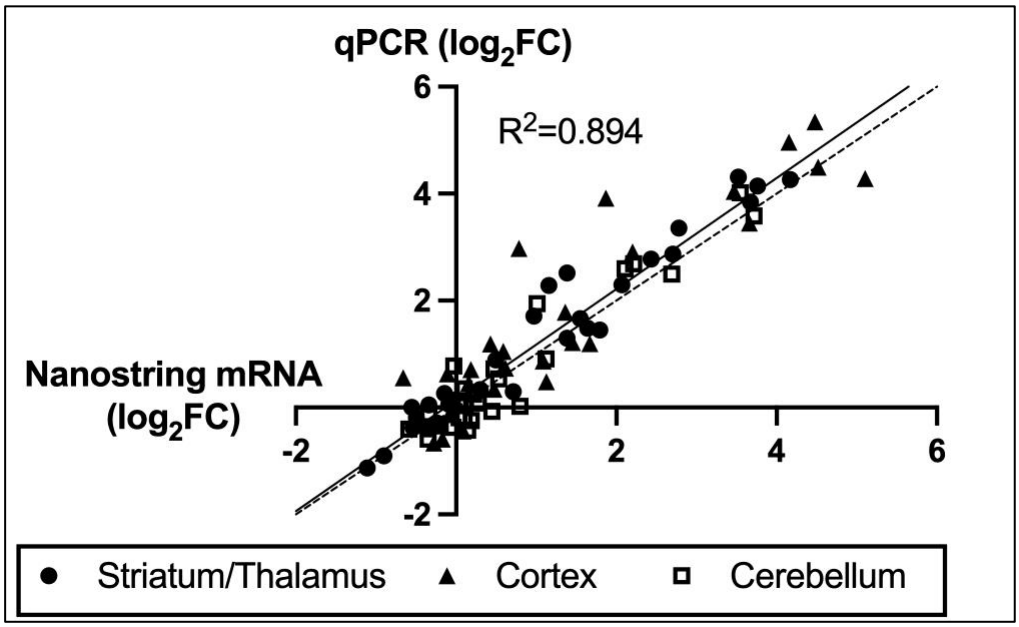

Figure 16. Correlation between Nanostring RNA sequencing and quantitative polymerase chain reaction (qPCR) validation *of seven highly expressed mRNAs. The x-axis values are Nanostring log_2 fold-change (hypoxic-ischemic brain injury versus control) values and y-axis are qPCR ΔΔCt log_2FC values. The solid line represents the best-fit regression of the data points with strong correlation (R^2=0.894) and the dashed line represents the ideal correlation line (x=y).*

Summary

This study represents the first brain region-specific profiling of miRNA expression after neonatal HIBI, finding 61 unique miRNAs with significant differential expression in at least one of the three regions studied. Additionally, Nanostring mRNA panel analyses were performed in order to attempt to link the miRNA changes that were seen to alterations in relevant mRNA pathways. Only two miRNAs were found to have direct pathway links to the mRNAs with significant differential expression, underscoring the differences in pathway targeting that were seen between the mRNAs and miRNAs. While the altered mRNAs were mostly made up of immediate early genes (IEG) such as Fos, Jun, and Arc that were associated with downstream inflammatory and apoptotic pathways on KEGG analysis, the miRNAs that demonstrated significant differential expression were mostly associated with pathways of metabolism and synthesis. Although any conclusions

regarding pathway analyses must take into consideration the somewhat limited scope of the mRNA analyses (using a specific panel rather than whole genome analyses), these data suggest differing roles of mRNAs versus miRNAs in the first 30 minutes after neonatal hypoxic-ischemic brain injury.

Additionally, in the previous study (Chapter 1), we demonstrated that the contralateral brain has limited utility as an “internal control” for miRNA studies in this model. The cerebellum in this study, however, demonstrated a unique miRNA profile from either of the other two regions (Figure 12C). This difference could potentially be caused by maturational differences between cerebellar and that of the rest of the brain (114), but is likely due at least in part to its sparing from the ischemic injury induced by the carotid artery ligation (113). Although this study only assessed the miRNA profiles at 30 minutes after injury, the findings here would suggest that the cerebellum may act as an adequate internal control at least in the first hour after injury.

There are a few limitations to this study that warrant discussion. They include a lack of a hypoxia-only control group. Though it may be reasonable to consider the cerebellum group as a hypoxia-only group, in comparing the cortex and striatum/thalamus data to the cerebellum it is not possible to separate whether differences are related to the inter-region differences or due to differences between hypoxia only and HIBI. Additionally, the mRNA analyses in this study were limited to only those mRNAs included in the Nanostring Neuroinflammation panel. Although this panel contains 770 genes relevant to neuroinflammation and brain injury, the network analyses performed were restricted to only those genes in the panel. Lastly, we were unable to study individual hippocampal sections due to low RNA yield. Future studies assessing hippocampal RNA signaling in this model could consider pooling samples.

In conclusion, this study demonstrated that miRNA expression varies by brain region after neonatal HIBI, and that the cerebellar miRNA profile is clearly distinct from those of the striatum/thalamus and cortex. Although miRNA-mRNA interactions may play more significant roles outside of the immediate period after HIBI, most of the mRNA with significant differential expression in this study were IEGs associated with downstream inflammatory and cell death pathways that were mostly distinct from the miRNA-targeted metabolic pathways. Future studies assessing brain miRNA expression to guide therapy development should consider evaluating individual brain regions rather than whole brain to ensure the sensitivity needed for targeted therapies.

CHAPTER 3: MIRNA CONTENT OF NEUROPROTECTIVE HYPOXIA-PRECONDITIONED EXTRACELLULAR VESICLES

Rationale

MSC transplantation has been shown to be a feasible and effective therapy for neonatal hypoxic ischemic brain injury in animal models (115). Significant concerns about the short- and long-term safety of MSC transplantation in this population remain, however, including associated risks of immunogenicity, proliferation, embolus formation, and malignant transformation (115-117). It is now widely believed that the stem cells elicit their therapeutic effects through paracrine signaling by several mechanisms including stem cell-secreted EVs that act as carriers to deliver protein, RNA, and miRNA contents to injured tissue (118-121). As such, EVs have recently been evaluated as potential therapy, with several studies demonstrating neuroregenerative potential and decreased brain injury following hypoxia-ischemia (115, 121), even when compared to therapy with MSCs (122). Additionally, EVs have not been associated with the same immunological or neoplastic risks as cell transplantation.

EVs are believed to be tissue-specific, and brain cells such as neurons and oligodendrocytes demonstrate preferential uptake of EVs derived from other neurons or microglia, respectively (121, 122). Given this potential for preferential uptake, EVs derived from NSCs and other brain-derived cells may provide increased specificity and more efficient targeting of the injured cellular environment than EVs derived from MSCs or other non-brain cells. Recent evidence supports that NSC-EVs exhibit more potent therapeutic potential than MSC-derived EVs in regenerative outcomes following thromboembolic stroke (118). In addition, most of the studies of MSC- and NSC-derived EVs have utilized naïve cultured cells grown in physiological conditions. It has been shown that the contents

of EVs are altered in response to hypoxia and brain injury (123, 124), however, and this EV conditioning in response to injury may allow for their contents to be altered in a manner that allows for even more specific targeting to hypoxia-ischemia injured brain tissue.

This study seeks to evaluate the effects of intranasal (IN) administration of naïve NSC-EVs on a mouse model of neonatal hypoxic-ischemic brain injury. Previous studies have demonstrated successful brain uptake of intranasally-administered EVs, with wide anatomic distribution (125), including neurons and microglia in the forebrain (126), hippocampus (127), and cortex (128). The neuroprotective effects of these naïve EVs will be compared to those of EVs derived from mouse brain tissue that has been preconditioned with hypoxia to potentially stimulate EVs with contents more specific to the hypoxic-ischemic brain. Understanding the comparative neuroprotective effects of NSC-EVs and brain-derived EVs following HIBI will allow for more targeted EV-based therapies in the future with the goal of improved lifelong outcomes for neonates with HIE.

Confirmation of Extracellular Vesicle Characteristics

All EVs underwent standard characterization to confirm EV features were present. Both the NSC-EVs and brain-EVs were positive for the EV marker CD9 and negative for calnexin (Figure 17A&B). EM demonstrated classic cup-shaped EV morphology (Figure 17C). Nanoparticle tracking analysis of the undiluted EV suspensions showed a concentration of $8.42 \times 10^{9} \pm 3.28 \times 10^{8}$ particles/mL of NSC-EVs and $1.27 \times 10^{13} \pm 8.65 \times 10^{11}$ particles/mL of brain-EVs. Both EV populations were primarily 80-300 nm in size with peaks between 152 and 208 nm (Figure 17D).

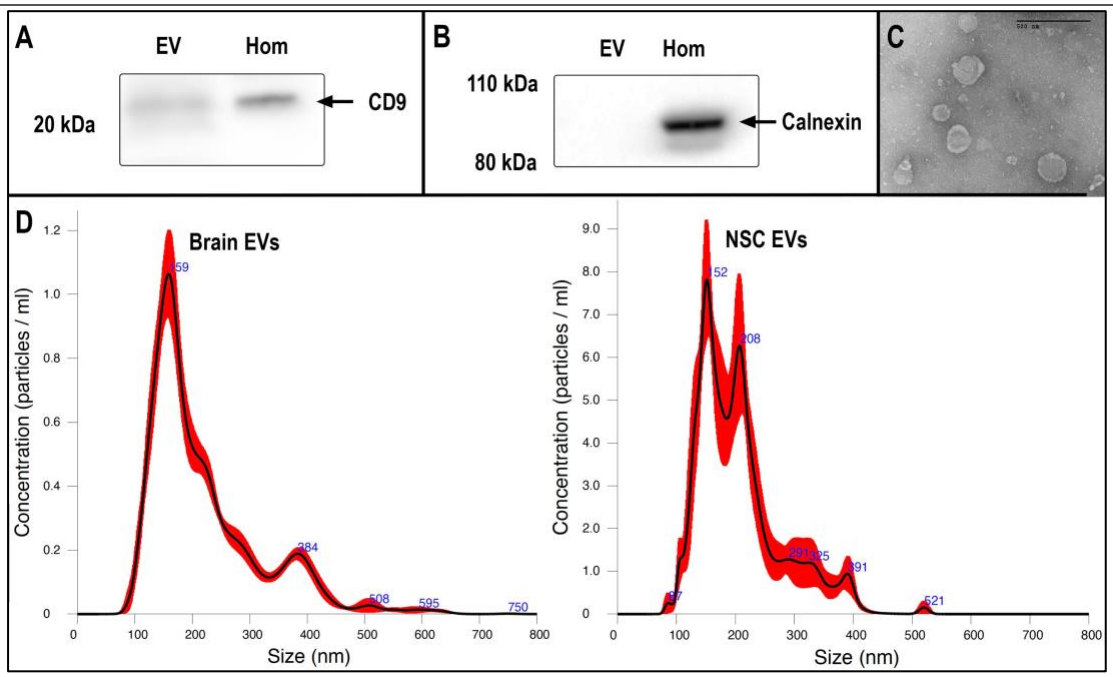

Figure 17. Confirmation of extracellular vesicle (EV) characteristics *by western blot of EVs and whole brain homogenate (Hom) as a positive control for A) the EV marker CD9 and B) the EV negative control calnexin; C) Electron microscopy demonstrating intact cup-shaped EVs; and D) nanoparticle tracking analysis of EV size distribution for both brain-derived and neural stem cell-derived (NSC) EVs.*

Infarct Size Comparison

TTC staining of coronal brain sections at the level of the optic chiasm demonstrated significantly more ipsilateral viable tissue between the HIBI + PBS group and the HIBI + brain-EV group (mean 28% and 72%, respectively, p=0.004) (Figure 18). The HIBI + NSC-EV group also demonstrated increased viable tissue, but this did not reach statistical significance (p=0.052).

Apoptosis as Measured by Caspase Signal and TUNEL Staining

Relative quantities of the apoptotic protein caspase-3 and its cleaved version were detected by western blot (Figure 19). No differences were seen between the HIBI + PBS group and the HIBI + NSC-EV group in either the cleaved form (p=0.372) or intact form of

caspase-3 (p=0.999). The brain-EV group, however, had significantly less cleaved caspase-3 (p=0.015) and a non-significant trend toward less intact caspase-3 (p=0.026).

TUNEL staining of the ipsilateral striatum demonstrated a non-significant decrease in the percent of TUNEL+ cells in both the NSC EV and brain EV groups versus the HIBI group (Figure 20A&C). This trend was similar when assessing both the combined ipsilateral striatum and cortex regions (Figure 20B).

miRNA Measurement of Hypoxia-Preconditioned Extracellular Vesicles

Next generation miRNA sequencing was performed on four samples of hypoxia-conditioned brain EVs. Twenty-four miRNA species were detected, with six of the species detectable in all four samples (Figure 21A). Of the miRNAs that were detectable in at least two of the four samples, miR-342-3p, -125a-5p, -330-3p, -128-2-5p, and -182-5p have all been shown to be altered in the first 24 hours after neonatal HIBI in animal models (including the studies described above in Chapters 1 and 2) (22, 38, 129). Additionally, miR-92b-3p, -328-3p, and -342-3p were each shown to have altered expression in umbilical cord blood of infants diagnosed with HIE (21, 22).

To assess whether the miRNA contents could be related to the anti-apoptotic effects seen with brain-EV administration, a KEGG pathway analysis was performed for the miRNAs expressed in the brain-EVs (Figure 21B). The significantly associated pathways included several anti-apoptotic pathways such as forkhead box O (FoxO), Hippo, transforming growth factor (TGF)-β, MAPK, and HIF1 signaling, as well as the caspase-3-related cGMP-dependent protein kinase G (cGMP-PKG) signaling pathway.

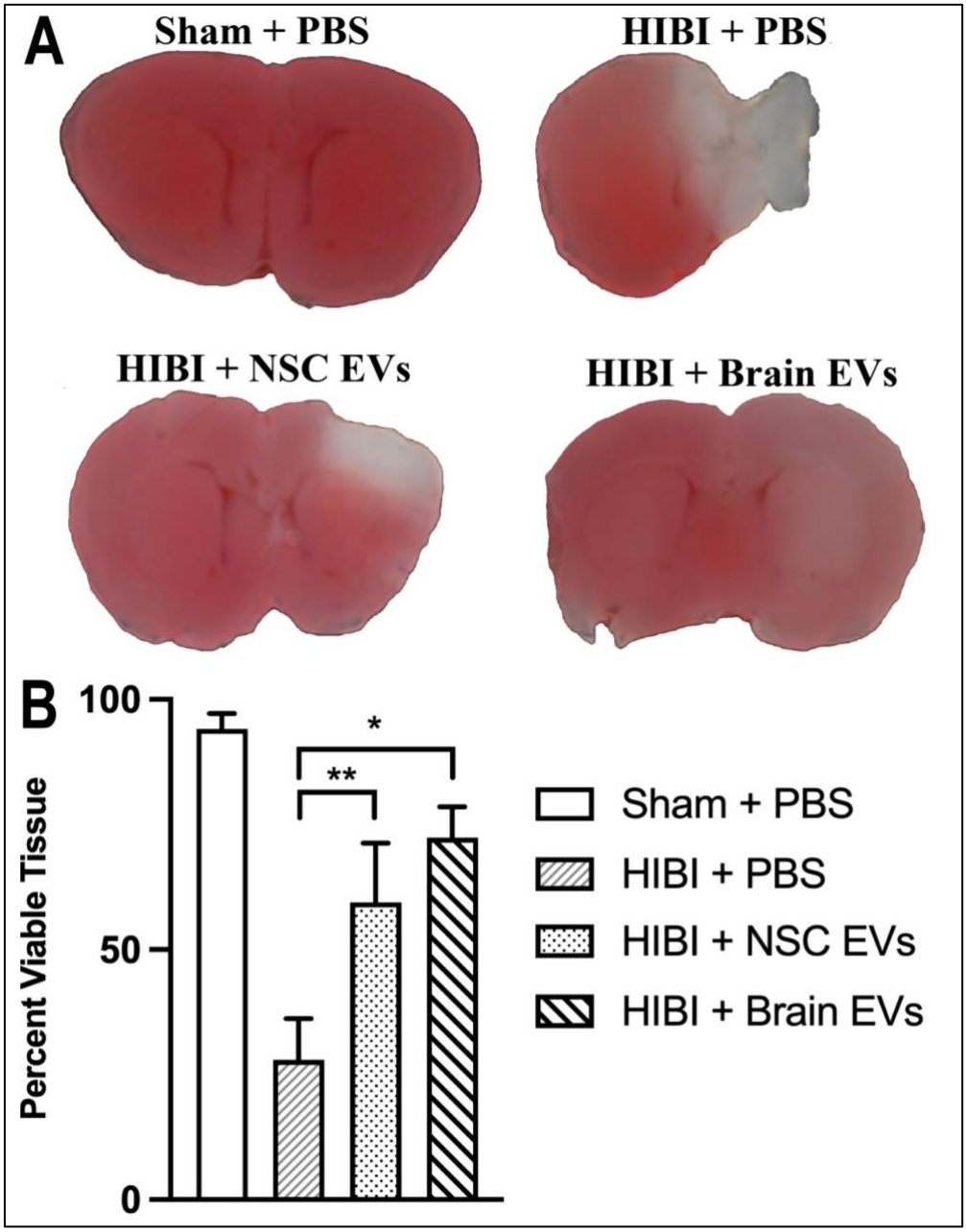

Figure 18. Measurement of relative tissue infarct area, *using A) representative 2,3,5-triphenyltetrazolium chloride (TTC) staining of coronal brain tissue sections in each intranasal treatment group, demonstrating viable tissue (pink) and infarcted area (white) in order to calculate B) the percent viable tissue in the ipsilateral hemisphere, calculated as area of viable tissue on ipsilateral side divided by area of viable tissue on contralateral side. *p=0.004; **p=0.052 EV, extracellular vesicles; HIBI, hypoxic-ischemic brain injury; NSC, neural stem cell; PBS, phosphate-buffered saline*

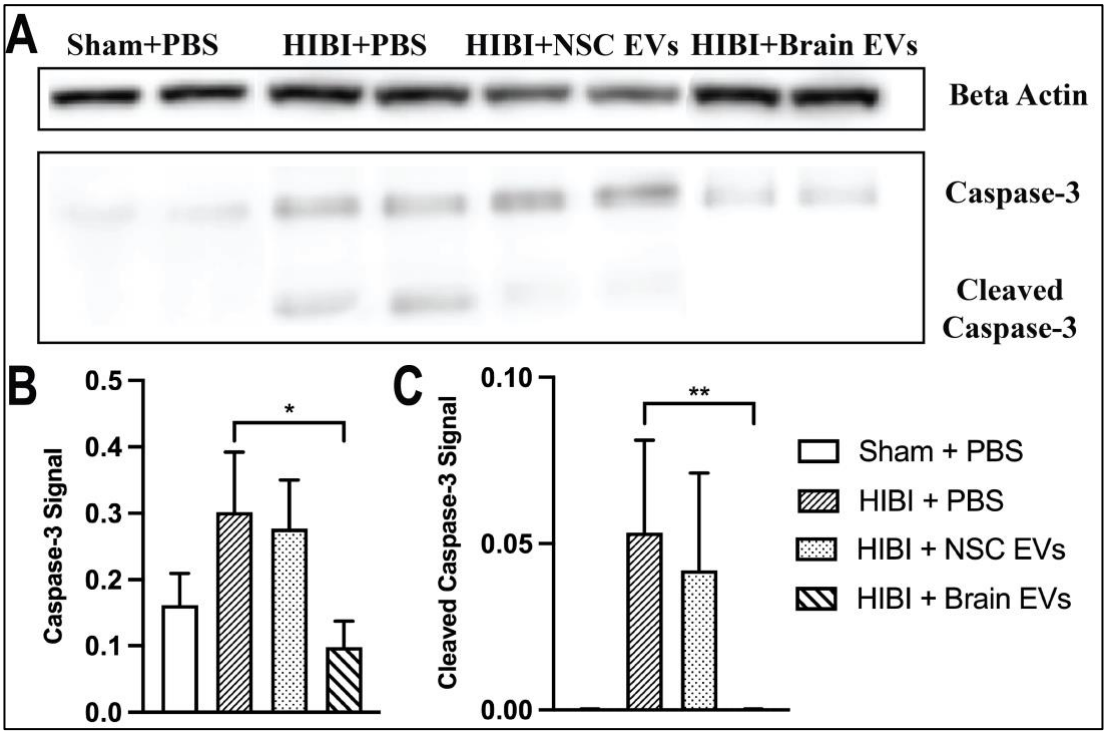

Figure 19. Signal ratio of caspase-3 and cleaved caspase-3 to β-actin control. *A) Representative images of western blots demonstrating B) a non-significant trend toward increased caspase-3 and C) significantly increased cleaved caspase-3 signal in the hypoxic-ischemic brain injury (HIBI) + hypoxia-preconditioned brain extracellular vesicles (EVs) compared to HIBI + phosphate-buffered saline (PBS). *p=0.026; **p=0.015 NSC, neural stem cell*

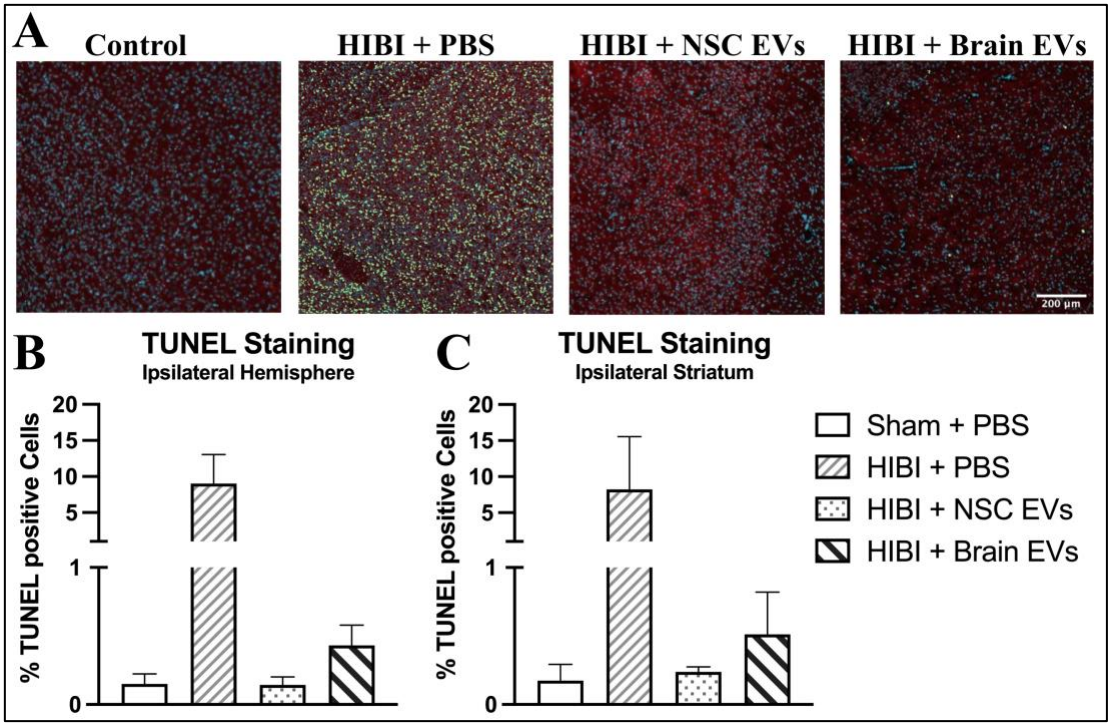

Figure 20. Terminal deoxynucleotidyl transferase dUTP nick end labeling (TUNEL) staining for apoptotic cells between treatment groups obtained in sections ~3.5 mm posterior to the rostral brain edge. *A) Representative images of the striatum with green TUNEL+ cells and blue DAPI TUNEL- cells; B) Analysis of the entire ipsilateral hemisphere, with the percent of cells positive for TUNEL stain versus DAPI positive cells; and C) analysis of only the ipsilateral striatum. HIBI, hypoxic-ischemic brain injury; PBS, phosphate-buffered saline; EV, extracellular vesicles; NSC, neural stem cell*

A

miRNA	Median (min-max) CPM
miR-92b-3p*	241,259 (116,352-306,977)
miR-541-5p	223,339 (162,791-298,742)
miR-434-3p	181,085 (146,530-229,560)
miR-328-3p*	144,525 (122,963-202,326)
miR-342-3p*†	77,463 (55,814-107,969)
miR-361-3p	56,524 (44,025-106,977)
miR-370-3p	14,710 (0-34,706)
miR-125a-5p†	7,560 (0-11,628)
miR-330-3p†	4,444 (0-15,723)
miR-329-3p	1,928 (0-7,404)
miR-148b-3p	1,904 (0-3,145)
miR-128-2-5p†	1,572 (0-24,422)
miR-182-5p†	1,163 (0-3,145)
miR-365-3p	0 (0-18,868)
miR-181a-5p†	0 (0-15,723)
miR-668-3p	0 (0-8,997)
miR-935	0 (0-8,997)
miR-667-5p	0 (0-8,889)
miR-6240†	0 (0-7,407)
miR-532-3p*	0 (0-6,289)
miR-340-3p	0 (0-3,145)
miR-351-5p	0 (0-2,963)
miR-130b-3p	0 (0-1,285)
miR-221-5p	0 (0-1,285)

B

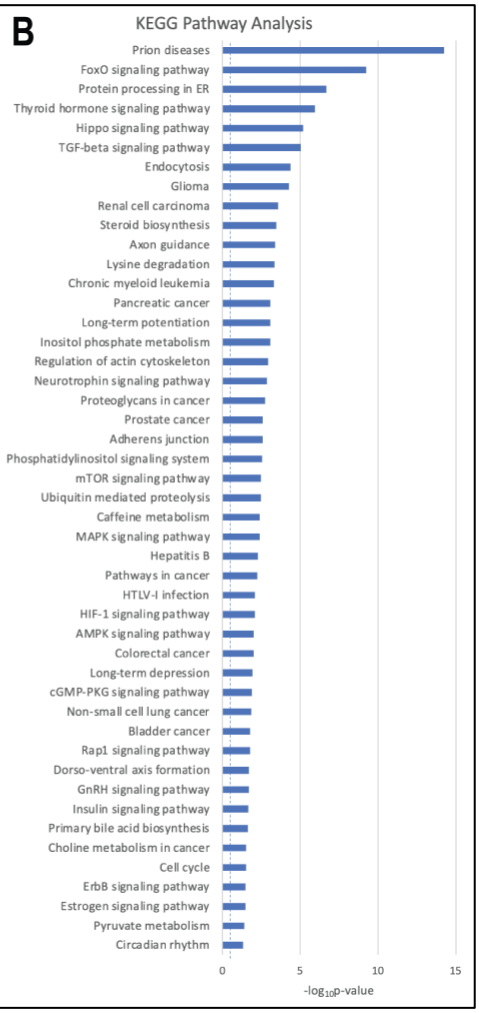

Figure 21. MicroRNAs (miRNA) expressed in hypoxia-preconditioned extracellular vesicles (EV)*. A) List of miRNAs sorted by relative counts and described as median (min-max) count per million (CPM) reads in each sample; and B) KEGG pathway analysis of the miRNAs that were detectable in the hypoxia preconditioned brain-derived EVs. *MiRNA that has been previously demonstrated to be altered after neonatal HIBI in one or more human study †MiRNA that has been previously demonstrated to be altered after HIBI in one or more animal study, including the current studies.*

Summary

These data suggest that treatment with intranasal extracellular vesicles (EVs) may confer neuroprotection following neonatal HIBI. Although IN administration of naïve NSC-derived EVs resulted in non-significant decreases in infarct size and caspase-3 levels, treatment with hypoxia-preconditioned brain-EVs resulted in a marked increase in ipsilateral viable tissue and decrease in cellular apoptosis after HBI. Some of the neuroprotective benefits of the brain-EVs may be related to their miRNA contents, many of which are involved in apoptotic pathways. These results demonstrate not only the therapeutic potential of pre-conditioned EVs but also that the EV contents may play a role in their neuroprotective effects.

This study primarily assessed apoptosis through the evaluation of the apoptotic marker caspase-3. However, the generation of free radicals and inflammation through the expression and activation of pro-inflammatory cytokines are also involved in the pathogenesis of HI brain injury (130-133). MSCs and NSCs have both shown inhibitory effects on mediators of inflammation and oxidative stress (134, 135). Although neuroapoptosis was the primary focus of this study, future studies assessing the effects of EV administration could assess other potential drivers of the neruoregenerative effects. An additional limitation to the current study was the lack of dose response assessment, as only a single dose level of EVs (given in two separate administrations) was used in this study. Moving forward, a dose-escalation study would be beneficial to optimize dosing and maximize regenerative potential.

Currently, therapeutic intervention for HIE in neonates is restricted to hypothermia, which provides limited effect. The results from this study demonstrated regenerative potential of EVs, particularly hypoxia-preconditioned brain-derived EVs. Further analyses of the contents of hypoxia-preconditioned EVs could allow for engineering of EVs with

optimal miRNA, RNA, and protein content to provide for a targeted cell-free therapy that could potentially improve the neurodevelopmental outcomes in infants diagnosed with HIE.

DISCUSSION

Overall, the studies described above provide a comprehensive analysis of the spatial and temporal endogenous brain miRNA signaling after neonatal HIBI as well as identifying miRNAs included in the neuroprotective hypoxia preconditioned EVs.

Chapter 1 provided a comprehensive assessment of the subacute brain miRNA expression changes at 24 and 72 hours after hypoxia or HIBI, including the identification of 16 miRNAs that had significant differential expression at 24 hours after HIBI, 26 at 72 hours, and five (miR-137-3p, -2137, -335-5p, -376c-3p, and -5126) which had significant altered expression at both 24 and 72 hours. Chapter 2 then provided brain region-specific profiling of miRNA expression at 30 minutes after neonatal HIBI, finding 61 unique miRNAs with significant differential expression in at least one of the three regions studied; most of which were associated with pathways of metabolism and synthesis. Additionally, several mRNAs demonstrated altered regulation at 30 minutes after injury; these were primarily made up of IEGs such as Fos, Jun, and Arc that were associated with downstream inflammatory and apoptotic pathways on KEGG analysis. Finally, Chapter 3 demonstrated that treatment with intranasal hypoxia preconditioned EVs resulted in neuroprotection following neonatal HIBI. These preconditioned EVs contained 24 miRNAs – many of which are involved in apoptotic pathways – that were at concentrations high enough to be consistently identified by miRNA sequencing.

Effects of Hypoxia Only Versus HIBI on Brain MicroRNA Expression

Given the significant role of hypoxamiRs in regulating the cell response to hypoxia, it is not surprising that many of the known hypoxamiRs (including miR-135a, -34a, -21a, -369, -128, and -92) (136, 137) demonstrated significant differential expression in the hypoxia only group versus controls in Chapter 1. The direction of differential expression

was consistent between 24 and 72 hours after hypoxic injury (as compared to HIBI where many of the miRNAs showed inverse differential expression at 24 versus 72 hours). Although there are very few time-series studies assessing temporal changes in miRNA expression after hypoxia, those that have been published demonstrate similarly persistent expression of hypoxamiRs up to 48 hours after hypoxia (138, 139).

In the current study, the primary value of assessing miRNA expression after hypoxia was in the comparison with the miRNA expression after HIBI in order to better understand the contribution of hypoxia versus ischemia in driving miRNA expression.

Temporal and Regional MicroRNA Changes After HIBI

In the HIBI tissue, four highly conserved miRNAs demonstrated significant differential expression at both 24 and 72 hours after injury: miR-2137, -335, -137, and -376c. Of these, miR-2137 was the only HIBI-specific miRNA that was upregulated at both 24 hours and 72 hours after injury.

MiR-2137 is involved in inflammation, has been associated with elevated levels of TNF-α, and its inhibition has been shown to increase the anti-inflammatory interleukin IL-10 (140). Increased miR-2137 expression has also been shown in the penumbral tissue after traumatic brain injury (141) and a previous study demonstrated upregulation of miR-2137 up to 7 days after injury in an adult ischemic stroke model (142). Contrary to our findings, however, the post-stroke data showed a decrease in miR-2137 differential expression between 1 and 3 days after injury while ours demonstrated an increase. This difference may be due to developmental differences between neonatal and adult brains, but could also be due to differences in the methodology of inducing HIBI in the neonatal versus adult models. It is notable that miR-2137 is the only of the four key miRNAs identified in HIBI in our study that has not yet been described as a hypoxamiR, and its

differential expression after HIBI was inverse to that of the hypoxia only group at both 24 and 72 hours, suggesting a unique association with ischemia rather than hypoxia. Additionally of note, miR-2137 is also significantly increased after ischemic cardiac injury (143), suggesting that its inhibition could have beneficial effects outside of the brain as well.

Consistent with the triphasic pattern seen in the pathophysiology of neonatal hypoxic-ischemic encephalopathy, we demonstrated multiphasic differential expression in several of the key HIBI-related miRNAs (Figure 22), including miR-335. MiR-335 is a hypoxamiR, regulates cholesterol metabolism (144-146), and acts as a direct regulator of HIF1α as well as being predicted to regulate several other mRNA known to be affected by neonatal HIBI (Table 1). MiR-335 has been shown to be downregulated in the cord blood of infants who suffered moderate to severe HIBI (22) and remains altered at 1-2 months after injury in infants with intraventricular hemorrhage and resulting abnormal muscle tone (147). In the adult stroke model, miR-335 has been shown to have a triphasic expression pattern: downregulated immediately after middle cerebral artery occlusion, peaked upregulation around 24 hours, and then downregulation again after 24 hours. Reflecting this pattern, miR-335 mimic has been shown to be neuroprotective when administered immediately after injury, when endogenous miR-355 expression is lowest, but miR-335 antagonist was neuroprotective when administered at 24 hours after injury, corresponding to increased

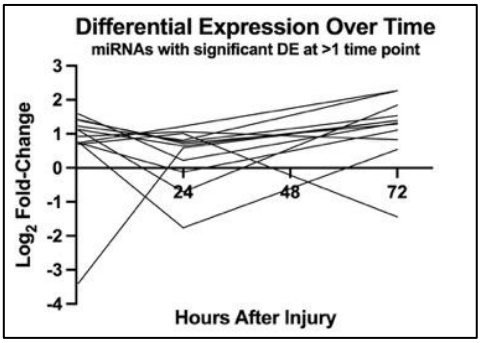

Figure 22. Change in differential expression (DE, hypoxic-ischemic brain injury vs. control) over time for microRNAs (miRNA) with DE at more than one time point *demonstrating the tri-phasic expression of many of the key miRNAs.*

endogenous expression (35). The current data showed similar trends, with upregulation at 24 hours after HIBI but downregulation by 72 hours.

In addition to miR-335, miR-376c was also seen in previous studies of cord blood after perinatal asphyxia or neonatal hypoxic-ischemic encephalopathy (21, 103). The relative downregulation of miR-376c demonstrated in the cord blood studies, in conjunction with relative upregulation at 24 hours and downregulation at 72 hours after HI injury in the current study, suggests that miR-376c also may have a triphasic response. This is further supported by an *in vitro* study demonstrating that overexpression of miR-376c-3p at the time of oxygen-glucose deprivation increased cell viability and decreased apoptosis by inhibiting inhibitor of growth family member 5 (ING5) in two neuroblast cell lines (148).

miR-137 is another hypoxamiR that has also been associated with the inflammatory response after cerebral ischemia (149). miR-137 may also play a significant role in brain development and neural stem cell differentiation (150), with decreased levels of miR-137 during brain development being associated with increased anxiety-like behaviors later in life (151). During brain development, miR-137 is known to be highly expressed, specifically in the dorsolateral nucleus and ventral posterolateral nucleus of the thalamus, the striatum, the nucleus accumbens of the telencephalon, and the cerebral peduncles (152); a spatial distribution suggesting a relationship with cholinergic neurotransmission neurons. Similar to the pattern observed in miR-335, the current study results showed upregulation of miR-137 at 24 hours after HIBI but downregulation at 72 hours. Although the multiphasic expression is not as well described as that of miR-335, it is likely that miR-137 also has a triphasic pattern, since overexpression of miR-137 at 30 minutes after cerebral ischemia attenuated brain levels of JAK1, STAT1, TNF-α, IL-1β, and IL-6 and resulted in decreased infarct size and neurological function score, suggesting that levels were low or downregulated early after ischemia (149).

As mentioned in the introduction, miR-210 is one of the most commonly studied hypoxia-related miRNAs and has been found to be elevated in rat brain after neonatal HIBI at 3 hours up to 24 hours (39). Although none of the studies presented here demonstrated significant changes in miR-210, there was a non-significant (1.8-fold, p=0.057) increase in HIBI versus controls at 72 hours after injury. This underscores the potential limitations from the smaller sample sizes in these studies, which may miss some physiologically relevant miRNAs. Additionally, as miR-210 has been closely associated with the effects of hypoxia, differences in oxygen concentrations and duration may affect its differential regulation. For instance, rat pups and some strains of mice, such as 129Sv, have been found to be more resistant to hypoxia-ischemia and so must receive longer and/or deeper hypoxia to result in the necessary brain injury to model HIBI (94).

An additional limitation of cross-species miRNA analyses (i.e. using rodent studies to design human interventions) is that miRNAs differ between species. Each of the studies above addressed the known conservation of miRNAs between mammalian species in the miRNAs that were detected, but there still exists the possibility of missing a pathologic miRNA that exists in humans but not in rodents. This is likely the case with miR-374a which was significantly altered in the Looney, et al umbilical cord blood study as well as that group's follow-up study, but miR-374a has not yet been identified in the house mouse (Mus musculus), so the sequencing alignment performed in these studies would not have identified it. Of note, however, miR-374b, which has a sequence with 96% similarity to miR-374a, was upregulated in HIBI versus controls at 24 hours in the current studies.

The final conclusions from chapters 1 and 2 centered around the use of various internal controls for this neonatal HIBI model. First, in chapter 1, the clustering analyses revealed distinct miRNA signatures between the sample groups, which were quite different at 24 and 72 hours. They suggested that the early subacute phase of the injury (at 24

hours) continues to evolve and change, giving rise to a less extensive, but more robust miRNA profile in HIBI animals at 72 hours. Additionally, the data suggested that using the contralateral hemisphere of the lesioned animals as a baseline control in the first 24 hours after HIBI is perhaps less than ideal. The unilateral lesion appears to have a strong effect on the miRNA expression level of the whole brain, and not only on the lesioned side. Contrary to the contralateral findings, in chapter 2, the cerebellum demonstrated distinct miRNA signatures at 30 minutes after injury, so may serve as an effective internal control at least in the immediate period after injury.

Downstream Pathways of Key MicroRNAs

Chapter 2 measured early mRNA expression levels after neonatal HIBI and demonstrated that, in the early phase of injury, there was limited clear interaction between miRNAs expressed at that time point and mRNA expression. Instead, most of the mRNAs that demonstrated significant differential expression were IEGs, including Atf3, Fos, Arc, Jun, and Tlr; IEGs that are largely involved in inflammatory and cell death pathways, including interleukin (IL-3, -8, -10, -17A), TNF receptor, HIF1α, and PI3K signaling. IEGs are genes that are rapidly transcribed in response to positive (e.g. neuronal activity) or negative (e.g. injury) stimuli and often ask as transcription factors and DNA-binding proteins (153). The regulation of the IEGs is complex but, of importance for the current studies, is closely tied with miRNA expression. IEGs can directly regulate the expression of various miRNAs (154). Specifically, Atf3 expression has been shown by multiple investigator groups to be regulated largely by a negative miRNA-based feedback loop (155, 156). Stimulating IEG expression briefly inhibits production of the negative feedback miRNAs (155, 156). This feedback relationship is a likely cause of the lack of predicted miRNA-mRNA interaction seen in Chapter 2; when IEGs are highly expressed, their associated miRNAs are repressed, and vice versa.

In each of the three chapters, additional predictions of miRNA targets were performed through KEGG pathway analyses. In Chapter 2, compared to the IEG mRNA expression described above, the miRNA KEGG analysis demonstrated that the miRNAs with altered regulation were primarily associated metabolic pathways, including that of fatty acid metabolism and biosynthesis, lysine metabolism, steroid biosynthesis, AMPK signaling, and sphingolipid metabolism. Many of the traditional hypoxia and cell death pathways, including mTOR, MAPK, and HIF1 were also present as significant targets in the KEGG analysis, but had considerably lower -log(p value) values.

For chapters 1 and 2, the KEGG pathways that were significantly associated with the differentially expressed miRNAs at all three time points are demonstrated in Figure 23. Overall, there were 23 pathways that were consistently targeted at 30 minutes, 24 hours, and 72 hours after injury. Twenty of the 23 pathways were also significantly associated with the miRNAs that were detected within the hypoxia preconditioned EVs in chapter 3.

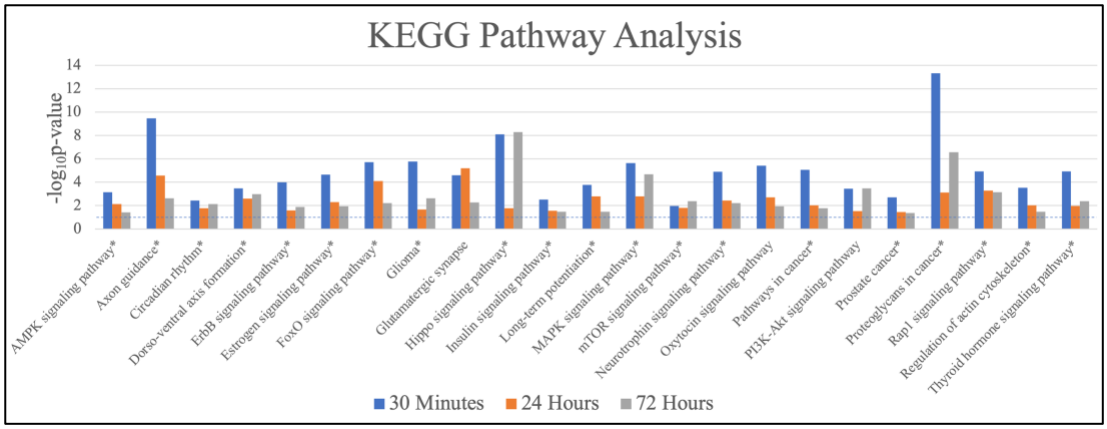

Figure 23. KEGG pathways consistently affected throughout the first 72 hours after injury. *KEGG pathway analyses performed by Diana-miRPath for miRNAs with significant differential expression at each time point. Figure lists all pathways demonstrating statistical significance at all three time points. *Pathways also significantly associated with miRNAs that were identified in neuroprotective hypoxia-preconditioned extracellular vesicles.*

Although there are many different pathways, many of them are closely associated with three of the primary pathways: the MAPK, mTOR, and PI3K-Akt signaling pathways.

MAPK Pathway

The MAPK pathway primarily consists of three families of genes: ERK, JNK/SAPK, and p38 MAPK. Each of these three sub-pathways can affect cell proliferation and differentiation, while the p38 and JNK/SAPK can also affect apoptosis, and p38 uniquely alters inflammation and stress response (157). The MAPK pathway is also closely linked to several other relevant pathways, including inhibiting the FoxO signaling pathway, stimulating the neurotrophin pathway and being stimulated by the Rap1 signaling pathway. Of the miRNAs highlighted in the current studies, miR-335, -137, -376c, -1264, -1298, -34b, -3473a, and -3473b are all predicted to target genes in the MAPK pathway. For instance, miR-335 and -34b are predicted to affect Rasa1 in the classical MAPK ERK pathway while miR-376c, -1264, -335, and -34b also target Map3k2 in the JNK pathway.

Both the ERK and JNK pathways have previously been shown to be targets for neuroprotective intervention after neonatal HIBI. Inhibition of the JNK pathway with the specific inhibitor TAT-JBD reduced neuronal injury and caspase-3 levels in the hours after neonatal HIBI as well as attenuating white and grey matter injury at 14 weeks after injury (158). For the ERK pathway, multiple studies in the rat model have demonstrated that the increased activation of ERK after neonatal HIBI can be neuroprotective (159-161). One study in the piglet model showed no difference in gross neuropathology after modulating the ERK pathways (162), but they used an ERK inhibitor rather than increasing activation, which primarily demonstrates that further inhibiting the ERK pathway (which is already downregulated by HIBI) does not further injure the brain.

mTOR Pathway

mTOR is a downstream kinase that can be activated by the PI3K/Akt, MAPK ERK, and AMPK signaling pathways, but can also be separately altered by several of the individual miRNAs that were found to be significantly altered in the current studies. Rapamycin-

insensitive companion of mTOR (Rictor), which codes for one of the protein components of the mTOR complex, is a predicted target of miR-137 and -1264. Rictor knockouts impairs brain development, resulting in decreased brain size, smaller neuronal somas, and shorter dendritic processes (163). Additionally, inhibition of mTOR complex 2 by Rictor deficiency has been shown to exacerbate ischemia reperfusion injury in the liver (164), but the role of Rictor specifically in brain hypoxia-ischemia has not yet been evaluated. One of the most well-studied of the mTOR pathway targets is HIF1α, which is directly activated by mTOR and is also a predicted target of miR-376c and -6240.

HIF1α is the 3' enhancer of the erythropoietin gene and contains three domains: the N-terminal domain, the C-terminal transactivation domain which primarily regulates gene transcription activity, and an oxygen-dependent degradation domain which mediates oxygen-dependent stability (165). As mentioned above, HIF1α expression demonstrates a multiphasic response after neonatal HIBI, with significant upregulation at 4-12 hours, decreasing to near-baseline by 24 hours and then subsequent elevation again between 2 and 8 days after injury (166). Although it is known to play a central role in hypoxic and hypoxic-ischemic brain injury, many questions still remain regarding the precise mechanisms by which HIF1α modulates brain injury after neonatal HIBI. For example, while acute HIF1α upregulation induces cellular apoptosis by both increasing the stability of p53 (167) and inducing expression of the BCL2/adenovirus E1B interacting protein 3 (BNIP3) (168), chronic upregulation of HIF1α through hypoxia preconditioning results in anti-apoptotic effects (169, 170), potentially through increasing erythropoietin expression (170) and/or increasing anaerobic metabolic potential (171). The neuroprotective effects of hypoxia preconditioning are not completely dependent on HIF1α, however, as the positive effects of preconditioning are retained in HIF1α-deficient mice (166).

Several studies have specifically assessed the role of endogenous HIF1α and the potential protective effects of downregulating HIF1α in neonatal HIBI. Inhibition of HIF1α using the inhibitor 2-methoxyestradiol immediately after HIBI resulted in decreased brain infarct volume, brain edema, and blood-brain barrier disruption (172). Contrary to these findings, however, neuron-specific HIF-1α knockout mice developed more necrotic and apoptotic cell death than control mice after neonatal HIBI (173). It is very possible that this contradiction could be explained by the non-specific nature of 2-methoxyestradiol inhibition. A study in an adult stroke model suggested that HIF1α knockout mice had no change in infarct or edema size, but when both HIF1α and HIF2α were knocked out, they demonstrated significantly reduced cell death and edema after ischemic brain injury (174), suggesting that the benefits seen in the 2-methoxyestradiol study may have been due to the drug's ability to inhibit both HIF1α and HIF2α (175).

PI3K-Akt Pathway

The PI3K-Akt pathway is involved in regulating cellular activation, inflammatory response, and apoptosis (176). Akt is the primary downstream effector in the pathway, and its activation promotes the phosphorylation of several downstream molecules, including Bcl-2, Fox03a, and mTOR, which each then act to reduce apoptosis (177). Several of the miRNAs that were highlighted in the current studies were closely associated with the downstream mRNAs from Akt. These include Casp9 (miR-137 and -3473a), Creb1 (miR-6240 and -410), and Bcl2 (miR-1264, -3473a, and -6240). Much like the other pathways already discussed, the PI3K-Akt pathway is also closely linked with several other pathways identified in the KEGG pathway analysis. The PI3K-Akt pathway can be activated by the RAP1 or ErbB signaling pathways and can in turn inhibit the FoxO signaling pathway.

Neonatal HIBI has been shown to result in inhibition of the PI3K-Akt signaling pathway. Further inhibition of PI3K by the inhibitor LY294002 in a rabbit model exacerbated neurological impairment beyond that seen in the injured controls (178). Additionally, LY294002 partially reversed the neuroprotective effects seen after administration of liraglutide (179) or L-cysteine (180), and the Akt inhibitor wortmannin did the same for the neuroprotective effects of progesterone (181) in the rodent models of neonatal HIBI, demonstrating the significant role that the PI3K-Akt pathway plays in neuroprotection.

Circadian Rhythm Pathway

Given the cyclical patterns of the miRNA expression it is not surprising that many of the miRNAs that were found to be altered after neonatal HIBI were related to the circadian rhythm pathway. Neonatal HIBI results in impaired circadian rhythms, likely in part due to decreased pineal melatonin levels (182). Clock protein, which is thought to be the master regulator of the circadian rhythm and is predicted as a target for both miR-335 and miR-182, was found to be upregulated after neonatal HIBI versus controls, but not until ~48 hours after injury (183). Melatonin levels, however, were decreased within the first 8 hours of injury (182), and one of the primary nuclear receptors of melatonin, retinoic acid receptor-related orphan receptor A (Rora), is a predicted target for miR-1264 and -137. Although not one of the miRNAs that demonstrated significant differential expression in the current studies, peripheral blood mononuclear cell levels of miR-325 have been positively associated with increased sleep rhythm problems in human infants after HIBI, and miR-325 knockout resulted in improved circadian rhythmicity and motor outcomes in mice after neonatal HIBI (184), suggesting that the circadian rhythm pathway may be yet another potential therapeutic target for neonatal HIBI.

Metabolic Pathways

One of the primary deficiencies in neonatal HIBI is metabolic failure, and as such, it is important to also consider the metabolic and synthetic pathways that may be altered by miRNAs. These include the ceramide and glycosphingolipid synthetic pathways which are known to be altered by HIBI, with decreased ceramide and sphingomyelin levels present for up to seven days after preterm HIBI (185). The glycosphingolipid pathways are predicted to be altered by miR-6240 and -125a-5p (which inhibit Fut1) as well as miR-182-5p and -1264-3p (which inhibit Fut9). Sterol synthesis and metabolism has also been found to be altered after neonatal HIBI (186) and is associated with several of the key miRNAs from the current study. For example, miR-335 expression is associated with decreased 3-hydroxy-3-methylglutaryl-CoA reductase (HMGCR) and synthase (HMGCS), suggesting a key role in astrocyte cholesterol synthesis (144), and may also affect lanosterol synthase and sterol-C5-desaturase (146). Similarly, miR-148a regulates LDL receptor and ABCA1 (187) and, along with the other miRNA modulators of the AMPK pathways (which includes 14 of the key miRNAs from the current study) may inhibit HMGCR (188).

High-Yield MicroRNAs for Future Neuroprotective Studies

Several promising miRNAs can be derived from the current studies, including miR-2137, -335, -137, and -376c from Chapter 1 and miR-410, -1264, -1298, -5126, -34b, -6240, -3963, -3473a, and -3473b from Chapter 2. Lastly, in Chapter 3, the miRNAs that were highly expressed in the neuroprotective EVs include miR-92b, -541, -434, -328, -342, and -361. Figure 24 demonstrates the clustering relationships between all of the miRNAs from chapters 1-3. Although the miRNA profiling in the first two chapters provides increased insight into the pathophysiology of neonatal HIBI and offers several potential high-yield targets for future therapeutic studies, it is important to note two significant

limitations: 1) differential expression of a miRNA after HIBI is not equivalent to pathologic expression, and 2) a lack of differential expression in a miRNA does not rule out therapeutic potential. The latter point is probably best exemplified by miR-210 which, as described in the introduction, has been demonstrated to be an effective target in multiple studies of neonatal HIBI and yet was not differentially expressed at any of the three time points assessed. This is often the case in the body's stress response, where the lack of upregulation (e.g. adrenal insufficiency resulting in a lack of cortisol elevation during stress) is pathologic.

Additionally, despite the inability of studies in the mouse model to detect human-specific miRNA such as miR-374a, it may still be possible to test the therapeutic potential of human-specific miRNA interventions in the rodent model. As an example, one study using the rat model of neonatal HIBI demonstrated significant attenuation of inflammatory cytokines and brain injury after intracerebroventricular injection of miR-374a-5p mimic (62). These investigators developed a mimic from the human hsa-miR-374a-5p and still demonstrated improvement in injury despite the rat, like the mouse, not having an identified rat-specific rno-miR-374a.

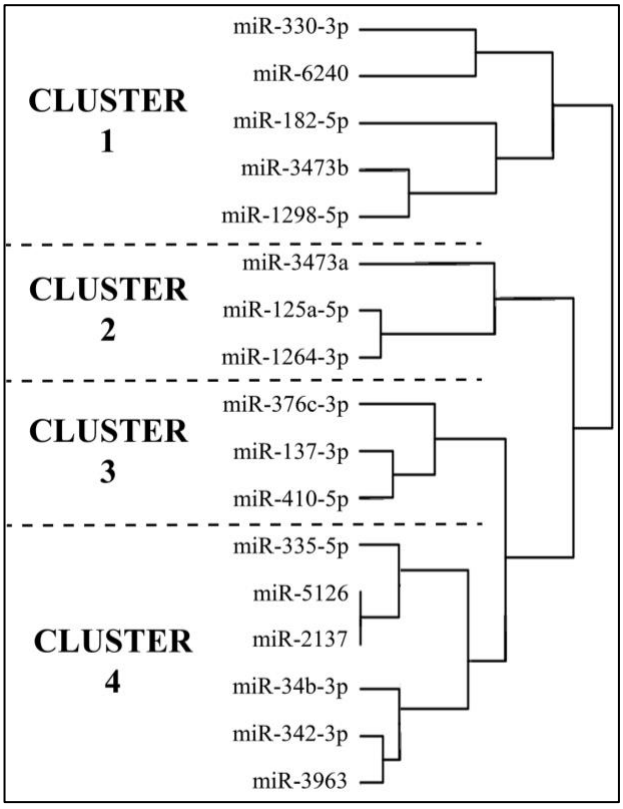

Figure 24. Hierarchical cluster pathway dendrogram of the promising miRNAs from chapters 1-3. *Pathway analyses performed by Diana-miRPath.*

Given the pre-clinical results already performed, both miR-210 and -374a certainly deserve continued attention in neonatal HIBI research despite their absence in the current studies. Further studies will be necessary to better identify potential stress response miRNAs that are not included in the following list of high-yield miRNAs for future studies of neuroprotective interventions. Since neonatal HIBI is a complex and multifactorial injury, developing effective therapies requires consideration of targeting multiple key pathways. As such, the following miRNAs are separated based on the pathway clusters in Figure 24.

Cluster 1

The miRNAs in this cluster target pathways including GABAergic synapse development, axon guidance, cGMP-PKG signaling pathway, and glycosphingolipid biosynthesis. Firstly, mir-182-5p was significantly downregulated at 24 hours after injury in whole brain, returns to control levels by 72 hours, and was detected in modest numbers in the preconditioned EVs. These findings are consistent with persistent downregulation that was seen for the first 48 hours after hypoxia plus inflammation induced by LPS (129) as well as a 5-fold downregulation at 48 hours after preterm HIBI (189). Additionally, miR-182 was downregulated at 12, 24, and 48 hours after HIBI in the neonatal rat model, and administration of miR-182 mimic to pineal gland cells after OGD resulted in attenuation of Clock protein elevation after injury (190) and thus miR-182 alterations may contribute to some of the circadian rhythm abnormalities that can be seen after neonatal HIBI.

Although not demonstrated to have significant differential expression at any of the three time points in the current study, miR-330 was expressed at a moderate level in the preconditioned EVs. Although its role in hypoxic and/or ischemic injury has not yet been explored in the literature, it may play a role in inflammation given that it was found to be consistently downregulated for the first 48 hours in the blood of a piglet model of neonatal hypoxic brain injury plus inflammation induced by LPS (129). Specifically, miR-330

expression was significantly lower in the hypoxia+LPS group compared to hypoxia alone. Its expression may also be developmentally regulated, as miR-330 was also downregulated 7-fold at 48 hours after preterm HIBI (189). Lastly, although it has been shown to inhibit Egr2 (191) which is a key protein in peripheral myelination (192), miR-330 expression does not appear to modulate myelin formation in the central nervous system (193).

miR-3473b expression was found to be upregulated in the striatum, thalamus, and cortex at 30 minutes after injury and remained significantly elevated at 72 hours. A study in BV2 microglial cells showed that miR-3473b induces pro-inflammatory factors such as inducible nitric oxide synthase (iNOS), COX-2, TNF-α, and IL-6 by targeting SOCS3 (194) and inhibits autophagy through TREM2 and ULK1 expression (195). Another possible mechanism of miR-3473b in neonatal HIBI is its effects on PTEN (196), a gene closely linked with the master hypoxia regulator HIF1α. Either pathway would suggest that downregulation of miR-3473b could attenuate cellular injury after HIBI.

Chapter 2 demonstrated significant increased expression of miR-1298 in the cortex, striatum, and thalamus at 30 minutes after injury, though a study using an adult model of brain hypoxia-ischemia demonstrated decreased expression in HIBI versus controls at 24 hours after injury, suggesting a multi-phasic expression (197). The physiologic targets and effects of miR-1298 in the brain, however, are still unknown at this time. Additionally, mir-6240 was significantly upregulated in the cortex and cerebellum at 30 minutes and remains elevated throughout the first 72 hours after injury, with significant elevation at 72 hours in the whole brain. It was also expressed in moderate quantity in the preconditioned EVs. Similar to miR-1298, though, little is known about the effects of miR-6240 expression outside of the *in silico* predicted effects.

Cluster 2

Some of the main pathways affected by the miRNAs in this cluster include the AMPK signaling pathway, galactose metabolism, and glycosphingolipid biosynthesis; all pathways related to metabolism and energy maintenance. This cluster includes miR-125a which targets Ppp2ca, a direct inhibitor of AMPK, as well as Fut1, a main driver of sphingolipid metabolism. miR-125a was downregulated in the cerebellum at 30 minutes after HIBI, but not the striatum or thalamus, suggesting that it is altered more by hypoxia (given that the cerebellum does not undergo ischemia in the mouse model) than ischemia, which is also supported by its significant downregulation at 24 hours after injury in hypoxia-only brains versus controls but not HIBI versus controls. Despite the endogenous downregulation of miR-125a after neonatal hypoxia in the current study, it may be that further inhibition of miR-125a – rather than upregulation – is actually therapeutic, as miR-125a silencing in an adult ischemic stroke model resulted in suppression of apoptosis through targeting of insulin-like growth factor binding protein 3 (IGFBP3) (198) and/or tissue inhibitor matrix metalloproteinase 1 (TIMP-1) (199). Additionally, miR-125a is highly expressed in cerebral spinal fluid (200), so could act as a potential cerebral spinal fluid biomarker.

The second miRNA in this cluster, miR-3473a, was upregulated in all three regions of the brain at 30 minutes after HIBI in the current study. It appeared to only be altered in the acute phase after injury, as it was not differentially expressed at 24 or 72 hours after injury. Although not much is known about its specific role in the brain, miR-3473a was one of the miRNAs found to be downregulated in the brain after preconditioning, suggesting that the relative decrease in expression may play a role in the neuroprotective effects of preconditioning (201).

miR-1264 also demonstrated increased expression in the cortex, striatum, and thalamus at 30 minutes after HIBI but, like miR-3473a, was only differentially expressed in the acute injury phase and returned to control levels by 24 hours. In adult stroke, upregulated miR-1264 expression was noted immediately after injury, peaking around 3 hours after injury, and gradually decreasing, remaining upregulated at 12 hours but not significantly altered at 24 hours after injury (202). Inhibition of miR-1264 attenuates apoptosis through targeting WNT/β-catenin signaling (203).

Cluster 3

For this cluster, the included miRNAs target the MAPK signaling pathway, biosynthesis of unsaturated fatty acids, circadian rhythm, and GABAergic synapse regulation. miR-137 has already been described in depth above.

miR-410 was found in the current studies to be downregulated in the cortex and upregulated in the cerebellum at 30 minutes after injury, with no differential expression at 24 or 72 hours. It was also downregulated in umbilical cord blood (21) as well as in circulating blood within 6 hours after delivery (30) in infants diagnosed with HIE. Overexpression of miR-410 attenuated apoptosis and inflammation in OGD models using both PC12 and SH-SY5Y cell lines (30). Furthermore, mesenchymal stem cell derived EVs that were neuroprotective when injected intraperitoneally after neonatal HIBI lost their positive effects on cerebral edema and infarct size after treatment with miR-410 antagonist (87).

miR-376c was found in the current studies to have increased expression at 24 hours and decreased expression at 72 hours after injury. Overexpression of miR-376c has been associated with increased cell viability, in part due to inhibition of ING5 (148). Although

miR-376c has been evaluated in several oncological studies, its role in brain development and/or injury has not yet been well defined.

Cluster 4

This final cluster includes six miRNAs that target pathways including FoxO signaling, PI3K-Akt signaling, and glutamatergic synapses. miR-2137 and -335 have already been described in depth, but mir-342 also has considerable promise as a therapeutic target, as it was significantly downregulated at 24 hours after injury in whole brain in the current study and was also highly expressed in the preconditioned EVs. Previous studies also showed miR-342 expression was downregulated in human umbilical cord blood at the time of neonatal HIBI (22) as well as in the blood after stroke in adults (204). Despite the several studies demonstrating its alterations, however, little is known about its true function in the brain.

One of the miRNAs that was highly differentially expressed at all three time points in the current study was miR-5126, which was upregulated in the cortex at 30 minutes and remained significantly upregulated in the whole brain at 24 and 72 hours after HIBI. It was also found to be downregulated in the cerebellum at 30 minutes, suggesting that it may be able to help differentiate between hypoxia only and HIBI, which is further supported by the finding that miR-5126 has significantly higher expression in HIBI versus hypoxia only at 24 hours (logFC 3.6) and 72 hours (logFC 5.7) after injury. This prolonged elevated expression and specificity for HIBI make miR-5126 an attractive candidate for a therapeutic target; however, it is unclear whether miR-5126 is adequately conserved between mammalian species.

miR-34b demonstrated increased expression in the striatum and thalamus at 30 minutes after HIBI and, although not differentially expressed at 24 hours, was significantly

increased again at 72 hours. Although the effects of miR-34b in the brain are not well known, it has been shown to increase cell apoptosis through increased p53 and Bax and decreased BCL2 (205). The final miRNA in this cluster, miR-3963, was upregulated in all three regions at 30 minutes but not at 24 hours or 72 hours. Although it has been found to be highly upregulated in microglia in the developing brain (206), it has unfortunately not been well studied and it's conservation between species is not known.

Conclusions

The current studies identified several promising miRNAs for future investigations into miRNA-based therapeutic interventions. Given the multifactorial nature of neonatal HIBI, it is likely that a combination of miRNAs would need to be targeted to achieve maximal benefit. Because of this, the list of promising miRNAs was grouped by targeted pathways, and future investigations should consider assessing the effects of altering one or more miRNA from each of the miRNA clusters. Additional mechanistic studies will be necessary to demonstrate whether the differential expression seen in chapters 1 and 2 are beneficial or pathologic and whether the miRNAs detected in the EVs in chapter 3 play a significant role in the neuroprotection seen after hypoxia preconditioned EV administration. Lastly, in order to better translate the pre-clinical miRNA studies to human infants, more sensitive analyses of postnatal circulating miRNAs must be performed. One possible method for specifically assessing brain-related miRNA expression could be identifying the miRNAs contained within circulating EV carrying brain-specific markers such as neuronal L1 cell adhesion molecule (L1CAM) (207). Ultimately, given their broad effect profile, ease of administration, and small size allowing for effective blood-brain barrier crossing, miRNAs represent promising targets for improving brain injury and reducing developmental impairments in neonates suffering from HIE.

BIBLIOGRAPHY

1. Lee ACC, Kozuki N, Blencowe H, Vos T, Bahalim A, Darmstadt GL, Niermeyer S, Ellis M, Robertson NJ, Cousens S, Lawn JE. Intrapartum-related neonatal encephalopathy incidence and impairment at regional and global levels for 2010 with trends from 1990. Pediatric research. 2013;74 Suppl 1(Suppl 1):50-72. doi: 10.1038/pr.2013.206. PubMed PMID: 24366463.

2. Jacobs SE, Berg M, Hunt R, Tarnow-Mordi WO, Inder TE, Davis PG. Cooling for newborns with hypoxic ischaemic encephalopathy. Cochrane Database Syst Rev. 2013(1):CD003311. doi: 10.1002/14651858.CD003311.pub3. PubMed PMID: 23440789.

3. Hassell KJ, Ezzati M, Alonso-Alconada D, Hausenloy DJ, Robertson NJ. New horizons for newborn brain protection: enhancing endogenous neuroprotection. Archives of disease in childhood Fetal and neonatal edition. 2015;100(6):F541-52. Epub 2015/06/13. doi: 10.1136/archdischild-2014-306284. PubMed PMID: 26063194; PMCID: PMC4680177.

4. Volpe JJ, Inder TE, Darras BT, de Vries LS, du Plessis AJ, Neil J, Perlman JM. Volpe's neurology of the newborn e-book: Elsevier Health Sciences; 2017.

5. Pauliah SS, Shankaran S, Wade A, Cady EB, Thayyil S. Therapeutic hypothermia for neonatal encephalopathy in low- and middle-income countries: a systematic review and meta-analysis. PloS one. 2013;8(3):e58834-e. Epub 2013/03/19. doi: 10.1371/journal.pone.0058834. PubMed PMID: 23527034.

6. Gluckman PD, Wyatt JS, Azzopardi D, Ballard R, Edwards AD, Ferriero DM, Polin RA, Robertson CM, Thoresen M, Whitelaw A. Selective head cooling with mild systemic hypothermia after neonatal encephalopathy: multicentre randomised trial. The Lancet. 2005;365(9460):663-70.

7. Eicher DJ, Wagner CL, Katikaneni LP, Hulsey TC, Bass WT, Kaufman DA, Horgan MJ, Languani S, Bhatia JJ, Givelichian LM. Moderate hypothermia in neonatal encephalopathy: efficacy outcomes. Pediatric neurology. 2005;32(1):11-7.

8. Battin MR, Dezoete JA, Gunn TR, Gluckman PD, Gunn AJ. Neurodevelopmental outcome of infants treated with head cooling and mild hypothermia after perinatal asphyxia. Pediatrics. 2001;107(3):480-4.

9. Jacobs SE, Morley CJ, Inder TE, Stewart MJ, Smith KR, McNamara PJ, Wright IM, Kirpalani HM, Darlow BA, Doyle LW. Whole-body hypothermia for term and near-term newborns with hypoxic-ischemic encephalopathy: a randomized controlled trial. Archives of pediatrics & adolescent medicine. 2011;165(8):692-700. Epub 2011/04/06. doi: 10.1001/archpediatrics.2011.43. PubMed PMID: 21464374.

10. Simbruner G, Mittal RA, Rohlmann F, Muche R. Systemic Hypothermia After Neonatal Encephalopathy: Outcomes of neo.nEURO.network RCT. Pediatrics. 2010;126(4):e771-e8. doi: 10.1542/peds.2009-2441.

11. Shankaran S, Laptook AR, Ehrenkranz RA, Tyson JE, McDonald SA, Donovan EF, Fanaroff AA, Poole WK, Wright LL, Higgins RD, Finer NN, Carlo WA, Duara S, Oh W, Cotten CM, Stevenson DK, Stoll BJ, Lemons JA, Guillet R, Jobe AH. Whole-Body Hypothermia for Neonates with Hypoxic–Ischemic Encephalopathy. New England Journal of Medicine. 2005;353(15):1574-84. doi: 10.1056/NEJMcps050929. PubMed PMID: 16221780.

12. Azzopardi DV, Strohm B, Edwards AD, Dyet L, Halliday HL, Juszczak E, Kapellou O, Levene M, Marlow N, Porter E, Thoresen M, Whitelaw A, Brocklehurst P. Moderate Hypothermia to Treat Perinatal Asphyxial Encephalopathy. New England

Journal of Medicine. 2009;361(14):1349-58. doi: 10.1056/NEJMoa0900854. PubMed PMID: 19797281.

13. Zhou W-h, Cheng G-q, Shao X-m, Liu X-z, Shan R-b, Zhuang D-y, Du L-z, Cao Y, Yang Q, Wang L-s. Selective head cooling with mild systemic hypothermia after neonatal hypoxic-ischemic encephalopathy: a multicenter randomized controlled trial in China. The Journal of pediatrics. 2010;157(3):367-72. e3.

14. De Rie D, Abugessaisa I, Alam T, Arner E, Arner P, Ashoor H, Åström G, Babina M, Bertin N, Burroughs AM. An integrated expression atlas of miRNAs and their promoters in human and mouse. Nature biotechnology. 2017;35(9):872-8.

15. Abdelfattah AM, Park C, Choi MY. Update on non-canonical microRNAs. Biomol Concepts. 2014;5(4):275-87. Epub 2014/11/06. doi: 10.1515/bmc-2014-0012. PubMed PMID: 25372759; PMCID: PMC4343302.

16. Denli AM, Tops BB, Plasterk RH, Ketting RF, Hannon GJ. Processing of primary microRNAs by the Microprocessor complex. Nature. 2004;432(7014):231-5.

17. Fareh M, Yeom K-H, Haagsma AC, Chauhan S, Heo I, Joo C. TRBP ensures efficient Dicer processing of precursor microRNA in RNA-crowded environments. Nature communications. 2016;7(1):1-11.

18. Yoda M, Kawamata T, Paroo Z, Ye X, Iwasaki S, Liu Q, Tomari Y. ATP-dependent human RISC assembly pathways. Nature structural & molecular biology. 2010;17(1):17-23.

19. Khvorova A, Reynolds A, Jayasena SD. Functional siRNAs and miRNAs exhibit strand bias. Cell. 2003;115(2):209-16.

20. Jo MH, Shin S, Jung S-R, Kim E, Song J-J, Hohng S. Human Argonaute 2 has diverse reaction pathways on target RNAs. Molecular cell. 2015;59(1):117-24.

21. Looney AM, Walsh BH, Moloney G, Grenham S, Fagan A, O'Keeffe GW, Clarke G, Cryan JF, Dinan TG, Boylan GB, Murray DM. Downregulation of Umbilical Cord Blood Levels of miR-374a in Neonatal Hypoxic Ischemic Encephalopathy. J Pediatr. 2015;167(2):269-73.e2. Epub 2015/05/24. doi: 10.1016/j.jpeds.2015.04.060. PubMed PMID: 26001314.

22. Casey S, Goasdoue K, Miller SM, Brennan GP, Cowin G, O'Mahony AG, Burke C, Hallberg B, Boylan GB, Sullivan AM, Henshall DC, O'Keeffe GW, Mooney C, Bjorkman T, Murray DM. Temporally Altered miRNA Expression in a Piglet Model of Hypoxic Ischemic Brain Injury. Molecular neurobiology. 2020;57(10):4322-44. doi: 10.1007/s12035-020-02018-w. PubMed PMID: 32720074.

23. Wang W, Jia L. Regulatory Mechanism of MicroRNA-30b on Neonatal Hypoxic-Ischemic Encephalopathy (HIE). J Stroke Cerebrovasc Dis. 2021;30(3):105553. Epub 2020/12/29. doi: 10.1016/j.jstrokecerebrovasdis.2020.105553. PubMed PMID: 33360521.

24. Jickling GC, Ander BP, Zhan X, Noblett D, Stamova B, Liu D. microRNA expression in peripheral blood cells following acute ischemic stroke and their predicted gene targets. PloS one. 2014;9(6):e99283-e. doi: 10.1371/journal.pone.0099283. PubMed PMID: 24911610.

25. Wang Z, Li L, Cui Y. miR-148a regulates inflammation in microglia induced by oxygen-glucose deprivation via MAPK signal pathways. INTERNATIONAL JOURNAL OF CLINICAL AND EXPERIMENTAL MEDICINE. 2019;12(5):5003-12.

26. O'Sullivan MP, Looney AM, Moloney GM, Finder M, Hallberg B, Clarke G, Boylan GB, Murray DM. Validation of Altered Umbilical Cord Blood MicroRNA Expression in

Neonatal Hypoxic-Ischemic Encephalopathy. JAMA neurology. 2019;76(3):333-41. doi: 10.1001/jamaneurol.2018.4182. PubMed PMID: 30592487.

27. Wang Z, Liu Y, Shao M, Wang D, Zhang Y. Combined prediction of miR-210 and miR-374a for severity and prognosis of hypoxic–ischemic encephalopathy. Brain and Behavior. 2018;8(1):e00835.

28. Looney A, Ahearne C, Hallberg B, Boylan G, Murray D. Downstream mRNA target analysis in neonatal hypoxic-ischaemic encephalopathy identifies novel marker of severe injury: A proof of concept paper. Molecular neurobiology. 2017;54(10):8420-8.

29. Looney A, O'Sullivan M, Ahearne C, Finder M, Felderhoff-Mueser U, Boylan G, Hallberg B, Murray DM. Altered expression of umbilical cord blood levels of miR-181b and its downstream target mUCH-L1 in infants with moderate and severe neonatal hypoxic-ischaemic encephalopathy. Molecular neurobiology. 2019;56(5):3657-63.

30. Meng Q, Yang P, Lu Y. MicroRNA-410 serves as a candidate biomarker in hypoxic-ischemic encephalopathy newborns and provides neuroprotection in oxygen-glucose deprivation-injured PC12 and SH-SY5Y cells. Brain and behavior. 2021;11(8):e2293-e. Epub 2021/07/31. doi: 10.1002/brb3.2293. PubMed PMID: 34331407.

31. Vonkova B, Blahakova I, Hruban L, Janku P, Pospisilova S. MicroRNA-210 expression during childbirth and postpartum as a potential biomarker of acute fetal hypoxia. Biomedical Papers. 2019;163(3):259-64.

32. Xu P, Ma Y, Wu H, Wang Y-L. Placenta-Derived MicroRNAs in the Pathophysiology of Human Pregnancy. Frontiers in Cell and Developmental Biology. 2021;9:540.

33. Reliszko Z, Gajewski Z, Kaczmarek M. Signs of embryo-maternal communication: miRNAs in the maternal serum of pregnant pigs. Reproduction. 2017;154(3):217-28.

34. Michniewicz B, Szpecht D, Sowińska A, Sibiak R, Szymankiewicz M, Gadzinowski J. Biomarkers in newborns with hypoxic-ischemic encephalopathy treated with therapeutic hypothermia. Child's Nervous System. 2020;36(12):2981-8.

35. Liu FJ, Kaur P, Karolina DS, Sepramaniam S, Armugam A, Wong PT, Jeyaseelan K. MiR-335 regulates Hif-1α to reduce cell death in both mouse cell line and rat ischemic models. PloS one. 2015;10(6):e0128432.

36. Chen H-j, Yang T-t. Expression and significance of serum miRNA-21 control HIF-1α in newborn with asphyxia. Chinese Journal of Child Health Care. 2015;23(1):32.

37. Ponnusamy V, Kapellou O, Yip E, Evanson J, Wong L-F, Michael-Titus A, Yip PK, Shah DK. A study of microRNAs from dried blood spots in newborns after perinatal asphyxia: a simple and feasible biosampling method. Pediatric research. 2016;79(5):799-805.

38. Garberg HT, Huun MU, Baumbusch LO, Åsegg-Atneosen M, Solberg R, Saugstad OD. Temporal profile of circulating microRNAs after global hypoxia-ischemia in newborn piglets. Neonatology. 2017;111(2):133-9.

39. Ma Q, Dasgupta C, Li Y, Bajwa NM, Xiong F, Harding B, Hartman R, Zhang L. Inhibition of microRNA-210 provides neuroprotection in hypoxic–ischemic brain injury in neonatal rats. Neurobiology of disease. 2016;89:202-12.

40. Li B, Dasgupta C, Huang L, Meng X, Zhang L. MiRNA-210 induces microglial activation and regulates microglia-mediated neuroinflammation in neonatal hypoxic-

ischemic encephalopathy. Cellular & Molecular Immunology. 2019. doi: 10.1038/s41423-019-0257-6.

41. Qiu J, Zhou X-y, Zhou X-g, Cheng R, Liu H-y, Li Y. Neuroprotective effects of microRNA-210 on hypoxic-ischemic encephalopathy. BioMed research international. 2013;2013.

42. Xiao P, Jin Y, Miao-Xia H, Yu-Dong P, Yan-Shan X. miR-210 Is Up-Regulated in the Peripheral Blood of Asphyxiated Neonates. Iranian Journal of Pediatrics. 2019;29(6).

43. O'Sullivan MP, Looney AM, Moloney GM, Finder M, Hallberg B, Clarke G, Boylan GB, Murray DM. Validation of Altered Umbilical Cord Blood MicroRNA Expression in Neonatal Hypoxic-Ischemic EncephalopathyValidation of Altered microRNA Expression in Neonatal Hypoxic-Ischemic EncephalopathyValidation of Altered microRNA Expression in Neonatal Hypoxic-Ischemic Encephalopathy. JAMA Neurology. 2019;76(3):333-41. doi: 10.1001/jamaneurol.2018.4182.

44. Yuan Y, Wang JY, Xu LY, Cai R, Chen Z, Luo BY. MicroRNA expression changes in the hippocampi of rats subjected to global ischemia. J Clin Neurosci. 2010;17(6):774-8. Epub 2010/01/19. doi: 10.1016/j.jocn.2009.10.009. PubMed PMID: 20080409.

45. Xu L-J, Ouyang Y-B, Xiong X, Stary CM, Giffard RG. Post-stroke treatment with miR-181 antagomir reduces injury and improves long-term behavioral recovery in mice after focal cerebral ischemia. Experimental neurology. 2015;264:1-7. Epub 2014/11/26. doi: 10.1016/j.expneurol.2014.11.007. PubMed PMID: 25433215.

46. Ouyang Y-B, Lu Y, Yue S, Xu L-J, Xiong X-X, White RE, Sun X, Giffard RG. miR-181 regulates GRP78 and influences outcome from cerebral ischemia in vitro and in

vivo. Neurobiology of disease. 2012;45(1):555-63. Epub 2011/09/24. doi: 10.1016/j.nbd.2011.09.012. PubMed PMID: 21983159.

47. Zhu J, Yao K, Wang Q, Guo J, Shi H, Ma L, Liu H, Gao W, Zou Y, Ge J. Circulating miR-181a as a potential novel biomarker for diagnosis of acute myocardial infarction. Cellular Physiology and Biochemistry. 2016;40(6):1591-602.

48. Griffiths BB, Arvola O, Bhutani A, Pastroudis J, Xu L, Stary C. Abstract WMP76: Sexually Dimorphic Response to Stroke of miR-181a and miR-200c in Aged Mice. Stroke; a journal of cerebral circulation. 2019;50(Suppl_1):AWMP76-AWMP.

49. Cho KHT, Xu B, Blenkiron C, Fraser M. Emerging roles of miRNAs in brain development and perinatal brain injury. Frontiers in physiology. 2019;10.

50. Greco S, Martelli F. MicroRNAs in Hypoxia Response. Antioxid Redox Signal. 2014;21(8):1164-6. doi: 10.1089/ars.2014.6083. PubMed PMID: 25098394.

51. Azzouzi HE, Leptidis S, Doevendans PA, De Windt LJ. HypoxamiRs: regulators of cardiac hypoxia and energy metabolism. Trends Endocrinol Metab. 2015;26(9):502-8. Epub 2015/07/23. doi: 10.1016/j.tem.2015.06.008. PubMed PMID: 26197955.

52. Koehler J, Sandey M, Prasad N, Levy SA, Wang X, Wang X. Differential Expression of miRNAs in Hypoxia (“HypoxamiRs”) in Three Canine High-Grade Glioma Cell Lines. Frontiers in Veterinary Science. 2020;7(104). doi: 10.3389/fvets.2020.00104.

53. Caballero-Garrido E, Pena-Philippides JC, Lordkipanidze T, Bragin D, Yang Y, Erhardt EB, Roitbak T. In vivo inhibition of miR-155 promotes recovery after experimental mouse stroke. Journal of Neuroscience. 2015;35(36):12446-64.

54. Cuomo O, Cepparulo P, Anzilotti S, Serani A, Sirabella R, Brancaccio P, Guida N, Valsecchi V, Vinciguerra A, Molinaro P, Formisano L, Annunziato L, Pignataro G. Anti-miR-223-5p Ameliorates Ischemic Damage and Improves Neurological Function by

Preventing NCKX2 Downregulation after Ischemia in Rats. Mol Ther Nucleic Acids. 2019;18:1063-71. Epub 2019/12/04. doi: 10.1016/j.omtn.2019.10.022. PubMed PMID: 31791013; PMCID: PMC6906731.

55. Kumar P, Wu H, McBride JL, Jung K-E, Kim MH, Davidson BL, Lee SK, Shankar P, Manjunath N. Transvascular delivery of small interfering RNA to the central nervous system. Nature. 2007;448(7149):39-43.

56. Huang L, Ma Q, Li Y, Li B, Zhang L. Inhibition of microRNA-210 suppresses pro-inflammatory response and reduces acute brain injury of ischemic stroke in mice. Experimental neurology. 2018;300:41-50.

57. Zhang H, Wu J, Wu J, Fan Q, Zhou J, Wu J, Liu S, Zang J, Ye J, Xiao M. Exosome-mediated targeted delivery of miR-210 for angiogenic therapy after cerebral ischemia in mice. Journal of nanobiotechnology. 2019;17(1):29.

58. Ma Q, Dasgupta C, Shen G, Li Y, Zhang L. MicroRNA-210 downregulates TET2 and contributes to inflammatory response in neonatal hypoxic-ischemic brain injury. J Neuroinflammation. 2021;18(1):6. Epub 2021/01/07. doi: 10.1186/s12974-020-02068-w. PubMed PMID: 33402183; PMCID: PMC7786974.

59. Ma Q, Dasgupta C, Li Y, Huang L, Zhang L. MicroRNA-210 downregulates ISCU and induces mitochondrial dysfunction and neuronal death in neonatal hypoxic-ischemic brain injury. Molecular neurobiology. 2019;56(8):5608-25.

60. Ma Q, Dasgupta C, Li Y, Huang L, Zhang L. MicroRNA-210 suppresses junction proteins and disrupts blood-brain barrier integrity in neonatal rat hypoxic-ischemic brain injury. International journal of molecular sciences. 2017;18(7):1356.

61. Qiu J, Zhou X-y, Zhou X-g, Cheng R, Liu H-y, Li Y. Neuroprotective Effects of MicroRNA-210 on Hypoxic-Ischemic Encephalopathy. BioMed Research International. 2013;2013:5. doi: 10.1155/2013/350419.

62. Chen Z, Hu Y, Lu R, Ge M, Zhang L. MicroRNA-374a-5p inhibits neuroinflammation in neonatal hypoxic-ischemic encephalopathy via regulating NLRP3 inflammasome targeted Smad6. Life Sciences. 2020:117664.

63. Chen R, Wang M, Fu S, Cao F, Duan P, Lu J. MicroRNA-204 may participate in the pathogenesis of hypoxic-ischemic encephalopathy through targeting KLLN. Experimental and therapeutic medicine. 2019;18(5):3299-306.

64. Xiong L, Zhou H, Zhao Q, Xue L, Al-Hawwas M, He J, Wu M, Zou Y, Yang M, Dai J. Overexpression of miR-124 Protects Against Neurological Dysfunction Induced by Neonatal Hypoxic–Ischemic Brain Injury. Cellular and Molecular Neurobiology. 2020:1-14.

65. Shi H, Xu Y, Cai W. Protective role of microRNA-454-3p in neonatal hypoxic-ischaemic encephalopathy by targeting ST18. Biotechnology & Biotechnological Equipment. 2020;34(1):211-20.

66. Wang X, Zhou H, Cheng R, Zhou X, Hou X, Chen J, Qiu J. Role of miR-326 in neonatal hypoxic-ischemic brain damage pathogenesis through targeting of the δ-opioid receptor. Molecular Brain. 2020;13(1):1-13.

67. Coenen-Stass AML, Pauwels MJ, Hanson B, Martin Perez C, Conceição M, Wood MJA, Mäger I, Roberts TC. Extracellular microRNAs exhibit sequence-dependent stability and cellular release kinetics. RNA Biol. 2019;16(5):696-706. Epub 2019/03/05. doi: 10.1080/15476286.2019.1582956. PubMed PMID: 30836828.

68. Mai H, Fan W, Wang Y, Cai Y, Li X, Chen F, Chen X, Yang J, Tang P, Chen H. Intranasal administration of miR-146a agomir rescued the pathological process and cognitive impairment in an AD mouse model. Molecular Therapy-Nucleic Acids. 2019;18:681-95.

69. Hanson LR, Frey WH, 2nd. Intranasal delivery bypasses the blood-brain barrier to target therapeutic agents to the central nervous system and treat neurodegenerative disease. BMC neuroscience. 2008;9 Suppl 3(Suppl 3):S5-S. doi: 10.1186/1471-2202-9-S3-S5. PubMed PMID: 19091002.

70. Tao H, Zhao J, Liu T, Cai Y, Zhou X, Xing H, Wang Y, Yin M, Zhong W, Liu Z, Li K, Zhao B, Zhou H, Cui L. Intranasal Delivery of miR-146a Mimics Delayed Seizure Onset in the Lithium-Pilocarpine Mouse Model. Mediators Inflamm. 2017;2017:6512620. Epub 2017/03/01. doi: 10.1155/2017/6512620. PubMed PMID: 28242958; PMCID: PMC5294386 publication of this article.

71. Maas SLN, Breakefield XO, Weaver AM. Extracellular Vesicles: Unique Intercellular Delivery Vehicles. Trends in cell biology. 2017;27(3):172-88. Epub 2016/12/17. doi: 10.1016/j.tcb.2016.11.003. PubMed PMID: 27979573; PMCID: PMC5318253.

72. Zaborowski MP, Balaj L, Breakefield XO, Lai CP. Extracellular Vesicles: Composition, Biological Relevance, and Methods of Study. Bioscience. 2015;65(8):783-97. Epub 2016/03/10. doi: 10.1093/biosci/biv084. PubMed PMID: 26955082; PMCID: PMC4776721.

73. Wang S, Cesca F, Loers G, Schweizer M, Buck F, Benfenati F, Schachner M, Kleene R. Synapsin I is an oligomannose-carrying glycoprotein, acts as an oligomannose-binding lectin, and promotes neurite outgrowth and neuronal survival

when released via glia-derived exosomes. J Neurosci. 2011;31(20):7275-90. Epub 2011/05/20. doi: 10.1523/JNEUROSCI.6476-10.2011. PubMed PMID: 21593312.

74. Zappulli V, Friis KP, Fitzpatrick Z, Maguire CA, Breakefield XO. Extracellular vesicles and intercellular communication within the nervous system. J Clin Invest. 2016;126(4):1198-207. Epub 2016/04/02. doi: 10.1172/jci81134. PubMed PMID: 27035811; PMCID: PMC4811121.

75. Zhuang X, Xiang X, Grizzle W, Sun D, Zhang S, Axtell RC, Ju S, Mu J, Zhang L, Steinman L. Treatment of brain inflammatory diseases by delivering exosome encapsulated anti-inflammatory drugs from the nasal region to the brain. Molecular Therapy. 2011;19(10):1769-79.

76. Drommelschmidt K, Serdar M, Bendix I, Herz J, Bertling F, Prager S, Keller M, Ludwig A-K, Duhan V, Radtke S, de Miroschedji K, Horn PA, van de Looij Y, Giebel B, Felderhoff-Müser U. Mesenchymal stem cell-derived extracellular vesicles ameliorate inflammation-induced preterm brain injury. Brain, Behavior, and Immunity. 2017;60:220-32. doi: https://doi.org/10.1016/j.bbi.2016.11.011.

77. Doeppner TR, Herz J, Gorgens A, Schlechter J, Ludwig AK, Radtke S, de Miroschedji K, Horn PA, Giebel B, Hermann DM. Extracellular Vesicles Improve Post-Stroke Neuroregeneration and Prevent Postischemic Immunosuppression. Stem Cells Transl Med. 2015;4(10):1131-43. Epub 2015/09/05. doi: 10.5966/sctm.2015-0078. PubMed PMID: 26339036; PMCID: PMC4572905.

78. Thery C, Witwer KW, Aikawa E, Alcaraz MJ, Anderson JD, Andriantsitohaina R, Antoniou A, Arab T, Archer F, Atkin-Smith GK, Ayre DC, Bach JM, Bachurski D, Baharvand H, Balaj L, Baldacchino S, Bauer NN, Baxter AA, Bebawy M, Beckham C, et al. Minimal information for studies of extracellular vesicles 2018 (MISEV2018): a position

statement of the International Society for Extracellular Vesicles and update of the MISEV2014 guidelines. J Extracell Vesicles. 2018;7(1):1535750. Epub 2019/01/15. doi: 10.1080/20013078.2018.1535750. PubMed PMID: 30637094; PMCID: PMC6322352.

79. Ghossoub R, Lembo F, Rubio A, Gaillard CB, Bouchet J, Vitale N, Slavik J, Machala M, Zimmermann P. Syntenin-ALIX exosome biogenesis and budding into multivesicular bodies are controlled by ARF6 and PLD2. Nat Commun. 2014;5:3477. doi: 10.1038/ncomms4477. PubMed PMID: 24637612.

80. Trajkovic K, Hsu C, Chiantia S, Rajendran L, Wenzel D, Wieland F, Schwille P, Brugger B, Simons M. Ceramide triggers budding of exosome vesicles into multivesicular endosomes. Science. 2008;319(5867):1244-7. doi: 10.1126/science.1153124. PubMed PMID: 18309083.

81. Yanez-Mo M, Siljander PR, Andreu Z, Zavec AB, Borras FE, Buzas EI, Buzas K, Casal E, Cappello F, Carvalho J, Colas E, Cordeiro-da Silva A, Fais S, Falcon-Perez JM, Ghobrial IM, Giebel B, Gimona M, Graner M, Gursel I, Gursel M, et al. Biological properties of extracellular vesicles and their physiological functions. J Extracell Vesicles. 2015;4:27066. Epub 2015/05/17. doi: 10.3402/jev.v4.27066. PubMed PMID: 25979354; PMCID: PMC4433489.

82. Airola MV, Hannun YA. Sphingolipid metabolism and neutral sphingomyelinases. Handb Exp Pharmacol. 2013(215):57-76. doi: 10.1007/978-3-7091-1368-4_3. PubMed PMID: 23579449; PMCID: PMC4043343.

83. Llorente A, Skotland T, Sylvanne T, Kauhanen D, Rog T, Orlowski A, Vattulainen I, Ekroos K, Sandvig K. Molecular lipidomics of exosomes released by PC-3 prostate cancer cells. Biochim Biophys Acta. 2013;1831(7):1302-9. Epub 2013/09/21. PubMed PMID: 24046871.

84. Morelli AE, Larregina AT, Shufesky WJ, Sullivan ML, Stolz DB, Papworth GD, Zahorchak AF, Logar AJ, Wang Z, Watkins SC, Falo LD, Jr., Thomson AW. Endocytosis, intracellular sorting, and processing of exosomes by dendritic cells. Blood. 2004;104(10):3257-66. Epub 2004/07/31. doi: 10.1182/blood-2004-03-0824. PubMed PMID: 15284116.

85. Laulagnier K, Motta C, Hamdi S, Roy S, Fauvelle F, Pageaux JF, Kobayashi T, Salles JP, Perret B, Bonnerot C, Record M. Mast cell- and dendritic cell-derived exosomes display a specific lipid composition and an unusual membrane organization. Biochem J. 2004;380(Pt 1):161-71. Epub 2004/02/18. doi: 10.1042/BJ20031594. PubMed PMID: 14965343; PMCID: PMC1224152.

86. Vidal M, Sainte-Marie J, Philippot JR, Bienvenue A. Asymmetric distribution of phospholipids in the membrane of vesicles released during in vitro maturation of guinea pig reticulocytes: evidence precluding a role for "aminophospholipid translocase". J Cell Physiol. 1989;140(3):455-62. Epub 1989/09/01. doi: 10.1002/jcp.1041400308. PubMed PMID: 2777884.

87. Han J, Yang S, Hao X, Zhang B, Zhang H, Xin C, Hao Y. Extracellular Vesicle-Derived microRNA-410 From Mesenchymal Stem Cells Protects Against Neonatal Hypoxia-Ischemia Brain Damage Through an HDAC1-Dependent EGR2/Bcl2 Axis. Frontiers in cell and developmental biology. 2021;8:579236-. doi: 10.3389/fcell.2020.579236. PubMed PMID: 33505958.

88. Yang J, Zhang X, Chen X, Wang L, Yang G. Exosome Mediated Delivery of miR-124 Promotes Neurogenesis after Ischemia. Mol Ther Nucleic Acids. 2017;7:278-87. Epub 2017/06/19. doi: 10.1016/j.omtn.2017.04.010. PubMed PMID: 28624203; PMCID: PMC5415550.

89. Xin H, Katakowski M, Wang F, Qian JY, Liu XS, Ali MM, Buller B, Zhang ZG, Chopp M. MicroRNA cluster miR-17-92 Cluster in Exosomes Enhance Neuroplasticity and Functional Recovery After Stroke in Rats. Stroke. 2017;48(3):747-53. Epub 2017/02/25. doi: 10.1161/strokeaha.116.015204. PubMed PMID: 28232590; PMCID: PMC5330787.

90. Li Y, Ren C, Li H, Jiang F, Wang L, Xia C, Ji X. Role of exosomes induced by remote ischemic preconditioning in neuroprotection against cerebral ischemia. NeuroReport. 2019;30(12).

91. Borosch S, Dahmen E, Beckers C, Stoppe C, Buhl EM, Denecke B, Goetzenich A, Kraemer S. Characterization of extracellular vesicles derived from cardiac cells in an in vitro model of preconditioning. Journal of extracellular vesicles. 2017;6(1):1390391. doi: 10.1080/20013078.2017.1390391.

92. Miao W, Bao T-H, Han J-H, Yin M, Zhang J, Yan Y, Zhu Y-H. Neuroprotection induced by post-conditioning following ischemia/reperfusion in mice is associated with altered microRNA expression. Molecular medicine reports. 2016;14(3):2582-8. Epub 2016/07/29. doi: 10.3892/mmr.2016.5576. PubMed PMID: 27485299.

93. Ti D, Hao H, Tong C, Liu J, Dong L, Zheng J, Zhao Y, Liu H, Fu X, Han W. LPS-preconditioned mesenchymal stromal cells modify macrophage polarization for resolution of chronic inflammation via exosome-shuttled let-7b. Journal of translational medicine. 2015;13:308. Epub 2015/09/21. doi: 10.1186/s12967-015-0642-6. PubMed PMID: 26386558; PMCID: PMC4575470.

94. Sheldon RA, Sedik C, Ferriero DM. Strain-related brain injury in neonatal mice subjected to hypoxia-ischemia. Brain Res. 1998;810(1-2):114-22. PubMed PMID: 9813271.

95. Tian C, Ambroz RJ, Sun L, Wang Y, Ma K, Chen Q, Zhu B, Zheng JC. Direct conversion of dermal fibroblasts into neural progenitor cells by a novel cocktail of defined factors. Curr Mol Med. 2012;12(2):126-37. Epub 2011/12/17. doi: 10.2174/156652412798889018. PubMed PMID: 22172100; PMCID: PMC3434966.

96. Lötvall J, Hill AF, Hochberg F, Buzás EI, Di Vizio D, Gardiner C, Gho YS, Kurochkin IV, Mathivanan S, Quesenberry P, Sahoo S, Tahara H, Wauben MH, Witwer KW, Théry C. Minimal experimental requirements for definition of extracellular vesicles and their functions: a position statement from the International Society for Extracellular Vesicles. Journal of extracellular vesicles. 2014;3:26913-. doi: 10.3402/jev.v3.26913. PubMed PMID: 25536934.

97. Bachurski D, Schuldner M, Nguyen P-H, Malz A, Reiners KS, Grenzi PC, Babatz F, Schauss AC, Hansen HP, Hallek M, Pogge von Strandmann E. Extracellular vesicle measurements with nanoparticle tracking analysis - An accuracy and repeatability comparison between NanoSight NS300 and ZetaView. Journal of extracellular vesicles. 2019;8(1):1596016-. doi: 10.1080/20013078.2019.1596016. PubMed PMID: 30988894.

98. Livak KJ, Schmittgen TD. Analysis of relative gene expression data using real-time quantitative PCR and the 2(-Delta Delta C(T)) Method. Methods. 2001;25(4):402-8. Epub 2002/02/16. doi: 10.1006/meth.2001.1262. PubMed PMID: 11846609.

99. Gallo-Oller G, Ordonez R, Dotor J. A new background subtraction method for Western blot densitometry band quantification through image analysis software. J Immunol Methods. 2018;457:1-5. Epub 2018/03/10. doi: 10.1016/j.jim.2018.03.004. PubMed PMID: 29522776.

100. Kiezun A, Artzi S, Modai S, Volk N, Isakov O, Shomron N. miRviewer: a multispecies microRNA homologous viewer. BMC Research Notes. 2012;5(1):92. doi: 10.1186/1756-0500-5-92.

101. Vlachos IS, Zagganas K, Paraskevopoulou MD, Georgakilas G, Karagkouni D, Vergoulis T, Dalamagas T, Hatzigeorgiou AG. DIANA-miRPath v3. 0: deciphering microRNA function with experimental support. Nucleic acids research. 2015;43(W1):W460-W6.

102. Qiu C, Wang J, Cui Q, editors. miR2Gene: pattern discovery of single gene, multiple genes, and pathways by enrichment analysis of their microRNA regulators. BMC systems biology; 2011: Springer.

103. O'Sullivan MP, Looney AM, Moloney GM, Finder M, Hallberg B, Clarke G, Boylan GB, Murray DM. Validation of altered umbilical cord blood microRNA expression in neonatal hypoxic-ischemic encephalopathy. JAMA neurology. 2019;76(3):333-41.

104. Kelly LA, O'Dea MI, Zareen Z, Melo AM, McKenna E, Strickland T, McEneaney V, Donoghue V, Boylan G, Sweetman D, Butler J, Vavasseur C, Miletin J, El-Khuffash AF, O'Neill LAJ, O'Leary JJ, Molloy EJ. Altered inflammasome activation in neonatal encephalopathy persists in childhood. Clin Exp Immunol. 2021. Epub 2021/03/27. doi: 10.1111/cei.13598. PubMed PMID: 33768526.

105. Zhao F, Qu Y, Liu J, Liu H, Zhang L, Feng Y, Wang H, Gan J, Lu R, Mu D. Microarray profiling and co-expression network analysis of LncRNAs and mRNAs in neonatal rats following hypoxic-ischemic brain damage. Scientific reports. 2015;5(1):1-11.

106. Xiong L-L, Xue L-L, Al-Hawwas M, Huang J, Niu R-Z, Tan Y-X, Xu Y, Su Y-Y, Liu J, Wang T-H. Single-nucleotide polymorphism screening and RNA sequencing of key

messenger RNAs associated with neonatal hypoxic-ischemia brain damage. Neural regeneration research. 2020;15(1):86.

107. O'Sullivan MP, Casey S, Finder M, Ahearne C, Clarke G, Hallberg B, Boylan GB, Murray DM. Up-Regulation of Nfat5 mRNA and Fzd4 mRNA as a Marker of Poor Outcome in Neonatal Hypoxic-Ischemic Encephalopathy. The Journal of Pediatrics. 2021;228:74-81. e2.

108. Juul SE, Beyer RP, Bammler TK, McPherson RJ, Wilkerson J, Farin FM. Microarray analysis of high-dose recombinant erythropoietin treatment of unilateral brain injury in neonatal mouse hippocampus. Pediatric research. 2009;65(5):485-92.

109. Douglas-Escobar MV, Weiss MD. Biomarkers of hypoxic-ischemic encephalopathy in newborns. Frontiers in neurology. 2012;3:144.

110. Massaro AN, Wu YW, Bammler TK, Comstock B, Mathur A, McKinstry RC, Chang T, Mayock DE, Mulkey SB, Van Meurs K. Plasma biomarkers of brain injury in neonatal hypoxic-ischemic encephalopathy. The Journal of pediatrics. 2018;194:67-75. e1.

111. Sharma S, Eghbali M. Influence of sex differences on microRNA gene regulation in disease. Biol Sex Differ. 2014;5(1):3-. doi: 10.1186/2042-6410-5-3. PubMed PMID: 24484532.

112. Hua Y-J, Tang Z-Y, Tu K, Zhu L, Li Y-X, Xie L, Xiao H-S. Identification and target prediction of miRNAs specifically expressed in rat neural tissue. BMC genomics. 2009;10(1):1-12.

113. Vannucci RC, Lyons DT, Vasta F. Regional cerebral blood flow during hypoxia-ischemia in immature rats. Stroke; a journal of cerebral circulation. 1988;19(2):245-50.

114. Sathyanesan A, Zhou J, Scafidi J, Heck DH, Sillitoe RV, Gallo V. Emerging connections between cerebellar development, behaviour and complex brain disorders. Nature Reviews Neuroscience. 2019;20(5):298-313. doi: 10.1038/s41583-019-0152-2.

115. Archambault J, Moreira A, McDaniel D, Winter L, Sun L, Hornsby P. Therapeutic potential of mesenchymal stromal cells for hypoxic ischemic encephalopathy: A systematic review and meta-analysis of preclinical studies. PloS one. 2017;12(12):e0189895. Epub 2017/12/21. doi: 10.1371/journal.pone.0189895. PubMed PMID: 29261798; PMCID: PMC5736208.

116. Patel DM, Shah J, Srivastava AS. Therapeutic potential of mesenchymal stem cells in regenerative medicine. Stem cells international. 2013;2013.

117. Drommelschmidt K, Serdar M, Bendix I, Herz J, Bertling F, Prager S, Keller M, Ludwig A-K, Duhan V, Radtke S. Mesenchymal stem cell-derived extracellular vesicles ameliorate inflammation-induced preterm brain injury. Brain, behavior, and immunity. 2017;60:220-32.

118. Webb RL, Kaiser EE, Scoville SL, Thompson TA, Fatima S, Pandya C, Sriram K, Swetenburg RL, Vaibhav K, Arbab AS. Human neural stem cell extracellular vesicles improve tissue and functional recovery in the murine thromboembolic stroke model. Translational stroke research. 2018;9(5):530-9.

119. Mathieu M, Martin-Jaular L, Lavieu G, Théry C. Specificities of secretion and uptake of exosomes and other extracellular vesicles for cell-to-cell communication. Nature cell biology. 2019;21(1):9-17.

120. Vogel A, Upadhya R, Shetty AK. Neural stem cell derived extracellular vesicles: attributes and prospects for treating neurodegenerative disorders. EBioMedicine. 2018;38:273-82.

121. Ophelders DR, Wolfs TG, Jellema RK, Zwanenburg A, Andriessen P, Delhaas T, Ludwig A-K, Radtke S, Peters V, Janssen L. Mesenchymal stromal cell-derived extracellular vesicles protect the fetal brain after hypoxia-ischemia. Stem cells translational medicine. 2016;5(6):754-63.

122. Doeppner TR, Herz J, Görgens A, Schlechter J, Ludwig A-K, Radtke S, de Miroschedji K, Horn PA, Giebel B, Hermann DM. Extracellular vesicles improve post-stroke neuroregeneration and prevent postischemic immunosuppression. Stem cells translational medicine. 2015;4(10):1131-43.

123. Zonneveld MI, Keulers TG, Rouschop K. Extracellular vesicles as transmitters of hypoxia tolerance in solid cancers. Cancers. 2019;11(2):154.

124. Huang S, Ge X, Yu J, Han Z, Yin Z, Li Y, Chen F, Wang H, Zhang J, Lei P. Increased miR-124-3p in microglial exosomes following traumatic brain injury inhibits neuronal inflammation and contributes to neurite outgrowth via their transfer into neurons. The FASEB Journal. 2018;32(1):512-28.

125. Perets N, Hertz S, London M, Offen D. Intranasal administration of exosomes derived from mesenchymal stem cells ameliorates autistic-like behaviors of BTBR mice. Mol Autism. 2018;9:57-. doi: 10.1186/s13229-018-0240-6. PubMed PMID: 30479733.

126. Kodali M, Castro OW, Kim D-K, Thomas A, Shuai B, Attaluri S, Upadhya R, Gitai D, Madhu LN, Prockop DJ, Shetty AK. Intranasally Administered Human MSC-Derived Extracellular Vesicles Pervasively Incorporate into Neurons and Microglia in both Intact and Status Epilepticus Injured Forebrain. International journal of molecular sciences. 2019;21(1):181. doi: 10.3390/ijms21010181. PubMed PMID: 31888012.

127. Losurdo M, Pedrazzoli M, D'Agostino C, Elia CA, Massenzio F, Lonati E, Mauri M, Rizzi L, Molteni L, Bresciani E, Dander E, D'Amico G, Bulbarelli A, Torsello A,

Matteoli M, Buffelli M, Coco S. Intranasal delivery of mesenchymal stem cell-derived extracellular vesicles exerts immunomodulatory and neuroprotective effects in a 3xTg model of Alzheimer's disease. STEM CELLS Translational Medicine. 2020;9(9):1068-84. doi: https://doi.org/10.1002/sctm.19-0327.

128. Long Q, Upadhya D, Hattiangady B, Kim D-K, An SY, Shuai B, Prockop DJ, Shetty AK. Intranasal MSC-derived A1-exosomes ease inflammation, and prevent abnormal neurogenesis and memory dysfunction after status epilepticus. Proceedings of the National Academy of Sciences of the United States of America. 2017;114(17):E3536-E45. doi: 10.1073/pnas.1703920114. PubMed PMID: PMC5410779.

129. Lingam I, Avdic-Belltheus A, Meehan C, Martinello K, Ragab S, Peebles D, Barkhuizen M, Tann CJ, Tachtsidis I, Wolfs TG. Serial blood cytokine and chemokine mRNA and microRNA over 48 h are insult specific in a piglet model of inflammation-sensitized hypoxia–ischaemia. Pediatric research. 2021;89(3):464-75.

130. Salmaso N, Jablonska B, Scafidi J, Vaccarino FM, Gallo V. Neurobiology of premature brain injury. Nature neuroscience. 2014;17(3):341-6.

131. Tannich F, Tlili A, Pintard C, Chniguir A, Eto B, Dang PM-C, Souilem O, El-Benna J. Activation of the phagocyte NADPH oxidase/NOX2 and myeloperoxidase in the mouse brain during pilocarpine-induced temporal lobe epilepsy and inhibition by ketamine. Inflammopharmacology. 2020;28(2):487-97.

132. Mai N, Miller-Rhodes K, Prifti V, Kim M, O'Reilly MA, Halterman MW. Lung-Derived SOD3 Attenuates Neurovascular Injury After Transient Global Cerebral Ischemia. Journal of the American Heart Association. 2019;8(9):e011801.

133. Zaghloul N, Patel H, Codipilly C, Marambaud P, Dewey S, Frattini S, Huerta PT, Nasim M, Miller EJ, Ahmed M. Overexpression of extracellular superoxide dismutase protects against brain injury induced by chronic hypoxia. PloS one. 2014;9(9):e108168.

134. Cao D, Qiao H, He D, Qin X, Zhang Q, Zhou Y. Mesenchymal stem cells inhibited the inflammation and oxidative stress in LPS-activated microglial cells through AMPK pathway. Journal of Neural Transmission. 2019;126(12):1589-97.

135. Edwards G, Gamez N, Armijo E, Kramm C, Morales R, Taylor-Presse K, Schulz PE, Soto C, Moreno-Gonzalez I. Peripheral Delivery of Neural Precursor Cells Ameliorates Parkinson's Disease-Associated Pathology. Cells. 2019;8(11):1359.

136. Cottrill KA, Chan SY, Loscalzo J. Hypoxamirs and mitochondrial metabolism. Antioxid Redox Signal. 2014;21(8):1189-201. Epub 2014/02/03. doi: 10.1089/ars.2013.5641. PubMed PMID: 24111795.

137. Hale AE, White K, Chan SY. Hypoxamirs in pulmonary hypertension: breathing new life into pulmonary vascular research. Cardiovascular diagnosis and therapy. 2012;2(3):200.

138. Gou D, Ramchandran R, Peng X, Yao L, Kang K, Sarkar J, Wang Z, Zhou G, Raj JU. miR-210 has an antiapoptotic effect in pulmonary artery smooth muscle cells during hypoxia. American Journal of Physiology-Lung Cellular and Molecular Physiology. 2012;303(8):L682-L91.

139. Fasanaro P, D'Alessandra Y, Di Stefano V, Melchionna R, Romani S, Pompilio G, Capogrossi MC, Martelli F. MicroRNA-210 modulates endothelial cell response to hypoxia and inhibits the receptor tyrosine kinase ligand Ephrin-A3. Journal of biological chemistry. 2008;283(23):15878-83.

140. Huck O, Al-Hashemi J, Poidevin L, Poch O, Davideau JL, Tenenbaum H, Amar S. Identification and Characterization of MicroRNA Differentially Expressed in Macrophages Exposed to Porphyromonas gingivalis Infection. Infect Immun. 2017;85(3). Epub 2017/01/11. doi: 10.1128/iai.00771-16. PubMed PMID: 28069815; PMCID: PMC5328478.

141. Meissner L, Gallozzi M, Balbi M, Schwarzmaier S, Tiedt S, Terpolilli NA, Plesnila N. Temporal Profile of MicroRNA Expression in Contused Cortex after Traumatic Brain Injury in Mice. J Neurotrauma. 2016;33(8):713-20. Epub 2015/10/02. doi: 10.1089/neu.2015.4077. PubMed PMID: 26426744.

142. Cai Y, Zhang Y, Ke X, Guo Y, Yao C, Tang N, Pang P, Xie G, Fang L, Zhang Z, Li J, Fan Y, He X, Wen R, Pei L, Lu Y. Transcriptome Sequencing Unravels Potential Biomarkers at Different Stages of Cerebral Ischemic Stroke. Front Genet. 2019;10:814. Epub 2019/11/05. doi: 10.3389/fgene.2019.00814. PubMed PMID: 31681398; PMCID: PMC6798056.

143. Zhou L, Zang G, Zhang G, Wang H, Zhang X, Johnston N, Min W, Luke P, Jevnikar A, Haig A, Zheng X. MicroRNA and mRNA signatures in ischemia reperfusion injury in heart transplantation. PloS one. 2013;8(11):e79805. Epub 2013/11/28. doi: 10.1371/journal.pone.0079805. PubMed PMID: 24278182; PMCID: PMC3835872.

144. Raihan O, Brishti A, Molla MR, Li W, Zhang Q, Xu P, Khan MI, Zhang J, Liu Q. The Age-dependent Elevation of miR-335-3p Leads to Reduced Cholesterol and Impaired Memory in Brain. Neuroscience. 2018;390:160-73. Epub 2018/08/21. doi: 10.1016/j.neuroscience.2018.08.003. PubMed PMID: 30125687.

145. Nakanishi N, Nakagawa Y, Tokushige N, Aoki N, Matsuzaka T, Ishii K, Yahagi N, Kobayashi K, Yatoh S, Takahashi A. The up-regulation of microRNA-335 is associated

with lipid metabolism in liver and white adipose tissue of genetically obese mice. Biochemical and biophysical research communications. 2009;385(4):492-6.

146. Hsu S-D, Lin F-M, Wu W-Y, Liang C, Huang W-C, Chan W-L, Tsai W-T, Chen G-Z, Lee C-J, Chiu C-M. miRTarBase: a database curates experimentally validated microRNA–target interactions. Nucleic acids research. 2011;39(suppl_1):D163-D9.

147. Chapman SD, Farina L, Kronforst K, Dizon M. MicroRNA Profile Differences in Neonates at Risk for Cerebral Palsy. Phys Med Rehabil Int. 2018;5(3):1148. Epub 2018/05/31. PubMed PMID: 30740584.

148. Zhang H, Zhou J, Zhang M, Yi Y, He B. Upregulation of miR-376c-3p alleviates oxygen-glucose deprivation-induced cell injury by targeting ING5. Cell Mol Biol Lett. 2019;24:67-. doi: 10.1186/s11658-019-0189-2. PubMed PMID: 31844418.

149. Zhang M, Ge D, Su Z, Qi B. miR-137 alleviates focal cerebral ischemic injury in rats by regulating JAK1/STAT1 signaling pathway. Human & Experimental Toxicology. 2020;39(6):816-27. doi: 10.1177/0960327119897103. PubMed PMID: 31961204.

150. Sun G, Ye P, Murai K, Lang MF, Li S, Zhang H, Li W, Fu C, Yin J, Wang A, Ma X, Shi Y. miR-137 forms a regulatory loop with nuclear receptor TLX and LSD1 in neural stem cells. Nat Commun. 2011;2:529. Epub 2011/11/10. doi: 10.1038/ncomms1532. PubMed PMID: 22068596; PMCID: PMC3298567.

151. Yan H-L, Sun X-W, Wang Z-M, Liu P-P, Mi T-W, Liu C, Wang Y-Y, He X-C, Du H-Z, Liu C-M, Teng Z-Q. MiR-137 Deficiency Causes Anxiety-Like Behaviors in Mice. Frontiers in Molecular Neuroscience. 2019;12(260). doi: 10.3389/fnmol.2019.00260.

152. Shu P, Wu C, Liu W, Ruan X, Liu C, Hou L, Zeng Y, Fu H, Wang M, Chen P. The spatiotemporal expression pattern of microRNAs in the developing mouse nervous system. Journal of Biological Chemistry. 2019;294(10):3444-53.

153. Minatohara K, Akiyoshi M, Okuno H. Role of Immediate-Early Genes in Synaptic Plasticity and Neuronal Ensembles Underlying the Memory Trace. Frontiers in Molecular Neuroscience. 2016;8(78). doi: 10.3389/fnmol.2015.00078.

154. Avraham R, Sas-Chen A, Manor O, Steinfeld I, Shalgi R, Tarcic G, Bossel N, Zeisel A, Amit I, Zwang Y. EGF decreases the abundance of microRNAs that restrain oncogenic transcription factors. Science signaling. 2010;3(124):ra43-ra.

155. Tindall MJ, Clerk A. Modelling Negative Feedback Networks for Activating Transcription Factor 3 Predicts a Dominant Role for miRNAs in Immediate Early Gene Regulation. PLOS Computational Biology. 2014;10(5):e1003597. doi: 10.1371/journal.pcbi.1003597.

156. Aitken S, Magi S, Alhendi AMN, Itoh M, Kawaji H, Lassmann T, Daub CO, Arner E, Carninci P, Forrest ARR, Hayashizaki Y, the FC, Khachigian LM, Okada-Hatakeyama M, Semple CA. Transcriptional Dynamics Reveal Critical Roles for Non-coding RNAs in the Immediate-Early Response. PLOS Computational Biology. 2015;11(4):e1004217. doi: 10.1371/journal.pcbi.1004217.

157. Zhang W, Liu HT. MAPK signal pathways in the regulation of cell proliferation in mammalian cells. Cell Research. 2002;12(1):9-18. doi: 10.1038/sj.cr.7290105.

158. Nijboer CH, van der Kooij MA, van Bel F, Ohl F, Heijnen CJ, Kavelaars A. Inhibition of the JNK/AP-1 pathway reduces neuronal death and improves behavioral outcome after neonatal hypoxic-ischemic brain injury. Brain Behav Immun. 2010;24(5):812-21. Epub 2009/09/22. doi: 10.1016/j.bbi.2009.09.008. PubMed PMID: 19766183.

159. Han BH, Holtzman DM. BDNF protects the neonatal brain from hypoxic-ischemic injuryin vivo via the ERK pathway. Journal of Neuroscience. 2000;20(15):5775-81.

160. Zhao B, Zheng Z. Insulin Growth Factor 1 Protects Neural Stem Cells Against Apoptosis Induced by Hypoxia Through Akt/Mitogen-Activated Protein Kinase/Extracellular Signal-Regulated Kinase (Akt/MAPK/ERK) Pathway in Hypoxia-Ishchemic Encephalopathy. Med Sci Monit. 2017;23:1872-9. doi: 10.12659/msm.901055. PubMed PMID: 28420864.

161. Wang L, Shao X, Yang Y, Chen L. Effects of moderate hypothermia on p-ERK/p38 MAPK signal pathway following hypoxic-ischemic brain injury in neonatal rats. Chin J Perinat Med. 2006;9:337-40.

162. Kovács V, Tóth-Szűki V, Németh J, Varga V, Remzső G, Domoki F. Active forms of Akt and ERK are dominant in the cerebral cortex of newborn pigs that are unaffected by asphyxia. Life Sci. 2018;192:1-8. Epub 2017/11/16. doi: 10.1016/j.lfs.2017.11.015. PubMed PMID: 29138115.

163. Thomanetz V, Angliker N, Cloëtta D, Lustenberger RM, Schweighauser M, Oliveri F, Suzuki N, Rüegg MA. Ablation of the mTORC2 component rictor in brain or Purkinje cells affects size and neuron morphology. Journal of Cell Biology. 2013;201(2):293-308.

164. Zhang T, Guo J, Gu J, Chen K, Li H, Wang J. Protective Role of mTOR in Liver Ischemia/Reperfusion Injury: Involvement of Inflammation and Autophagy. Oxidative Medicine and Cellular Longevity. 2019;2019:7861290. doi: 10.1155/2019/7861290.

165. Fan X, Heijnen CJ, van der Kooij MA, Groenendaal F, van Bel F. The role and regulation of hypoxia-inducible factor-1α expression in brain development and neonatal hypoxic–ischemic brain injury. Brain Research Reviews. 2009;62(1):99-108. doi: https://doi.org/10.1016/j.brainresrev.2009.09.006.

166. Baranova O, Miranda LF, Pichiule P, Dragatsis I, Johnson RS, Chavez JC. Neuron-Specific Inactivation of the Hypoxia Inducible Factor 1α Increases Brain Injury in a Mouse Model of Transient Focal Cerebral Ischemia. The Journal of Neuroscience. 2007;27(23):6320-32. doi: 10.1523/jneurosci.0449-07.2007.

167. Chen D, Li M, Luo J, Gu W. Direct interactions between HIF-1α and Mdm2 modulate p53 function. Journal of Biological Chemistry. 2003;278(16):13595-8.

168. Guo K, Searfoss G, Krolikowski D, Pagnoni M, Franks C, Clark K, Yu KT, Jaye M, Ivashchenko Y. Hypoxia induces the expression of the pro-apoptotic gene BNIP3. Cell Death & Differentiation. 2001;8(4):367-76. doi: 10.1038/sj.cdd.4400810.

169. Greijer A, Van der Wall E. The role of hypoxia inducible factor 1 (HIF-1) in hypoxia induced apoptosis. Journal of clinical pathology. 2004;57(10):1009-14.

170. Bianciardi P, Fantacci M, Caretti A, Ronchi R, Milano G, Morel S, Von Segesser L, Corno A, Samaja M. Chronic in vivo hypoxia in various organs: hypoxia-inducible factor-1α and apoptosis. Biochemical and biophysical research communications. 2006;342(3):875-80.

171. Akakura N, Kobayashi M, Horiuchi I, Suzuki A, Wang J, Chen J, Niizeki H, Kawamura K-i, Hosokawa M, Asaka M. Constitutive expression of hypoxia-inducible factor-1α renders pancreatic cancer cells resistant to apoptosis induced by hypoxia and nutrient deprivation. Cancer research. 2001;61(17):6548-54.

172. Chen W, Jadhav V, Tang J, Zhang JH. HIF-1 alpha inhibition ameliorates neonatal brain damage after hypoxic-ischemic injury. Acta Neurochir Suppl. 2008;102:395-9. Epub 2008/01/01. doi: 10.1007/978-3-211-85578-2_77. PubMed PMID: 19388354.

173. Liang X, Liu X, Lu F, Zhang Y, Jiang X, Ferriero DM. HIF1α signaling in the endogenous protective responses after neonatal brain hypoxia-ischemia. Developmental neuroscience. 2018;40(5-6):617-26.

174. Barteczek P, Li L, Ernst A-S, Böhler L-I, Marti HH, Kunze R. Neuronal HIF-1α and HIF-2α deficiency improves neuronal survival and sensorimotor function in the early acute phase after ischemic stroke. Journal of Cerebral Blood Flow & Metabolism. 2017;37(1):291-306.

175. Aquino-Gálvez A, González-Ávila G, Delgado-Tello J, Castillejos-López M, Mendoza-Milla C, Zúñiga J, Checa M, Maldonado-Martínez HA, Trinidad-López A, Cisneros J. Effects of 2-methoxyestradiol on apoptosis and HIF-1α and HIF-2α expression in lung cancer cells under normoxia and hypoxia. Oncology Reports. 2016;35(1):577-83.

176. Cantley LC. The phosphoinositide 3-kinase pathway. Science (New York, NY). 2002;296(5573):1655-7.

177. Zhang Z, Yao L, Yang J, Wang Z, Du G. PI3K/Akt and HIF-1 signaling pathway in hypoxia-ischemia. Molecular medicine reports. 2018;18(4):3547-54.

178. Luo Z, Zhang M, Niu X, Wu D, Tang J. Inhibition of the PI3K/Akt signaling pathway impedes the restoration of neurological function following hypoxic-ischemic brain damage in a neonatal rabbit model. J Cell Biochem. 2019;120(6):10175-85. Epub 2019/01/08. doi: 10.1002/jcb.28302. PubMed PMID: 30614032.

179. Zeng SS, Bai JJ, Jiang H, Zhu JJ, Fu CC, He MZ, Zhu JH, Chen SQ, Li PJ, Fu XQ, Lin ZL. Treatment With Liraglutide Exerts Neuroprotection After Hypoxic-Ischemic Brain Injury in Neonatal Rats via the PI3K/AKT/GSK3β Pathway. Front Cell Neurosci.

2019;13:585. Epub 2020/02/23. doi: 10.3389/fncel.2019.00585. PubMed PMID: 32082121; PMCID: PMC7003644.

180. Li T, Li J, Li T, Zhao Y, Ke H, Wang S, Liu D, Wang Z. L-Cysteine Provides Neuroprotection of Hypoxia-Ischemia Injury in Neonatal Mice via a PI3K/Akt-Dependent Mechanism. Drug Design, Development and Therapy. 2021;15:517.

181. Li X, Zhang J, Zhu X, Wang P, Wang X, Li D. Progesterone reduces inflammation and apoptosis in neonatal rats with hypoxic ischemic brain damage through the PI3K/Akt pathway. International journal of clinical and experimental medicine. 2015;8(5):8197-203. PubMed PMID: 26221393.

182. Yang Y, Sun B, Huang J, Xu L, Pan J, Fang C, Li M, Li G, Tao Y, Yang X, Wu Y, Miao P, Wang Y, Li H, Ren J, Zhan M, Fang Y, Feng X, Ding X. Up-regulation of miR-325-3p suppresses pineal aralkylamine N-acetyltransferase (Aanat) after neonatal hypoxia–ischemia brain injury in rats. Brain Research. 2017;1668:28-35. doi: https://doi.org/10.1016/j.brainres.2017.05.001.

183. Sun B, Feng X, Ding X, Bao L, Li Y, He J, Jin M. Expression of Clock genes in the pineal glands of newborn rats with hypoxic-ischemic encephalopathy. Neural regeneration research. 2012;7(28):2221-6. doi: 10.3969/j.issn.1673-5374.2012.028.008. PubMed PMID: 25538743.

184. Sha N, Wang H-W, Sun B, Gong M, Miao P, Jiang X-L, Yang X-F, Li M, Xu L-X, Feng C-X, Yang Y-Y, Zhang J, Zhu W-J, Gao Y-Y, Feng X, Ding X. The role of pineal microRNA-325 in regulating circadian rhythms after neonatal hypoxic-ischemic brain damage. Neural regeneration research. 2021;16(10):2071-7. doi: 10.4103/1673-5374.308101. PubMed PMID: 33642396.

185. Vlassaks E, Mencarelli C, Nikiforou M, Strackx E, Ferraz MJ, Aerts JM, De Baets MH, Martinez-Martinez P, Gavilanes AWD. Fetal asphyxia induces acute and persisting changes in the ceramide metabolism in rat brain. J Lipid Res. 2013;54(7):1825-33. Epub 2013/04/26. doi: 10.1194/jlr.M034447. PubMed PMID: 23625371.

186. Dave AM, Peeples ES. Cholesterol metabolism and brain injury in neonatal encephalopathy. Pediatric Research. 2020:1-8.

187. Goedeke L, Rotllan N, Canfrán-Duque A, Aranda JF, Ramírez CM, Araldi E, Lin C-S, Anderson NN, Wagschal A, De Cabo R. MicroRNA-148a regulates LDL receptor and ABCA1 expression to control circulating lipoprotein levels. Nature medicine. 2015;21(11):1280-9.

188. Hardie DG. AMP-activated protein kinase: a cellular energy sensor with a key role in metabolic disorders and in cancer. Biochem Soc Trans. 2011;39(1):1-13. Epub 2011/01/27. doi: 10.1042/bst0390001. PubMed PMID: 21265739.

189. Cui H, Yang L. Analysis of microRNA expression detected by microarray of the cerebral cortex after hypoxic-ischemic brain injury. J Craniofac Surg. 2013;24(6):2147-52. Epub 2013/11/14. doi: 10.1097/SCS.0b013e3182a243f3. PubMed PMID: 24220425.

190. Ding X, Sun B, Huang J, Xu L, Pan J, Fang C, Tao Y, Hu S, Li R, Han X, Miao P, Wang Y, Yu J, Feng X. The role of miR-182 in regulating pineal CLOCK expression after hypoxia-ischemia brain injury in neonatal rats. Neuroscience Letters. 2015;591:75-80. doi: https://doi.org/10.1016/j.neulet.2015.02.026.

191. Liu X, Shi H, Liu B, Li J, Liu Y, Yu B. miR-330-3p controls cell proliferation by targeting early growth response 2 in non-small-cell lung cancer. Acta biochimica et biophysica Sinica. 2015;47(6):431-40.

192. Tammia M, Mi R, Sluch VM, Zhu A, Chung T, Shinn D, Zack DJ, Höke A, Mao H-Q. Egr2 overexpression in Schwann cells increases myelination frequency in vitro. Heliyon. 2018;4(11):e00982.

193. Cervellini I, Annenkov A, Brenton T, Chernajovsky Y, Ghezzi P, Mengozzi M. Erythropoietin (EPO) increases myelin gene expression in CG4 oligodendrocyte cells through the classical EPO receptor. Molecular Medicine. 2013;19(1):223-9.

194. Wang X, Chen S, Ni J, Cheng J, Jia J, Zhen X. miRNA-3473b contributes to neuroinflammation following cerebral ischemia. Cell Death Dis. 2018;9(1):11. Epub 2018/01/11. doi: 10.1038/s41419-017-0014-7. PubMed PMID: 29317607; PMCID: PMC5849032 SN were the inventors of a patent on application of one miRNA antagomir, which was approved by China Intellectual Property Office.

195. Lv Q, Zhong Z, Hu B, Yan S, Yan Y, Zhang J, Shi T, Jiang L, Li W, Huang W. MicroRNA-3473b regulates the expression of TREM2/ULK1 and inhibits autophagy in inflammatory pathogenesis of Parkinson disease. J Neurochem. 2021;157(3):599-610. Epub 2021/01/16. doi: 10.1111/jnc.15299. PubMed PMID: 33448372.

196. Wu C, Xue Y, Wang P, Lin L, Liu Q, Li N, Xu J, Cao X. IFN-γ primes macrophage activation by increasing phosphatase and tensin homolog via downregulation of miR-3473b. The Journal of Immunology. 2014;193(6):3036-44.

197. Wang C, Pan Y, Cheng B, Chen J, Bai B. Identification of conserved and novel microRNAs in cerebral ischemia-reperfusion injury of rat using deep sequencing. J Mol Neurosci. 2014;54(4):671-83. Epub 2014/07/27. doi: 10.1007/s12031-014-0383-7. PubMed PMID: 25063377.

198. Song B, Xu J, Zhong P, Fang L. MiR-125a-5p silencing inhibits cerebral ischemia-induced injury through targeting IGFBP3. Folia Neuropathol. 2021;59(2):121-30. Epub 2021/07/22. doi: 10.5114/fn.2021.107109. PubMed PMID: 34284540.

199. Ghoshal-Gupta S, Kutiyanawalla A, Lee BR, Ojha J, Nurani A, Mondal AK, Kolhe R, Rojiani AM, Rojiani MV. TIMP-1 downregulation modulates miR-125a-5p expression and triggers the apoptotic pathway. Oncotarget. 2018;9(10):8941.

200. Martín M-S, Gomez I, Miguela A, Belchí O, Robles-Cedeño R, Quintana E, Ramió-Torrentà L. Description of a CSF-Enriched miRNA Panel for the Study of Neurological Diseases. Life. 2021;11(7):594.

201. Miao W, Yan Y, Bao T-h, Jia W-j, Yang F, Wang Y, Zhu Y-h, Yin M, Han J-h. Ischemic postconditioning exerts neuroprotective effect through negatively regulating PI3K/Akt2 signaling pathway by microRNA-124. Biomedicine & Pharmacotherapy. 2020;126:109786. doi: https://doi.org/10.1016/j.biopha.2019.109786.

202. Uhlmann S, Mracsko E, Javidi E, Lamble S, Teixeira A, Hotz-Wagenblatt A, Glatting K-H, Veltkamp R. Genome-wide analysis of the circulating miRNome after cerebral ischemia reveals a reperfusion-induced MicroRNA cluster. Stroke; a journal of cerebral circulation. 2017;48(3):762-9.

203. Zou L, Xia P-f, Chen L, Hou Y-y. XIST knockdown suppresses vascular smooth muscle cell proliferation and induces apoptosis by regulating miR-1264/WNT5A/β-catenin signaling in aneurysm. Bioscience Reports. 2021;41(3). doi: 10.1042/bsr20201810.

204. Sepramaniam S, Tan J-R, Tan K-S, DeSilva DA, Tavintharan S, Woon F-P, Wang C-W, Yong F-L, Karolina D-S, Kaur P, Liu F-J, Lim K-Y, Armugam A, Jeyaseelan K. Circulating microRNAs as biomarkers of acute stroke. International journal of

molecular sciences. 2014;15(1):1418-32. doi: 10.3390/ijms15011418. PubMed PMID: 24447930.

205. Zhang L, Ma T, Tao Q, Tan W, Chen H, Liu W, Lin P, Zhou D, Wang A, Jin Y, Tang K. Bta-miR-34b inhibits proliferation and promotes apoptosis via the MEK/ERK pathway by targeting MAP2K1 in bovine primary Sertoli cells. Journal of Animal Science. 2020;98(10). doi: 10.1093/jas/skaa313.

206. Varol D, Mildner A, Blank T, Shemer A, Barashi N, Yona S, David E, Boura-Halfon S, Segal-Hayoun Y, Chappell-Maor L. Dicer deficiency differentially impacts microglia of the developing and adult brain. Immunity. 2017;46(6):1030-44. e8.

207. Cicognola C, Brinkmalm G, Wahlgren J, Portelius E, Gobom J, Cullen NC, Hansson O, Parnetti L, Constantinescu R, Wildsmith K. Novel tau fragments in cerebrospinal fluid: relation to tangle pathology and cognitive decline in Alzheimer's disease. Acta neuropathologica. 2019;137(2):279-96.